

# Lunar Transportation System Final Report

Spacecraft Design Team  
University of Minnesota  
Twin Cities

July 21, 1993

(NASA-CR-195540) LUNAR  
TRANSPORTATION SYSTEM Final Report  
(Minnesota Univ.) 106 p

N94-24805

Unclas

G3/37 0204275

# Table of Contents

Table of Contents	i	
List of Tables and Figures	iii	
List of Acronyms and Abbreviations	vi	
1.0	INTEGRATION	1
1.1	Motivation	1
1.2	Mission Statement	1
1.3	Executive Summary	1
2.0	MISSION ANALYSIS	1
2.1	Mission Goals and Objectives	2
2.2	Earth to Orbit Vehicle	3
2.3	On-Orbit Operations	5
2.4	Piloted Mission Scenario	6
2.5	Cargo Mission Scenario	10
2.6	Landing Site	10
2.7	Contingency Planning	11
2.8	Conclusion	12
3.0	SYSTEM LAYOUT	12
3.1	Scope	12
3.2	Design Process	12
3.3	Design Configurations	12
3.4	Final Configuration	16
3.5	Vibration	18
4.0	ORBITAL MECHANICS	19
4.1	Introduction	19
4.2	Orbit Mode Selections	19
4.3	Interplanetary Trajectories	20
4.4	Lunar Ascent / Descent Trajectories	23
4.5	Earth Orbit Activities	24
4.6	Abort Scenarios	25
4.7	Delta V Requirements	25
4.8	Conclusion	25
5.0	PROPULSION	25
5.1	Introduction	25
5.2	LTV Primary Propulsion	26
5.3	LEV Primary Propulsion	30
5.4	RCS	31
5.5	Fuel Requirements	34
5.6	Conclusion	34
6.0	STRUCTURAL AND THERMAL ANALYSIS	35
6.1	Structural Developments	35
6.2	Physical Testing of LTS System	42
6.3	Thermal Analysis Development	42

## **Table of Contents (cont.)**

7.0	CREW SYSTEMS, AVIONICS AND POWER	49
7.1	Crew Systems Introduction	49
7.2	Avionics Introduction	59
7.3	Power System Introduction	62
8.0	CONCLUSION	69
Appendix A	Crew Activity Timeline	70
Appendix B	Specification Sheet	73
Appendix C	Propulsion Spreadsheet	76
Appendix D	Thermal Analysis Program	90
Appendix E	MLI Analysis and Code	93
Appendix F	LTVCM Structure	100
Appendix G	LTS Power Requirements	102
Appendix H	LEVCM Structure	103
Appendix I	LEV Avionics	105
Appendix J	LTV Avionics	106
References		107
Contributors		110

# List of Tables and Figures

Table 2.1	Lunar Outpost Timeline	2
Table 2.2	Possible Heavy Lift Launch Vehicles	3
Figure 2.1	Payload Shroud	4
Figure 2.2	Heavy Lift Launch Vehicles	5
Figure 2.3	LTV in Low Earth Orbit	6
Figure 2.4	Earth - Moon Transit	7
Figure 2.5	LEV in Low Lunar Orbit	8
Figure 2.6	LEV ascending to LTV	9
Figure 2.7	LEV propulsively brakes into LEO	10
Figure 2.8	Lunar Outpost Landing Site	11
Figure 2.9	Contingency Plans	11
Table 3.1	LEV Masses	18
Table 3.2	LTV Masses	18
Figure 3.1	TLI Stage for Cryogenic Propulsion Layout	13
Figure 3.2	TEI Stage for Cryogenic Propulsion Layout	13
Figure 3.3	One-Tank Nuclear Configuration	14
Figure 3.4	Four-Tank Layout with Nuclear Propulsion	14
Figure 3.5	Layout with TLI Tanks away from Propulsion	15
Figure 3.6	Layout with Large and Small Truss Sections	15
Figure 3.7	LEV Configuration	16
Figure 3.8	LTV Configuration	17
Figure 3.9	Mode 1 Vibration	18
Figure 3.10	Mode 2 Vibration	18
Figure 3.11	Mode 3 Vibration	19
Table 4.1	Delta V Table	25
Figure 4.1	Earth Departure	20
Figure 4.2	Trans-Lunar Injection	21
Figure 4.3	Trans-Lunar Trajectory	21
Figure 4.4	Earth Departure	21
Figure 4.5	Maneuvers between Orbits	22
Figure 4.6	Lunar Departure	22
Figure 4.7	Trans-Earth Injection	22
Figure 4.8	Lunar Descent	23
Figure 4.9	Lunar Ascent	24
Figure 4.10	Earth Orbits	24
Figure 4.11	Abort Scenarios	25
Table 5.1	Burn Times for Piloted & Unpiloted Missions	29
Table 5.2	RL10A-4 Engine Specifications	31
Table 5.3	LOX/LH2 RCS Engine	31
Table 5.4	Shuttle Primary Thrusters	32
Table 5.5	Storable Lander RCS Engine	33

## List of Tables and Figures (cont.)

Figure 5.1	Comparison of Vehicle & Fuel Masses	27
Figure 5.2	NTR Operating Cycle	27
Figure 5.3	Diagram of Two Fuel Elements	29
Figure 5.4	Fuel Requirements for Mission Phases	34
Table 6.1	Material Properties	38
Table 6.2	Duration of Tank Exposure	47
Table 6.3	Physical Properties of Tanks	48
Table 6.4	MLI Thicknesses and Masses	49
Figure 6.1	Worst-Case Landing Orientation	35
Figure 6.2	Unstable Equilibrium Point	35
Figure 6.3	Initial Values of Spring Constants	36
Figure 6.4	Modified Spring Constants	37
Figure 6.5	LEV Truss Configuration	37
Figure 6.6	I-DEAS Finite Element Model of LEV	38
Figure 6.7	Tank Loads on the Four Nearest Nodes	39
Figure 6.8	Mohr's Circle of Stress	40
Figure 6.9	LTV Truss Configuration	41
Figure 6.10	I-DEAS Model of LTV Truss	41
Figure 6.11	I-DEAS Predicted Deformed Geometry For LTV Truss	42
Figure 6.12	Physical Test Article Geometry	42
Figure 6.13	Thermal Loads in Low Earth Orbit	43
Figure 6.14	Thermal Loads in Transit	43
Figure 6.15	Thermal Loads in Low Lunar Orbit	44
Figure 6.16	Definition of Heat Transfer Terms	44
Figure 6.17	Single Model Element and Heat Transfer Modes	44
Figure 6.18	Minimum and Maximum Element Temperatures	45
Figure 6.19	Rotating Louvers Configuration	46
Figure 6.20	Heat Pipe for LTS	46
Figure 6.21	Thermal Environment on Lunar Surface	47
Figure 6.22	Tank Configuration	47
Figure 6.23	MLI Layers	48
Table 7.1	Mass Loop Closure Comparison	49
Table 7.2	Human Daily Consumable Requirements	50
Table 7.3	Effects of Reduced O <sub>2</sub> Partial Pressure	52
Table 7.4	Standard Sea Level Partial Pressure	52
Table 7.5	Short Term Dose Equivalent	57
Table 7.6	Career Whole Body Dose Equivalent Limits	58
Table 7.7	Avionics Subsystem Masses	62
Table 7.8	LTS Power Requirements (LEV and LTV Docked)	63
Table 7.9	LEV Power Requirements (undocked and occupied)	63
Table 7.10	LTV Power Requirements (unoccupied on orbit)	63
Table 7.11	LEV Power Requirements (unoccupied on surface)	64
Table 7.12	Battery Chemical Types	64

## List of Tables and Figures (cont.)

Table 7.13	Solar Cell Conversion Efficiencies	65
Table 7.14	Silicon Solar Cells with Rigid Array Technologies	65
Table 7.15	Performance of Solar Cells with Rigid Arrays	67
Table 7.16	Power Parameters of the Octagonal Truss Section	67
Table 7.17	Power Parameters of the Square Truss Section	67
Table 7.18	Array Output and Mass to Meet Peak Power Demand	67
Table 7.19	Fuel Cell Reaction Rates	68
Table 7.20	Fuel Cell Power System	68
Table 7.21	LEV and LTV Power System Mass Summary	69
Figure 7.1	THC Schematic	50
Figure 7.2	Space Shuttle WMF	51
Figure 7.3	LTVCM External Dimensions	53
Figure 7.4	LTVCM Internal Dimensions	53
Figure 7.5	LTVCM Component Layout	54
Figure 7.6	Space Shuttle Galley	54
Figure 7.7	LEVCM Internal Dimensions	55
Figure 7.8	LEVCM Flight Deck Layout	55
Figure 7.9	Mission Specialist Seat	56
Figure 7.10	Mission Specialist Seat in Stowed Position	56
Figure 7.11	Pilot Seat	56
Figure 7.12	Water Dispenser	57
Figure 7.13	BATH Radiation Shield Location	59
Figure 7.14	Power Requirements vs. Mission	62
Figure 7.15	Regenerative Fuel Cell Schematic	65
Figure 7.16	Octagonal Cross Section of Truss	66
Figure 7.17	Square Cross Section of Truss	66
Figure 7.18	Normalized Solar Array Power Output	66

## Table Of Acronyms and Abbreviations

ACS	Atmosphere Control and Supply
AMO	Air Mass Zero
AR	Air Revitalization
ASE	Advanced Space Engine
ASRM	Advanced Solid Rocket Motor
ATDRSS	Advanced Tracking and Data Relay Satellite System
BATH	Borated Aluminum Titanium Hydride
BFO	Blood Forming Organs
CAD/CAM	Computer Aided Design / Computer Aided Manufacturing
CDR	Commander
CHX	Heat Exchanger
CIS	Commonwealth of Independent States
CM	Command or Crew Module
DoD	Department of Defense
DSN	Deep Space Network
ECLS	Environmental Control and Life Support
ECLSS	Environmental Control and Life Support System
ELVIS	Expendable Launch Vehicle in Space
EOC	Earth Orbit Capture
EOI	Earth Orbit Insertion
EPD&C	Electrical Power Distribution and Control
ET	External Tank
ETO	Earth To Orbit
EVA	Extra-Vehicular Activity
FDS	Fire Detection and Suppression
FLO	First Lunar Outpost
GCR	Galactic Cosmic Radiation
GN&C	Guidance, Navigation, & Control
HEPA	High Particulate Atmosphere
HLLV	Heavy Lift Launch Vehicle
HM	Habitation Module
IMU	Inertial Mass Unit
JSC	Johnson Space Center
KSC	Kennedy Space Center
LAM	Lunar Abort Module
LEO	Low Earth Orbit
LEV	Lunar Excursion Vehicle
LEVCM	See LEV and CM
LH <sub>2</sub>	Liquid Hydrogen
LLO	Low Lunar Orbit
LOI	Lunar Orbit Insertion
LOX	Liquid Oxygen
LRB	Liquid Rocket Booster
LTS	Lunar Transportation System
LTV	Lunar Transfer Vehicle

## Table Of Acronyms and Abbreviations (cont.)

LTVCM	See LTV and CM
MLI	Multi-Layer Insulation
MS	Mission Specialist
MSFC	Marshall Space Flight Center
NA	Not Applicable
NASA	National Aeronautics and Space Administration
NERVA	Nuclear Engine for Rocket Vehicle Application
NIR	Non-Ionizing Radiation
NLS	National Launch System
NSO	Nuclear Safe Orbit
NTR	Nuclear Thermal Rocket
OMV	Orbital Maneuvering Vehicle
PLS	Personnel Launch System
PLT	Pilot
RBE	Relative Biological Effectiveness
RCS	Reaction Control System
Rem	Roentgen Equivalent Man
RGA	Rate Gyro Assembly
RHC	Rotational Hand Controller
SCEVA	Sample Collection / Extra-Vehicular Activity
SEI	Space Exploration Initiative
SPE	Solar Particle Event
SRB	Solid Rocket Booster
SSCM	Space Station Crew Module
SSF	Space Station Freedom
SSME	Space Shuttle Main Engine
STME	Space Transportation Main Engine
STS	Space Transportation System
Sv	Sievert
TBD	To Be Determined
TCCA	Trace Contaminate Control Assembly
TDRSS	Tracking and Data Relay Satellite System
TEI	Trans-Earth Injection
THC	Temperature and Humidity Control
TLI	Trans-Lunar Injection
WMF	Waste Management Facility
WFS	Waste Management System



***"Destiny is not a matter of chance, it is a matter of choice; it is not a thing to be waited for, it is a thing to be achieved."***

**-William Jennings Bryan**

## **1.0 SYSTEM INTEGRATION**

### **1.1 Motivation**

If America is to regain the lead in space endeavors and become a spacefaring nation, a significant presence on the Moon will be required. The Moon is the gateway to the solar system, acting as a transportation node as well as a source of raw materials. For this reason, a major investment in a Lunar transportation infrastructure must be made. The University Space Research Association (USRA) requested the University of Minnesota Spacecraft Design Team design just such an infrastructure. This task was a year long design effort culminating in a complete conceptual design and presentation at Johnson Space Center. The design team was divided disciplines to ensure all aspects of the project were investigated.

### **1.2 Mission Statement**

In order to stay focused a design group must have a well defined mission task. This is the reason for declaring a mission statement. The design group has formulated the following statement for just that purpose:

"Design a system of vehicles to bring a habitation module, cargo, and crew to the Lunar surface from LEO and return either or both crew and cargo safely to LEO while emphasizing component commonality, reusability, and cost effectiveness."

Elaborating on this statement, the goal of the Lunar Transportation System (LTS) is to return America to the Moon to stay. The scope of this project is significantly larger than Apollo and will require a significantly larger infrastructure to support it. This large infrastructure will require massive amounts of funding. To help reduce the cost and complexity of the mission, components such as the Lunar lander will be reusable. This permits a functional infrastructure to be emplaced in cis Lunar space which can be used multiple times before requiring replacement. It is simply not feasible to throw away large portions of a space transportation system and retain a permanent presence on the Moon without horrendous expenditures.

## **1.3 Executive Summary**

During the course of the design, the LTS has taken on many forms. The final design of the system is composed of two vehicles, an Lunar Transfer Vehicle (LTV) and a Lunar Excursion Vehicle (LEV). The LTV serves as an efficient orbital transfer vehicle between the Earth and the Moon. The LEV carries crew and cargo to the Lunar surface. The reason for using a Lunar Orbit Rendezvous is to reduce the amount of fuel. This also give a lifeboat capability to the LEV in case of emergencies.

The LTV has seen the most drastic design changes of the two vehicles. After an initial configuration using all cryogenic propellants was analyzed, it was found to require inordinately large fuel masses. For this reason, a nuclear propulsion system for the LTV was investigated. This system was found to be superior to a comparable chemical system in many ways and was baselined for the LTV primary propulsion system.

After the choice was made to use nuclear propulsion on the LTV, the next major revision of the LTV design was the elimination of the aerobrake. This was done for two reasons. First, the nuclear propulsion package was efficient enough to allow the LTV to propulsively brake into Earth orbit. Second, it was considered unacceptable to aerobrake a nuclear reactor into the Earth's atmosphere and risk a nuclear accident.

An added concern of using a nuclear reactor is the placement of the reactor in between missions. The orbit of the reactor must be sufficiently high to ensure that in the event of a catastrophe no radioactive products reach the ground in any concentration. Furthermore, the orbit selected must be as free of orbiting debris as possible to ensure that nothing will collide with the reactor. The first requirement resulted in an initial parking orbit of 1200km (720 miles). However, this orbit contained much debris from Soviet weapons testing. Finally, it was decided to park the LTV in an orbit 10km (6 miles) higher than Freedom's orbit.

The choice of a nuclear rocket also influenced the structural design of the LTV. The reactor had to be maintained at a distance sufficiently far from the crew so

as to offer no significant radiation hazard. This distance was approximately 33m (108.3 ft). Initially, it was thought that a single large hydrogen tank could serve as both a fuel tank and a main structural element. However, this introduced other complications related to fuel transfer. Instead, the hydrogen fuel was broken up into four tanks and the single large tank was replaced by a 33m (108.3 ft) truss.

Since it is easy to lose sight of the overall mission goals, it is important to dedicate a portion of the design to defining the mission characteristics

## 2.0 MISSION ANALYSIS

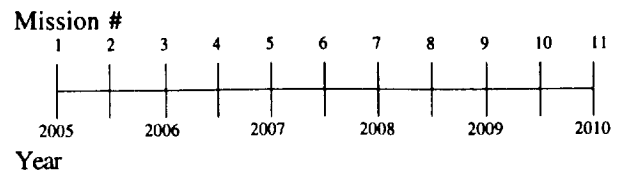
### 2.0.1 Introduction

The Mission Analysis discipline is responsible for the definition, safety, and reliability of the overall mission. Specific responsibilities include: mission goals and objectives; selection of the Earth To Orbit (ETO) vehicle; operations on-orbit, in transit, and on the Lunar surface; site selection; mission timelines; and contingency planning and abort scenarios.

### 2.1 Mission Goals and Objectives

The first major goal of the Space Exploration Initiative (SEI) is to establish a permanent Lunar outpost. Returning to the Moon to stay will require a series of cargo and crew missions. This objective is divided into three phases. The first phase missions will send large habitation and research modules to be assembled into a Lunar base. Several crews will be sent to accomplish this task. Once this architecture is complete, the next phase is to reach steady state operation. This involves extended stays for crews who will be resupplied on a regular basis. The last phase and long range goal is to attain a level of self-sufficiency by utilizing the Moon's resources to supply oxygen and materials for the outpost.

The initial phase timeline is as follows:



Lunar Mission Outline	
1.	First Habitation Module with Solar Power
2.	Lunar Abort Module and Equipment
3.	First crew of four - 14 day stay
4.	SCEVA Module
5.	Second crew of four - 14 day stay
6.	First Living Quarters and Nuclear Power
7.	Third crew of six - 30 to 60 day stay
8.	Science and Research Module
9.	Fourth crew of six - 30 to 60 day stay
10.	Second Living Quarters
11.	Fifth crew of six - 30 to 60 day stay

**Table 2.1** Lunar Outpost Timeline

As shown in Table 2.1, the first two Lunar missions will send the Habitation Module (HM) and a Lunar Abort Module (LAM) along with construction equipment to begin the initial phase of the Lunar base. The first piloted mission will consist of a crew of four who will stay for one Lunar day (14 days). Their primary mission will be to bring the HM to full operational status. The next cargo sent will be the Sample Collection and Extra-Vehicular Activity (SCEVA) module. This module will serve as a storage facility for EVA equipment and Lunar soil samples. The addition of this module will allow the next crew to begin in-situ resource utilization studies which are very important for attaining self-sufficiency. The second crewed mission will also consist of a crew of four who will stay for 14 days. The fourth cargo flight will deliver a living quarters module and a nuclear power source. This will allow for a larger crew of six and extended stays from 30 to 60 days. The Lunar outpost will be completed with the addition of a science research module and a second living quarters. The steady-state phase of the Lunar base will begin after the year 2010<sup>2,1</sup>. The Lunar base will be permanently occupied with crews of up to twelve people.

The Lunar Transportation System (LTS) has been designed to meet the goal of building and supporting a Lunar base. The first step in implementing this plan is to literally "get it off the ground."

## 2.2 Earth To Orbit Vehicle

During the initial stage of design the mission analysis discipline determined the ETO vehicle to be used for the LTS. This has been an on-going, evolutionary process. Any change in the LTS usually required a change in the launch scenario. The LTS and the ETO vehicle are mutually dependent systems. The requirements of each will drive the design or selection of the other. The launch vehicle selection is important since it imposes size and weight constraints on the LTS design.

### 2.2.1 HLLV Candidates

The United States currently has no heavy lift capability. A new launch system or one derived from existing components must be developed to support the SEI requirements. It is estimated that a direct launch Lunar mission would require a 75 to 105 metric ton payload capacity at post Trans-Lunar Injection (TLI). Future Mars missions require a lift capacity of about 250 metric tons to Low Earth Orbit (LEO). Both of these requirements can be met with the same Heavy Lift Launch Vehicle (HLLV). NASA's Marshall Space Flight Center (MSFC) has been investigating the development of a HLLV to meet these requirements. Various configuration possibilities which met these requirements are listed in Table 2.2.2.<sup>2</sup> All lift capacities are metric tons of payload to LEO.

Possible Heavy Lift Launch Vehicles	Lift Capacity
ET Core with 2 ASRM boosters	61t
ET Core with 4x2 F-1A boosters	265t
ET Core with 8x1 F-1A boosters	265t
ET Core with 3x3 F-1A boosters	280t
ET Core with 8 Energia boosters	250t
Saturn 5 derivative with 2x2 F-1A	254t
Energia with 8 Zenit boosters	200t

**Table 2.2**  
Possible Heavy Lift Launch Vehicles

One proposed concept of an HLLV is derived from the current Space Transportation System (STS). A Shuttle External Tank (ET) is utilized as the first stage by extending the tank an extra five feet and adding a propulsion module at the base. The propulsion module consists of four Space Transportation Main Engines (STME). The STME is a new engine currently under development by the Space Transportation Propulsion Team, a partnership formed by Aerojet, Pratt & Whitney, and Rocketdyne. The will be a cost efficient, more

reliable engine, with performance characteristics comparable to the Space Shuttle Main Engine (SSME).<sup>2.3</sup> This first stage is the center core of many possible configurations. The Advanced Solid Rocket Motor (ASRM) is the new booster currently under development for the STS. It will replace the currently used Solid Rocket Booster (SRB) providing an additional 5.5t of payload lifting capacity to the STS.<sup>2.4</sup> The F-1A booster is a Liquid Rocket Booster (LRB) based on a redesigned F-1 motor from the Saturn 5.

Another option for an HLLV is a Saturn 5 derivative consisting of the first and second stages of the Saturn 5 with the ET core as the third stage. Like the STS derived option, this option remains in the conceptual design stage. There is no Saturn 5 hardware that could be refurbished. Thus, it is not feasible to resurrect the Saturn 5.

The last possibility available is the Energia rocket of the Commonwealth of Independent States (CIS). The Energia consists of a LH<sub>2</sub> / LOX central core with four engines and up to eight strap-on LOX / kerosene Zenit boosters. It is currently the only existing HLLV in the world and has flown successfully with four Zenit boosters.<sup>2.5</sup>

### 2.2.2 Shroud Size

All possible HLLV's would use the same payload shroud whose sizing was a constraint on the LTS design. The concern was to determine if the HM needed to be down sized in order to be placed in the shroud. For a crew of six, the module would have a length of 16.0m (52.5 ft) and a diameter of 4.4m (14.4 ft). The current configuration of the payload fairing has a length of 18.3m (60 ft) along the mid-section and 11.0m (36.1 ft) outside diameter. The usable volume inside has a diameter of 10m (32.8 ft)<sup>2.3</sup> as shown in Figure 2.1. The HM will fit within the shroud if it is oriented vertically. With proper structural support, this orientation should not present any loading problems during launch.

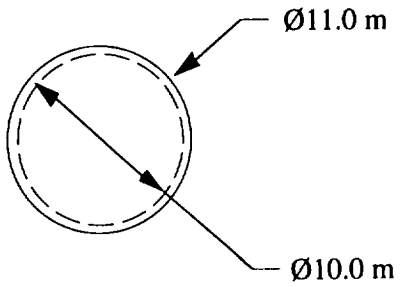
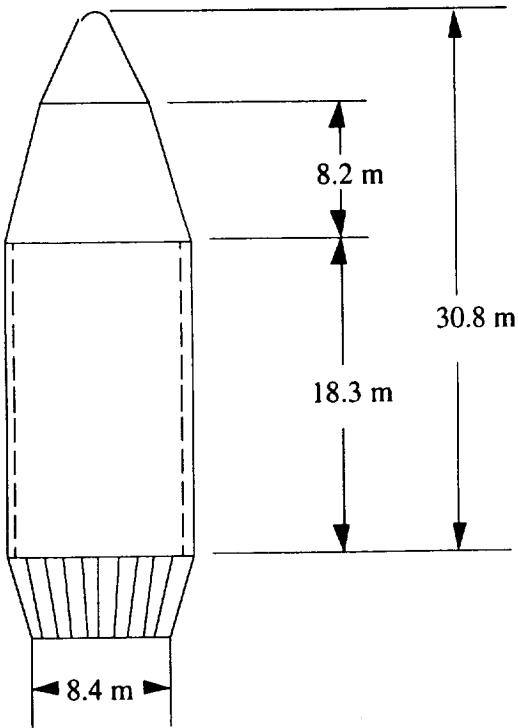


**Figure 2.1** Payload Shroud

### 2.2.3 Final Selections

The STS derived HLLV was selected as the launch vehicle for the LTS. This design was chosen for its versatility in configurations for specific missions as listed below. Also, this design is the most cost effective and feasible launch vehicle for the near future. The vehicle provides a maximum lift capability of 265t to LEO and should not impose a design constraint on the LTS.

The HLLV with ASRM's in Figure 2.2 is capable of lifting 61t into LEO. This vehicle will be used to place the Lunar Transportation Vehicle (LTV) truss, crew module, and Lunar Excursion Vehicle (LEV) into orbit in a single launch.

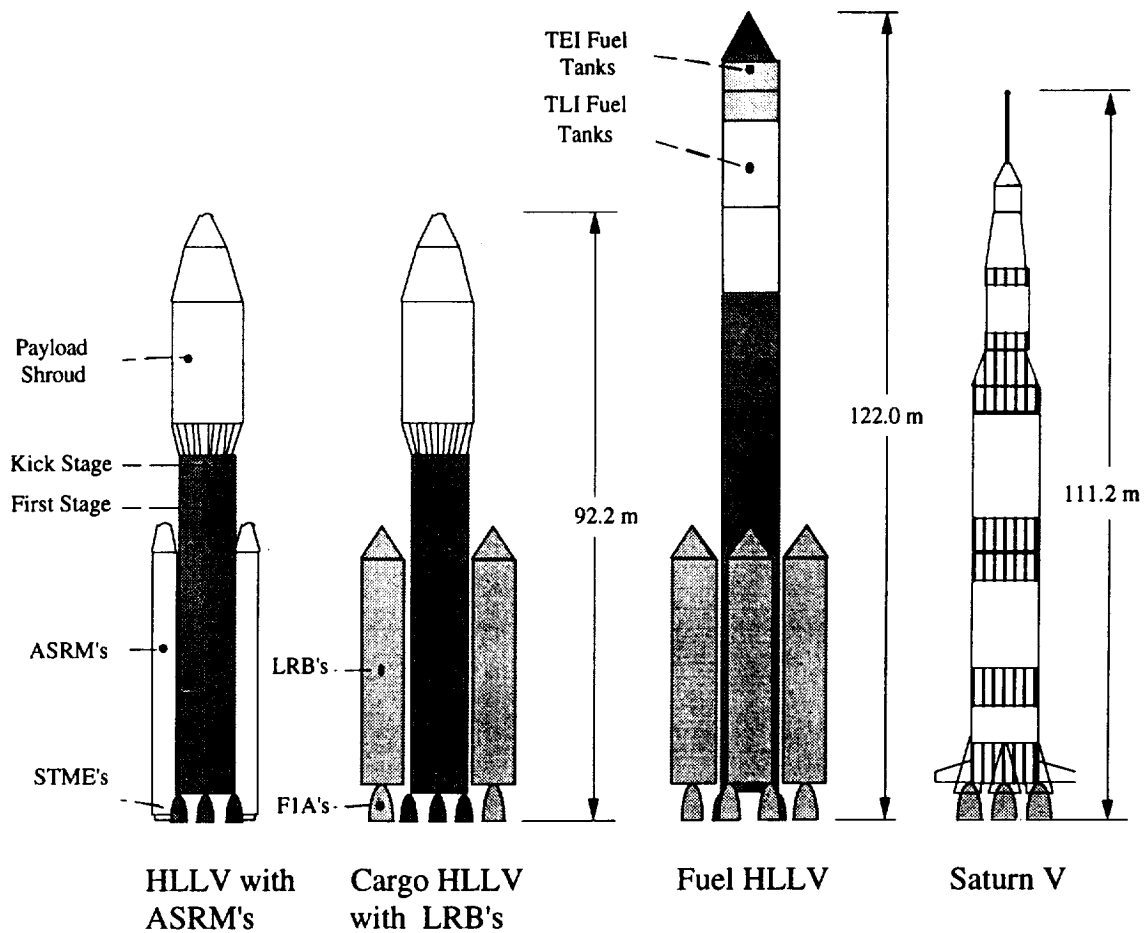


**Figure 2.2** Heavy Lift Launch Vehicles

The HLLV with two LRB's in Figure 2.2 is capable of lifting 123t into LEO. This vehicle will be used to place various cargo such as the HM into orbit.

The current mission requires 130t of Liquid Hydrogen (LH<sub>2</sub>) fuel for the Nuclear Thermal Rocket (NTR). The density of LH<sub>2</sub> is 0.071 t/m<sup>3</sup> which translates into a volume with a diameter of 10 m (maximum) and a length of 23 m. This is too long to fit in the payload shroud of the HLLV. One possible way of avoiding this sizing constraint is to integrate the tanks into an upper stage of the HLLV. A conversation with Steve Cook, lead engineer for the HLLV project at MSFC, confirmed that this is feasible. The outside diameter of each tank is 8.4m (27.6 ft). The third HLLV configuration in Figure 2.2 will be used to lift the LTS fuel into orbit.

### 2.3 On-Orbit Operations

Preparing for any mission requires on-orbit operations. Initially, the entire LTV must be launched and assembled.

This will require two launches. One vehicle carries the three major truss sections, crew modules, and the LEV. The other transports the NTR which is launched separately on a Titan III for safety reasons as outlined in Section 2.7. Assembly in a parking orbit near Space Station Freedom (SSF) follows. The major components will require minimal on-orbit construction utilizing Orbital Maneuvering Vehicles (OMV) from SSF. Rendezvous and docking of the components will be all that is necessary for assembly.

Once the LTV is completed in LEO, cargo missions to the Moon will begin. Each cargo mission will require two HLLV launches. One launch will consist of LH<sub>2</sub> fuel, the other would deliver the heavy lander with its cargo to the LTV.

A piloted mission would involve one HLLV launch for the fuel. The crew arrives by the shuttle or a personnel launch system (PLS) to SSF and then transfer to the LTV in the LEV which will be initially docked at SSF.

## 2.4 Piloted Mission Scenario

See Appendix A for a detailed crew activity timeline.

### 2.4.1 Low Earth Orbit

At the start of the mission, the LTV is in LEO as shown in Figure 2.3. The fuel tanks are attached by an orbital maneuvering vehicle (OMV) from SSF. A wet tank

transfer was chosen for its simplicity and level of safety. The fuel launch, attachment, and vehicle check out will take no more than one week. After the vehicle is fully assembled, the crew transfers from SSF to the LTV in the LEV. The LEV docks with the LTV for the trip to the Moon. Once the LTV has been checked out in LEO, the crew prepares for the TLI burn. Finally, the NTR is engaged and the TLI burn initiated.

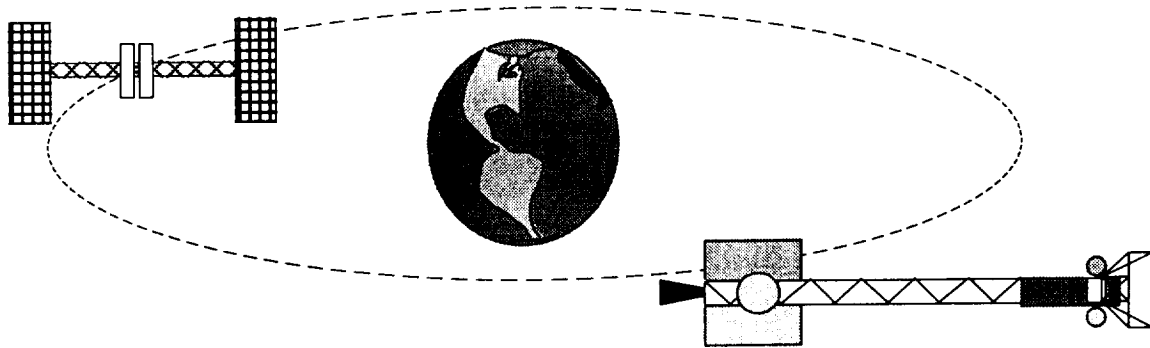
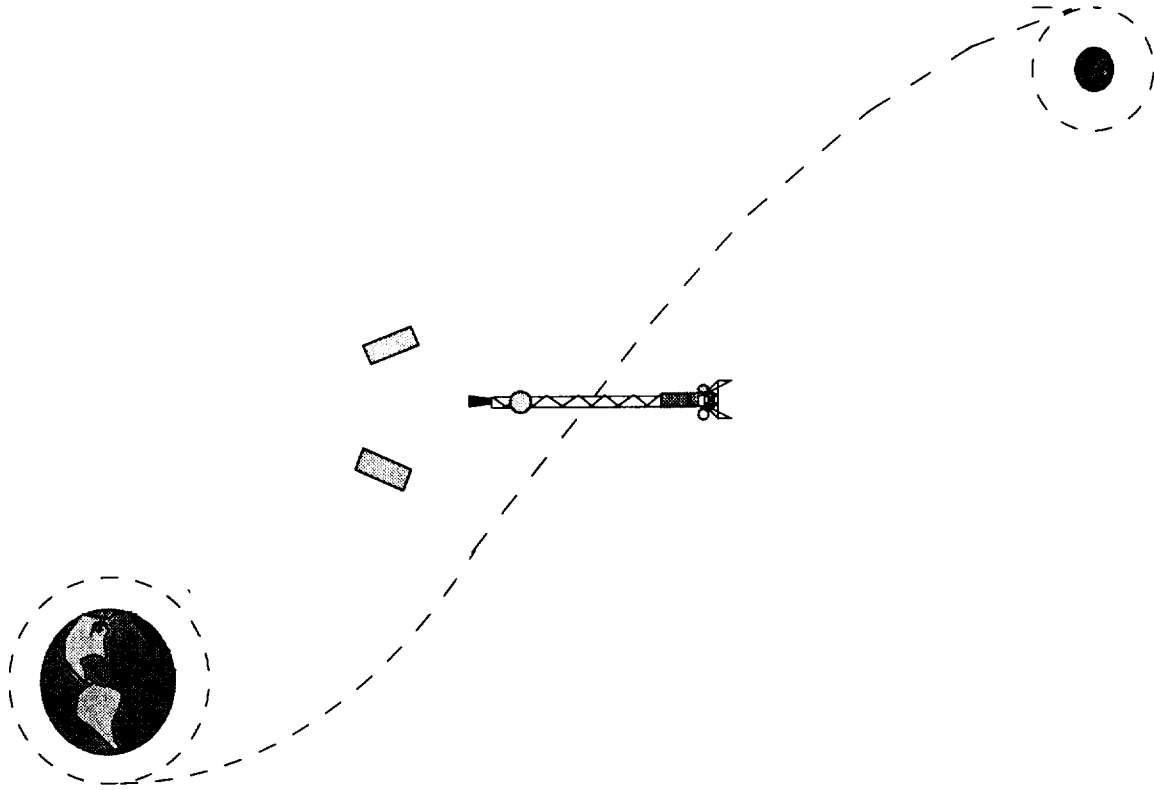


Figure 2.3 LTV in Low Earth Orbit

### 2.4.2 Trans-Lunar Injection

The TLI burn lasts for 35 minutes, after which the LTV coasts for approximately three days until reaching Low Lunar Orbit (LLO). During transit, various crew activities and experiments are performed. First the maneuver to drop the TLI tanks is initiated as displayed in Figure 2.4. The tanks will be targeted for Lunar impact at some designated location on the surface. This would require a delta V of 5 m/s.<sup>2.7</sup> Since the tanks have no

avionics or reaction control system (RCS), the disposal maneuver will be made by the LTV which will then have to be realigned to its planned course. The LTV is designed for accurate targeting which would be necessary for tank disposal. Performance of the disposal maneuver takes the LTV off course from the free-return trajectory designed for mission abort contingencies. This does add some risk should a total RCS or avionics failure occur. Then a reorientation of the LTV is executed to prepare for the Lunar Orbital Insertion (LOI) burn of the NTR.



**Figure 2.4 Earth - Moon Transit**

**2.4.3 Lunar Orbit Insertion**

At this point the LTV undergoes a 9.05 minute LOI burn decelerating the spacecraft into LLO.

**2.4.4 Low Lunar Orbit**

Now in LLO, the LTV undergoes an orbital adjustment to the desired inclination for a landing. The crew at this time must enter the LEV. Now the LEV separates from the LTV and maneuvers to leave its orbit and descend as shown in Figure 2.5. At this point, the mission elapsed time is at T+72 hours.

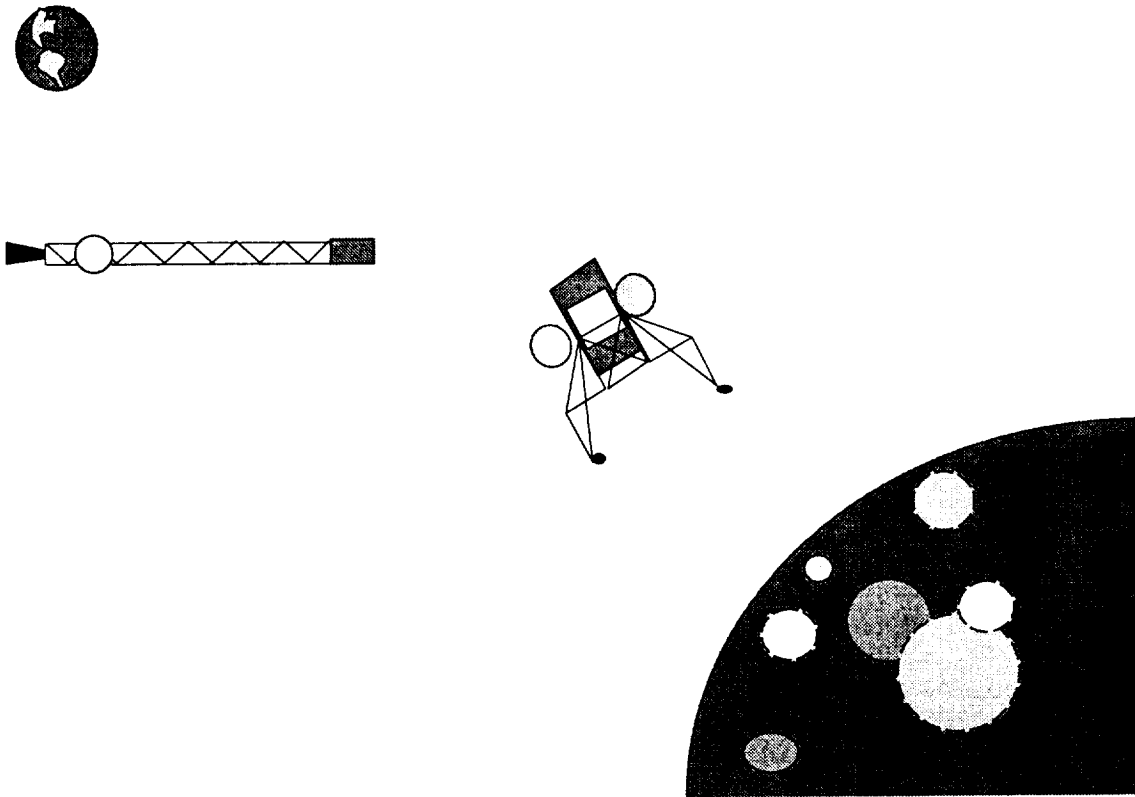


**Figure 2.5** LEV in Low Lunar Orbit

#### **2.4.5 Descent To Lunar Surface**

The LEV descends to the lunar surface using its RL10 engines. for a duration of 17.64 minutes.

Once on the lunar surface, the crew must execute a number of activities. In order, these tasks are:

- a. The crew will conduct an LEV systems check.
- b. The crew will change into Extra-Vehicular Activity (EVA) suits.
- c. The crew then leaves the LEV and enters the HM.
- d. The HM is secured with activities to be determined.
- e. The total Lunar surface stay for this mission is 14 days.

f. The crew will then reenter the LEV and prepare for ascent.

g. Finally, the crew ignites the RL10 engines for the ascent to LLO.

#### **2.4.6 Ascent to LLO, rendezvous with LTV**

The ascent burn of the RL10 engines is 10.13 minutes. Now back in LLO, the LEV rendezvous with the LTV as shown in Figure 2.6. An orbital adjustment is made to prepare for the Trans-Earth Injection (TEI) trajectory. The NTR is prepared to be engaged for the TEI burn and the return mission elapsed time is at T+ 5 hours.



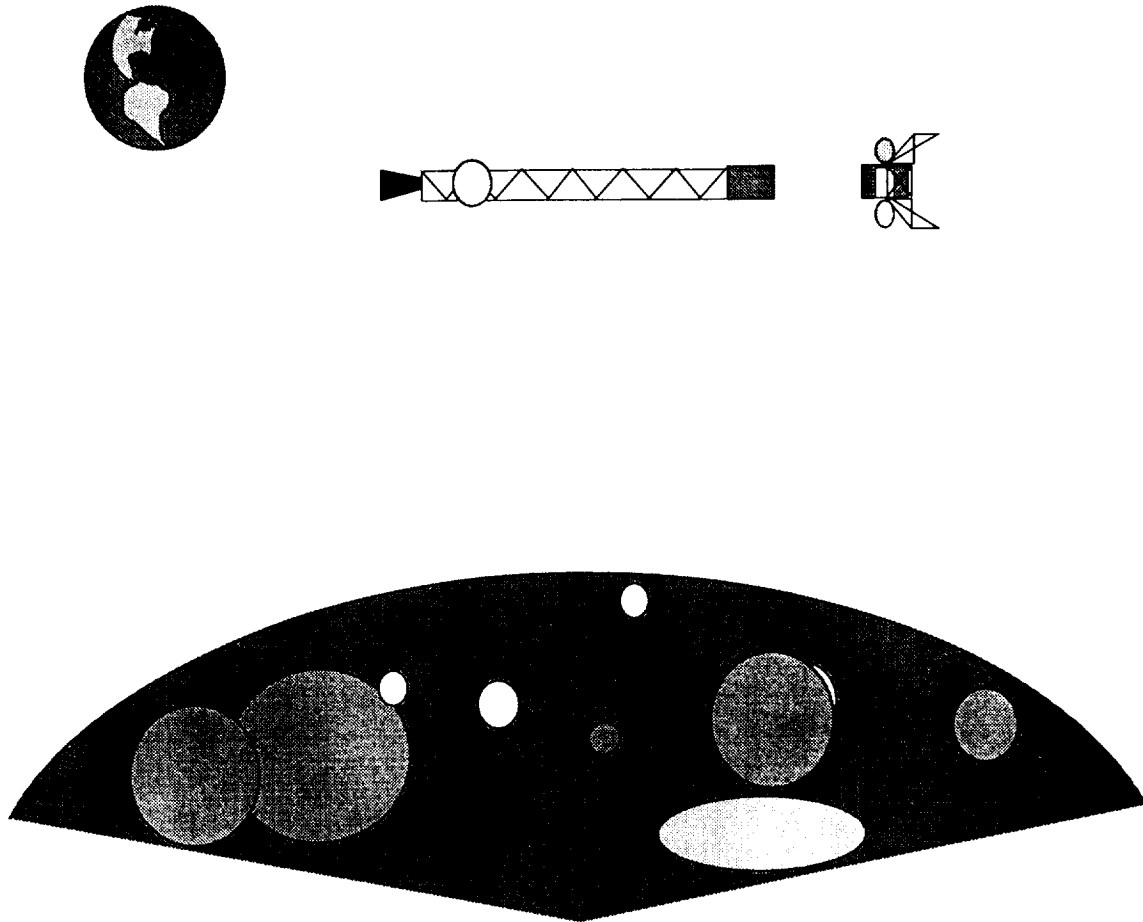


**Figure 2.6** LEV ascending to LTV

### **2.4.7 Trans-Earth Injection**

The NTR is engaged for a 5.15 minute TEI burn. Transit back to LEO will take about two days in which many tasks must be executed. In-transit crew activities will be performed. The LTV will execute a series of mid-course corrections. Finally, the LTV must be reoriented to the proper position needed for Earth orbital insertion (EOI). At this time determination of the status of the NTR for EOI will be performed.

### **2.4.8 Earth Orbit Insertion**

On approach to Earth, the EOI burn is performed placing the LTV into LEO as illustrated in Figure 2.7. The EOI burn lasts for 10.82 minutes. The orbit of the LTV is adjusted to rendezvous with SSF. After sustaining LEO and completing the required orbital adjustments, the mission clock is at T+ 20 days.

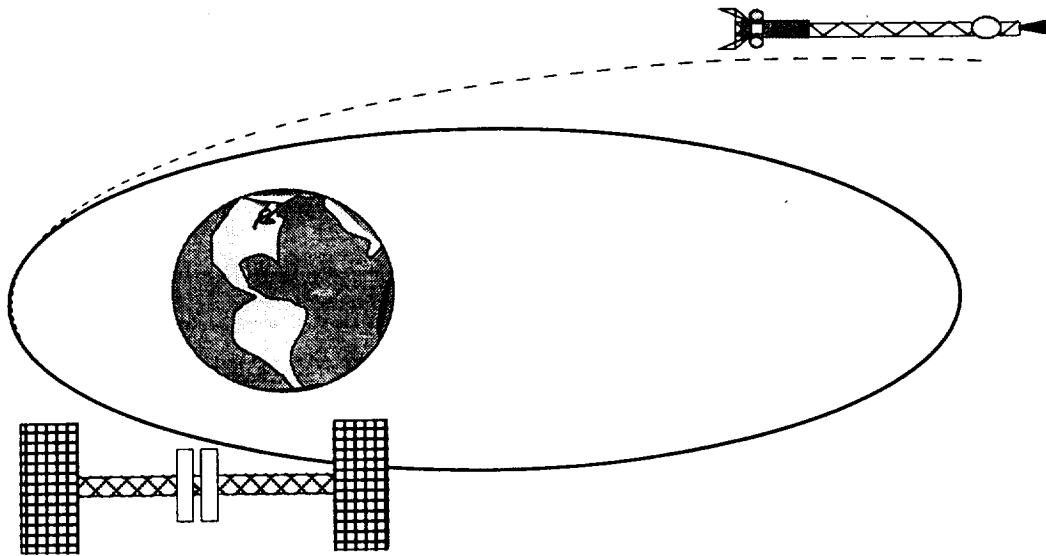


Figure 2.7 LEV propulsively brakes into LEO

## 2.5 Cargo Mission Scenario

The cargo scenario is very similar to the piloted case except that nothing is returned from the Lunar surface. The flight is completely automated and monitored from Mission Control at Johnson Space Center (JSC) in Houston.

### 2.5.1 Low Earth Orbit

The LTV including the NTR is initially in LEO. The cargo and heavy lander are attached to the LTV. When the LTV is fully functional, the NTR is engaged, and the TLI burn is initiated.

### 2.5.2 Trans-Lunar Injection

After the TLI burn is completed, the LTV will travel for three days before reaching LLO. The maneuver to drop the TLI tanks is initiated and the reorientation of the LTV is executed to prepare for the LOI burn of the NTR.

### 2.5.3 Lunar Orbit Insertion

In order to put the LTV in LLO, the craft utilizes a decelerating burn and undergoes LOI.

### 2.5.4 Low Lunar Orbit

Now in LLO, the LTV undergoes an orbital adjustment to the desired inclination for a landing.

### 2.5.5 Descent To Lunar Surface

Now the heavy lander with cargo separates from the LTV and maneuvers to leave orbit and descend to the Lunar surface. The heavy lander then descends using its RL10 engines. The heavy lander remains on the Lunar surface. There is no ascent or rendezvous with the LTV.

### 2.5.6 Trans-Earth Injection

The LTV prepares for the TEI trajectory immediately after the descent of the heavy lander. The NTR is engaged for the TEI burn.

### 2.5.7 Earth Orbit Insertion

Transit back to LEO will take two days in which many tasks must be executed. The LTV will execute a series of mid-course corrections. The LTV must be reoriented to the proper position needed for EOI. On approach to Earth, the EOI burn is fired putting the LTV in LEO. The orbit of the LTV is adjusted to rendezvous with SSF.

## 2.6 Landing Site

Mare Cognitum (Known Sea) has been chosen as a preliminary landing site for the Lunar outpost. This site is for reference purposes only. The actual site will be selected based on data received from the Lunar precursor missions. Mare Cognitum is on the edge of Oceanus Procellarum (Ocean of Storms). This is the landing site of Apollo 12 and Surveyor 3 as illustrated in Figure 2.8.<sup>2.8</sup> The coordinates are latitude: 3° 12' South and longitude: 23° 23' West.

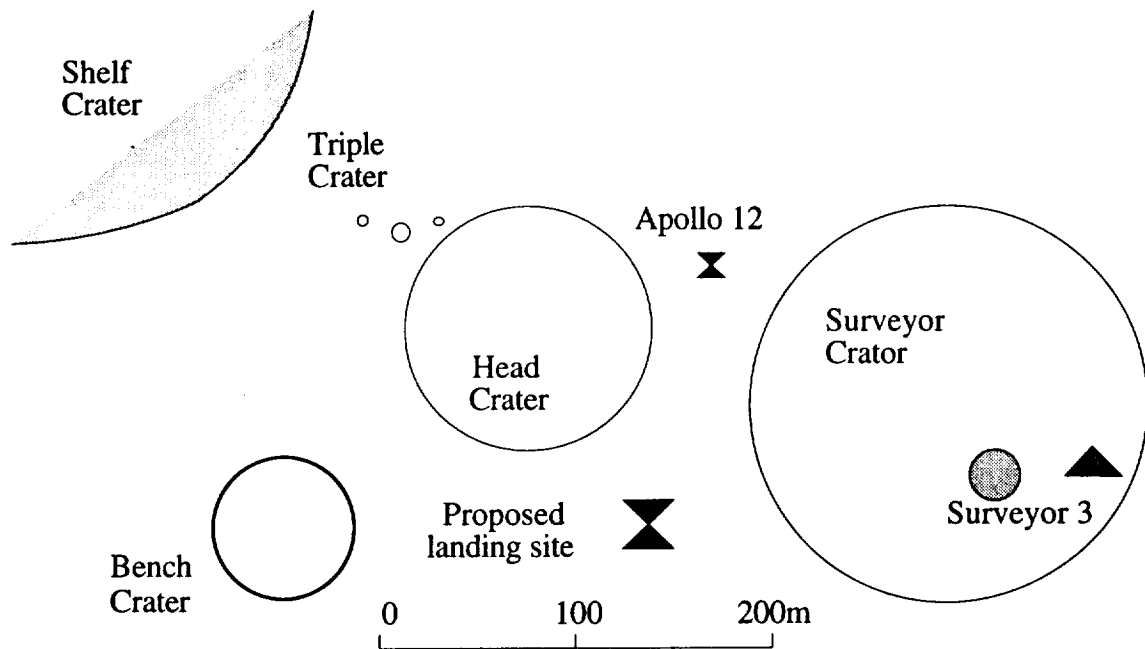


Figure 2.8 Lunar Outpost Landing Site

This site was selected for several reasons. The location is within the  $\pm 5^\circ$  latitude limits set by the orbital mechanics of the mission. In addition, this site has been surveyed and photographed in detail. Finally, the Apollo 12 Lunar descent stage and Surveyor spacecraft should provide valuable data on the long term effects of the Lunar environment on materials used in the construction of the Lunar outpost.

## 2.7 Contingency Planning

Contingency plans must be made for many different system failures. Every possible scenario could not possibly be studied in the amount of time available. Only the "worst case" scenarios which could lead to mission failure or loss of life are included.

### 2.7.1 Possible failures for critical systems

#### Launch:

The NTR will be launched separately from the rest of the LTV to reduce mission risks. Launching from Kennedy Space Center (KSC) provides a unique hydrological feature known as the Blake Escarpment 400km (240 miles) downrange of the launch site. The ocean depth before this point is 1100m (3609 ft). The depth then increases to several kilometers and extends for 8000km (4800 miles). The interchange of water from the surface to the bottom takes hundreds of years in this region. Thus, in the event of a launch failure, this hydrological region provides an

excellent disposal option. For this reason, the launch from KSC will maintain a flight path over water up to the orbital injection point.<sup>2.9</sup>

#### NTR:

All of the following contingency plans for NTR failure refer to Figure 2.9 below.

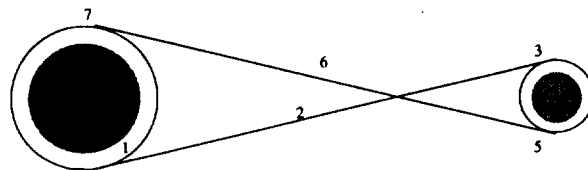


Figure 2.9 In Transit Contingency Plans

1. While in LEO, if a malfunction should arise before the NTR is ignited, the LTV will remain in orbit.

2. After TLI, a NTR failure requires either a fly-by around the Moon and flight back to LEO in the LEV or an abort to the Lunar surface. This latter option allows the crew to complete their mission and return to Earth in the LAM.

3. In LLO prior to descent, an NTR failure requires the LEV fuel for TEI. An LEV failure requires the use of the NTR as planned to complete the trip back to Earth. Alternatively, an automated launch and rendezvous of the LAM with the LTV in LLO is also possible.

4. A problem with the LTV while the crew is on the surface requires returning to Earth in the LAM.

5. After ascent, there will be no fuel in the LEV. An NTR failure at this point requires an automated launch and rendezvous of the LAM with the LTV in LLO. The crew transfers to the LAM for the trip back to Earth.

6. After TEI, NTR failures are again considered. In the event that the NTR does not fire, there are no options for braking into LEO. The large delta V required in any type of abort at this point results in an unacceptably large mass increase on the LTV. This type of failure is considered unlikely and was deemed an acceptable risk for the mission.

7. An NTR failure in LEO also has possible solutions. The crew could be rescued with the use of an ETO such as the shuttle. In the event of a core failure, the NTR can be disposed of with the use of a core ejection system (CES), an independent means for launching the reactor core to a higher orbit with an orbital decay period on the order of thousands of years.

#### **LEV:**

A single engine failure on the LEV can be compensated by the remaining engine and the RCS system. Descent and ascent can be accomplished with a single engine.

#### **Crew Modules :**

Failure of any critical system in the crew modules are covered by redundant systems.

### **2.8 Conclusion**

The mission scenarios outlined above reflect a concern for safety, reliability, and cost efficiency. All possible contingencies were analyzed and necessary abort scenarios have been devised.

## **3.0 SYSTEMS LAYOUT**

### **3.1 Scope**

The following section details the design process and trial configurations leading up to the final configuration. Also, the final configuration is presented in detail through all phases of the piloted mission.

### **3.2 Design Process**

The primary tasks of the Systems Layout Discipline are to conceptually assemble the subsystems of the LTS into a functional, efficient system, to investigate and optimize the

stability and control of that system, and to prepare detailed drawings of the system's final configuration layout. To complete these tasks, a design process was followed to accumulate many trial configurations and to then choose and optimize a layout that is functional, stable, and efficient.

To obtain trial configurations, a process of gathering information about each subsystem and all design parameters had to be completed. This process included gaining a complete understanding of the geometric attributes, mass distributions, and operational function of each subsystem. This was completed by interacting with each discipline in the Spacecraft Design Team to gather information and layout ideas about the disciplines' individual subsystems. Once a reasonable level of understanding of the LTS and its required components and design parameters was attained, sketches and block diagrams of layout ideas were produced and analyzed.

The sketches that were created provided a means of viewing and analyzing the attributes of each subsystem when assembled with all of the other components. Such drawings were especially helpful in analyzing the geometric constraints that had to be dealt with and the stability of each layout idea.

As can be expected, the use of Computer Aided Design (CAD) software proved to be very valuable in designing the layout of the LTS. Three-dimensional views of an object, for example, were very simple to obtain from the CAD software, once the object's geometry was defined. This also helped in the determination of geometric constraints, since hand-made three-dimensional sketches were often difficult to construct and interpret. The software used was Pro/ENGINEER (by Parametric Technology Corporation), a user-friendly package with many powerful drafting capabilities. This CAD package not only helped in sketching and analyzing trial configurations, but was very useful in the addition and modification of the many details that had to be included in the drawings of the final configuration of the LTS.

### **3.3 Design Configurations**

Analyzing the trial configurations was the next step in choosing an optimum layout. This was done individually and by comparing the accumulated layouts. This analysis led to the elimination of many proposed designs because of a lack of agreement with the design parameters gathered previously or obvious lack of efficiency. The following sections describe a few of the candidates for the LTS layout and an analysis of the advantages and disadvantages of each.

### 3.3.1 All Cryogenic

Earlier in the year, the Spacecraft Design Team had decided to utilize cryogenic propulsion on the LTS during the TLI and TEI stages of the mission. This decision led to an analysis of many possible configurations, which were eventually narrowed down to one optimum layout. Shown in Figure 3.1, the LTS in the TLI stage in this layout consists of six major components: the LEV, the TLI fuel tanks, the aerobrake, the LTVCM, the TEI fuel tanks, and the TLI propulsion system.

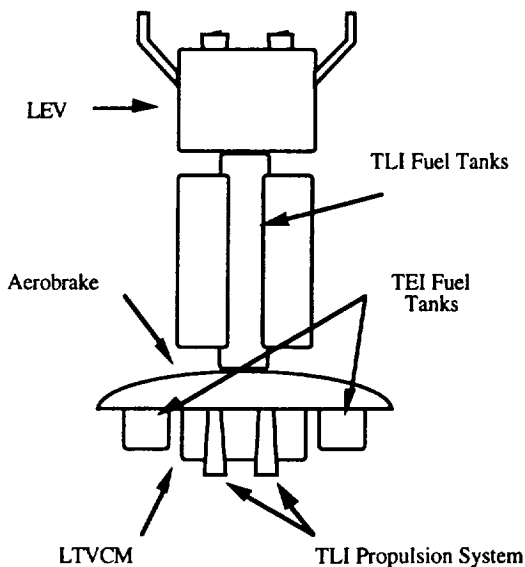


**Figure 3.1**  
TLI stage for Cryogenic Propulsion Layout

During the TEI stage (shown in Figure 3.2), the LTS would then consist of only three major components: the aerobrake, the TEI fuel tanks, and the LEV (the LEV's propulsion system would be used for TEI propulsion).

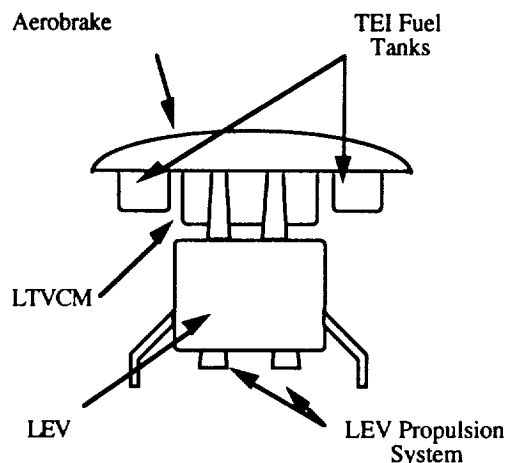


**Figure 3.2**  
TEI Stage for Cryogenic Propulsion Layout

Referring to Figure 3.1 and Figure 3.2, the TLI tanks are jettisoned in LLO and the LEV re-docks with the LTV after its Lunar missions with the orientation shown in Figure 3.2. The LEV's propulsion system, as stated previously, provides the TEI burn needed, and the aerobrake then slows the LTS down to allow for docking with SSF. The largest disadvantage of this layout is the extensive amount of fuel needed for the complete mission.

### 3.3.2 NTR LTV

As further analysis progressed, it was determined that a nuclear propulsion system for the TLI and TEI stages would be a more efficient system, due to the decreased amount of fuel needed. This then produced new challenges for the layout of the LTS. One example of such a challenge was how to provide adequate radiation protection for the crew. Furthermore, the aerobrake was deemed necessary only for a possible abort scenario due to the fact that the nuclear propulsion system could efficiently slow the LTS down enough for docking with SSF. The following figures, therefore, have an optional aerobrake sketched in to show where it would be placed if it was chosen to be included for abort reasons.

#### 3.3.2.1 NTR LTV 1 Tank

A preliminary layout of an LTS with a nuclear propulsion system is shown in Figure 3.3. With only one type of fuel needed (liquid hydrogen), a one tank layout, as shown, could be designed. Such a huge tank could provide the needed radiation shielding for the crew, and also serve as the main truss structure of the LTS.

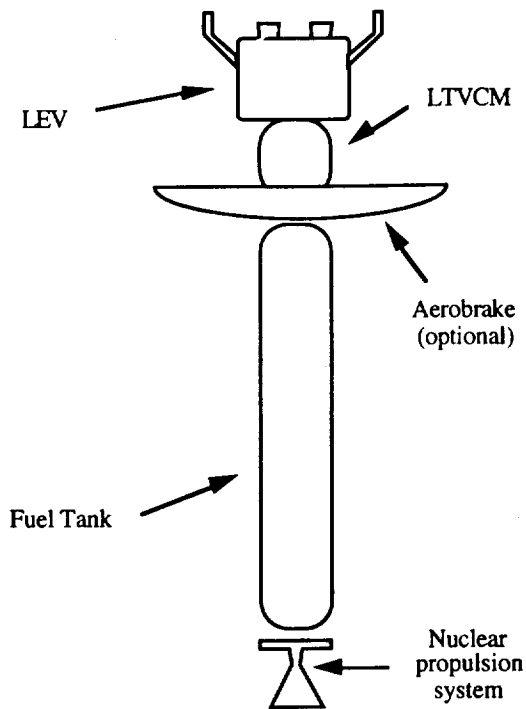


**Figure 3.3**  
One-Tank Nuclear Configuration

However, since it has been determined, through previous Spacecraft Design Team research, that a wet-tank transfer is much more desirable than a refueling fluid transfer, especially in such a large scale as this, a massive orbital rendezvous operation would be necessary at the start of each mission. This would involve the handling and maneuvering of a potentially dangerous nuclear reactor quite frequently. Also a disadvantage would be the fact that the whole mass of the tank would be hauled along throughout the entire mission, causing a loss in efficiency.

### 3.3.2.1 NTR LTV 4 Tanks

With these problems in mind, a layout with four fuel tanks (two for the TLI stages and two for the TEI stages) attached to a long truss was produced and is shown in Figure 3.4. The symmetry of this design is an obvious advantage while the four tank layout allows for jettisoning of the TLI tanks after use, limiting the amount of extra mass being carried by the LTS.

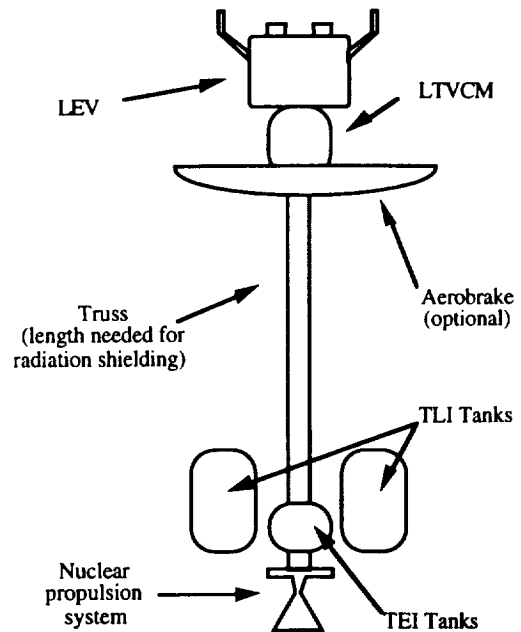


**Figure 3.4**  
Four-Tank Layout with Nuclear Propulsion

However, with a one meter square truss, a structurally sound layout, the fuel tanks have to be set radially outward from the truss by one and a half meters to keep the tanks from interfering with one another. This would present a fairly difficult problem in structurally attaching the tanks to the truss. Two approaches were then taken to encounter this problem.

One way to avoid this attachment problem was to move the TLI tanks away from the propulsion system just enough to keep them from interfering with the TEI tanks. This configuration is shown in Figure 3.5. This layout seems to solve the attachment difficulty quite well, but it also produces another problem.

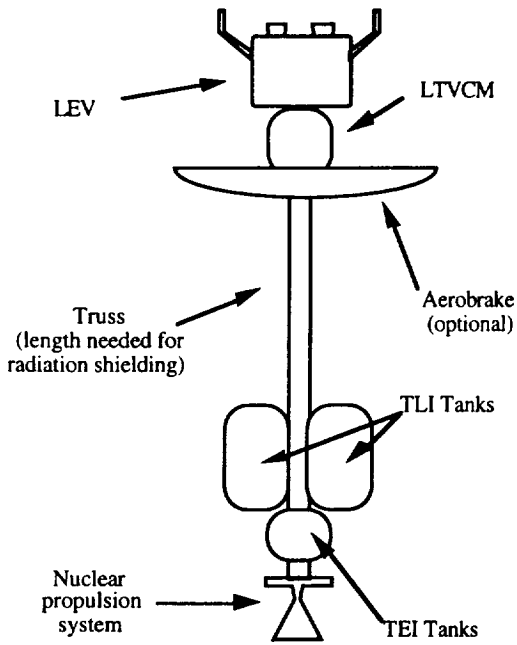


**Figure 3.5**  
Layout with TLI Tanks away from propulsion

In order to place the TLI fuel tanks as shown in Figure 3.5, fuel lines of eight meters in length or more would have to be utilized, which would thus cause a fairly inefficient means of fuel transfer.

Another means of countering the attachment problem was then produced. As shown in Figure 3.6, a smaller truss is still used for the majority of the length of the LTV, but a larger one (four meters square) is used for the area where the tanks are attached. This design allows for all of the tanks to be placed fairly close to the propulsion system, without interference, thus eliminating the lengthy fuel lines.

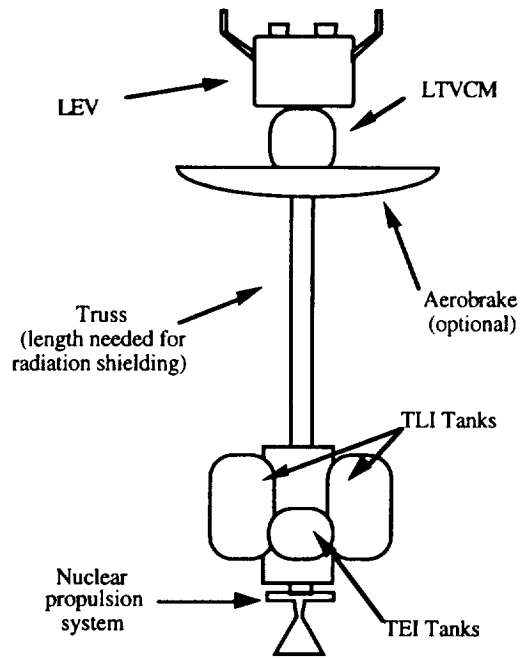


**Figure 3.6**  
Layout with Large and Small Truss Sections

With continuous modifications of the layout shown in Figure 3.6, and the inclusion of extensive details, an optimum layout of the LTS was then produced.

### 3.4 Final Configuration

The final LTV configuration consists of the LEV, NTR, and fuel tanks attached to a truss. The length of the truss provides the crew with adequate radiation protection. Tank sizes were determined working under the assumption that the TLI fuel would be contained in two large tanks, while the

remaining fuel for LOI, TEI, and EOI will be contained in two smaller tanks. This allows the TLI tanks to be jettisoned. The final LTV layout with major dimensions is included as Figure 3.7 and 3.8. Masses are included in Tables 3.1 and 3.2. The specification sheet of this vehicle is located in Appendix B.

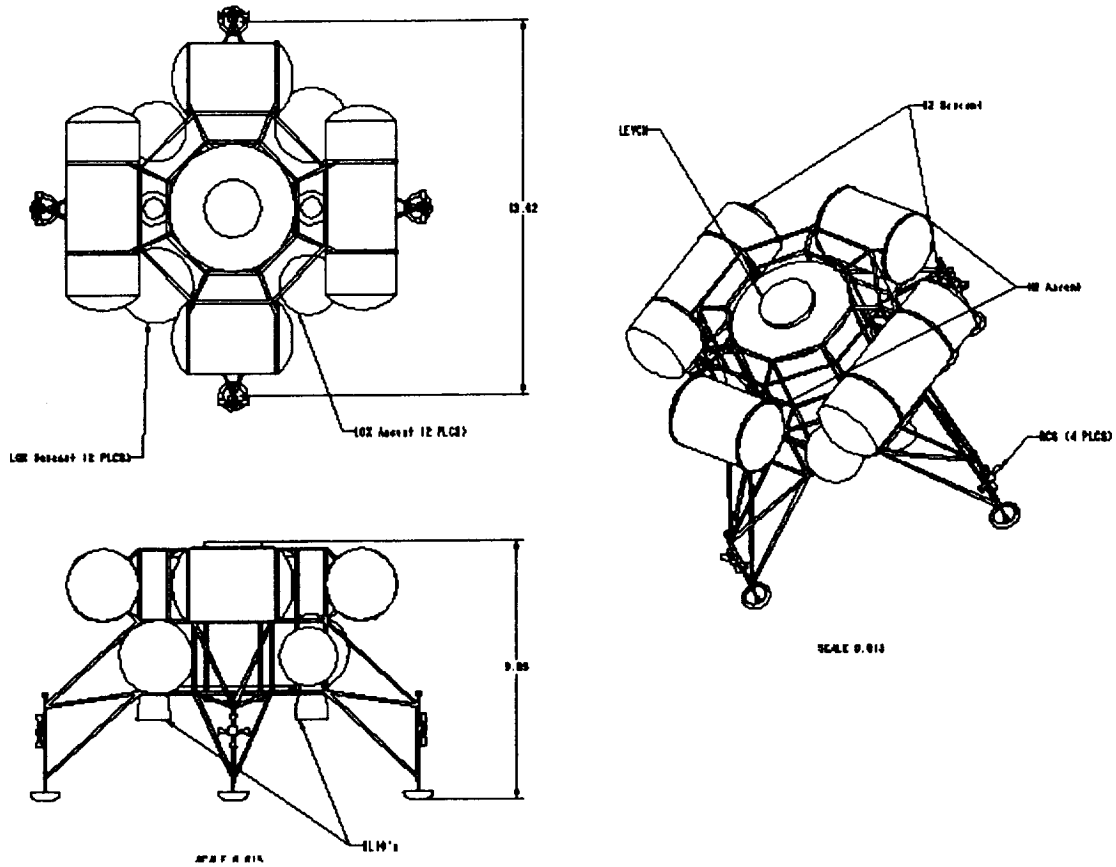


Figure 3.7 LEV Configuration



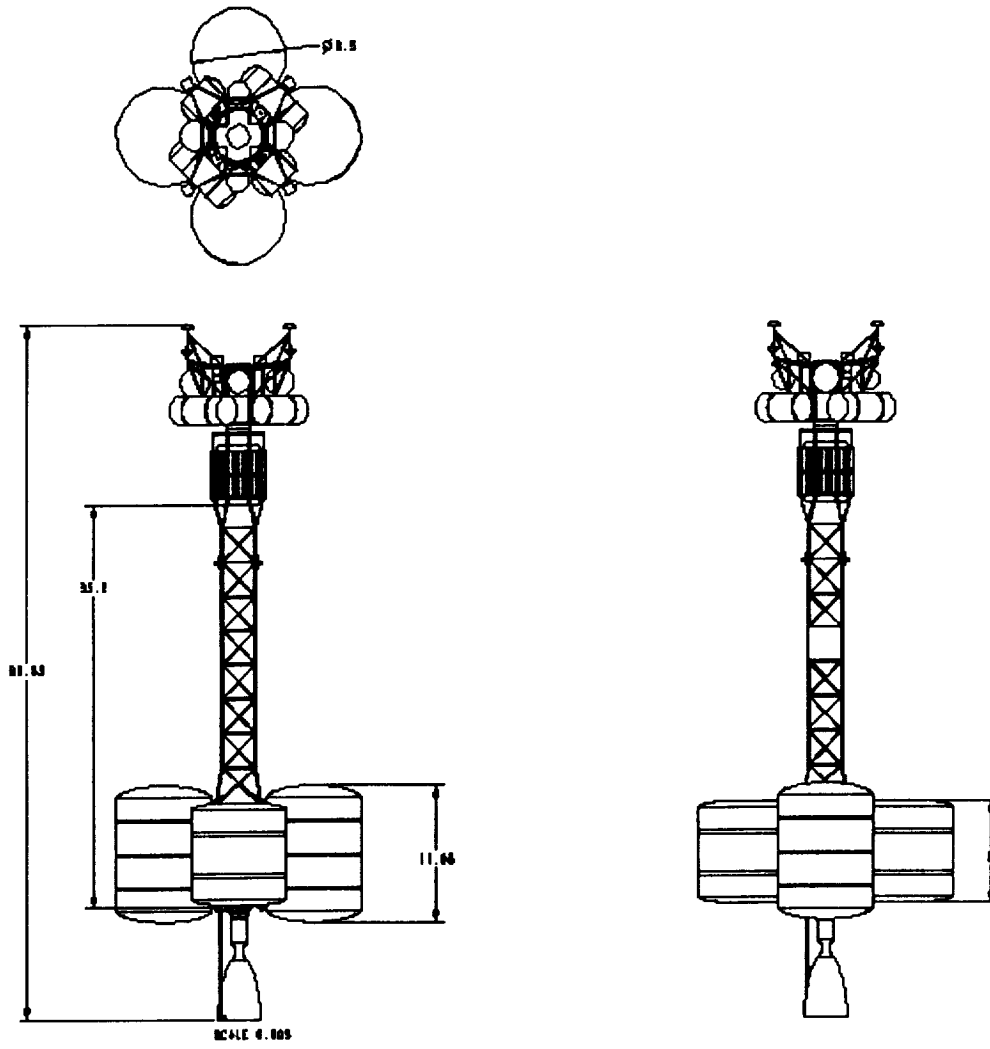


Figure 3.8 LTV Configuration

Component	Mass (mT)	
Truss	3.75	
Crew Module	9.95	
Power	1.746	
Prim.Prop.	.344	
Dry Tanks	1.977	
<b>Total Dry</b>	<b>17.84</b>	
<b>Fuel</b>		
<b>Burn</b>	<b>LH2</b>	<b>LOX</b>
Xfer from SSF	.028	.139
Descent	3.6	18.0
Ascent	2.12	10.6
Xfer to SSF	.009	.044
RCS	.48 (Hydrazine)	
<b>Total Fuel</b>	<b>5.76</b>	<b>28.78</b>

Table 3.1 LEV Masses

Component	Mass(mT)
Truss	5.5
Crew Mod	10.068
Power	1.345
Prim.Prop.	13
RCS	.692
Dry Tanks	14.367
<b>Total Dry</b>	<b>44.97</b>
<b>Fuel</b>	
<b>Burn</b>	<b>LH2</b>
TLI	78.2
LOI	19.99
TEI	12.39
EOC	26.58
RCS	2.07 (Storable)
<b>Total Fuel</b>	<b>137.17</b>

Table 3.2 LTV Masses

### 3.5 Vibration

Vibrational analysis consisted of the analysis of the LTV truss only. Because of the unusually long length of this truss, it was determined that this truss would be the most sensitive to vibrations out of all the LTS structures. The analysis involved the determination of the frequency, deformation, and maximum displacement for the first three

modes of vibration. The results are contained in Figures 3.9, 3.10, and 3.11.

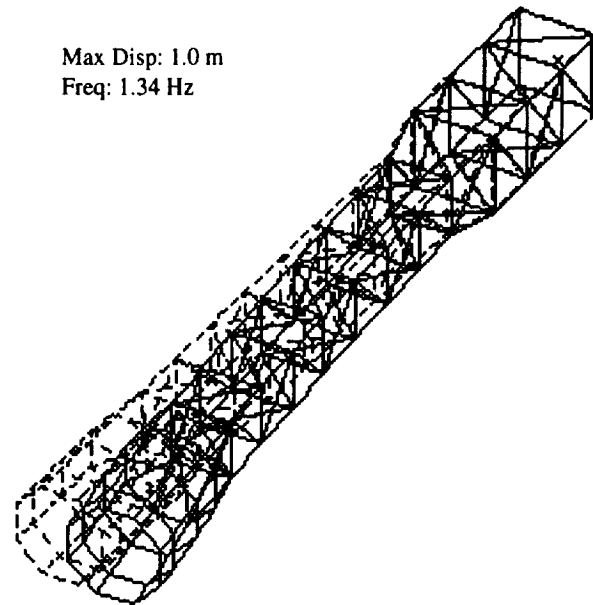


Figure 3.9 Mode 1 Vibration

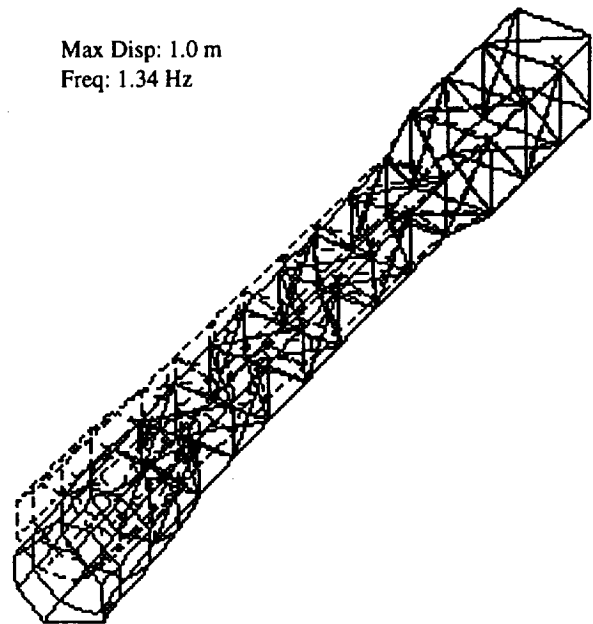
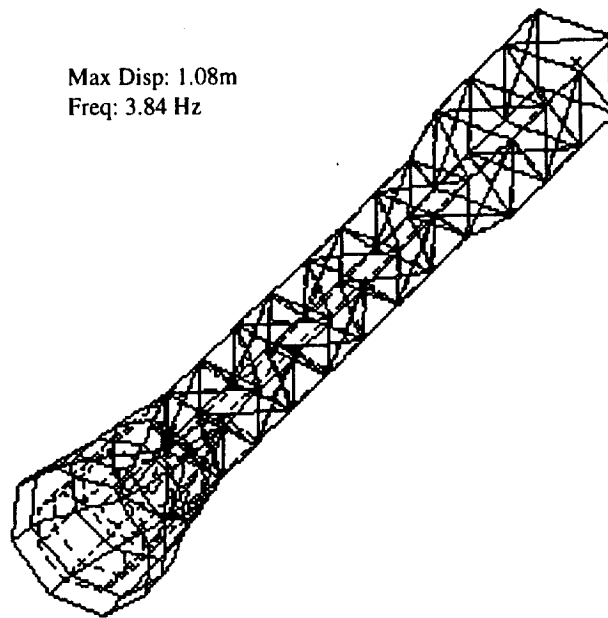


Figure 3.10 Mode 2 Vibration



**Figure 3.11 Mode 3 Vibration**

Three modes of vibration were checked using the I-DEAS solid modeling program. The results were within the structures tolerance levels so at maximum acceleration and deceleration the structure could withstand the vibrational stresses.

## 4.0 ORBITAL MECHANICS

### 4.1 Introduction

The goal of the orbital mechanics discipline is to determine the orbits and trajectories necessary to accomplish the mission of the LTS. This includes selecting orbit modes, determining trajectories between the Earth and Moon, planning the Lunar descent and ascent, coordinating Earth orbit activities, and preparing abort scenarios. In conjunction with the mission statement, emphasis was placed on minimizing propulsion requirements in order to maximize cost efficiency.

### 4.2 Orbit Mode Selections

The goal in selecting orbit modes is essentially to determine which modes are the most feasible according to certain mission parameters such as safety, cost effectiveness, and weight limitations. A brief synopsis of available options for orbit modes will be presented.

### 4.2.1 Earth Orbit Modes

To accomplish its mission, the LTV must be placed in a specific position at a specific time in LEO in order to perform a TLI burn. The most practical and efficient technique for Earth departure is launching the transfer vehicle(s) into circular parking orbits prior to injection. These parking orbits allow greater mission flexibility by providing: (1) Sufficient time for final on-board and ground checkouts before injection, (2) Injection capability any time of the month, twice a day, and (3) The same ascent and injection trajectory profile for any mission. The only disadvantage to parking orbits are the increased requirements for tracking and communications, however this problem will be minimized as more ground tracking facilities become operational in the future.

There are two basic launch techniques that can be used to obtain launch frequencies, direct and indirect ascents. In the direct launch technique, the LTV arrives directly at its appointed TLI time and position from launch. This method solves the timing problem on the ground prior to launch, but only allows launch windows of a few minutes. An indirect ascent involves launching the LTV into LEO at any time and solving the timing problem while in orbit. This option involves longer launch windows, but also requires additional propulsive burns in orbit. Since the mission statement assumes rendezvous with SSF prior to injection, the indirect launch scenario will be used.

Prior to injection, the LTV will maneuver into the appropriate parking orbit. The required change in velocity ( $\Delta V$ ) needed for TLI is a function of a number of parameters including Earth orbit inclination, orbit altitude, and trans-Earth trajectory inclination, to name a few. Once the particular mission has been planned, an optimum configuration for the LTS voyage can be determined, and the required  $\Delta V$  necessary to accomplish the mission can be calculated.

### 4.2.2 Lunar Orbit Modes

As with Earth orbit modes, there are two choices for descent upon reaching Lunar orbit, direct and indirect descent. Direct descent involves a straight shot to the Lunar surface directly from the trans-Lunar orbit. In this case, the entire space vehicle becomes a multipurpose landing module. This method is the least complex, since it avoids orbital rendezvous with a LTV prior to Earth departure. The major disadvantage of this option is the requirement of lifting off more weight from the Lunar surface upon departure for Earth. However, this scenario is ideal for unpowered cargo or probe missions that will require little or no lift-off capabilities.

The second orbit mode involves injecting the LTV into a Lunar satellite orbit upon arrival. Next, the landing module is separated from the LTV for descent to the Moon's surface. The LEV is landed on the Lunar surface, and later launched to rendezvous with the LTV. This approach presents smaller fuel requirements, since less weight needs to be lifted off from the Moon's surface, however it limits landing sites to low latitudes.

### 4.3 Interplanetary Trajectories

#### 4.3.1 Earth Departure

Interplanetary trajectory analysis begins with looking at the parameter requirements for Earth departure. The Earth-Moon distance has been chosen as a mean of 56 Earth radii. The Earth injection altitude corresponds to 250km (150 miles), and the Lunar altitude corresponds to 185km (111 miles). For piloted missions, it is desirable to limit the exposure any astronauts would have to harmful space radiation, therefore one of the mission priorities is to minimize flight times to and from the Moon. Also, in order to maximize the cost efficiency of the mission, the required delta Vs will be minimized.

##### 4.3.1.1 Earth Departure Requirements

Figure 4.1 shows our Earth departure configuration on a translunar plane inclined at an angle to the Moon orbital plane,  $i_a$ , which is 60 degrees. The inclination of the Moon orbital plane to the Earth equatorial plane,  $i_b$ , is 28 degrees. It is assumed to be constant, neglecting the rate of nodal regression due to the Earth's oblateness. Also constant is  $i_c$ , the inclination angle of the parking orbit, at 30 degrees. The Moon lead angle,  $f$ , is measured at 37 degrees. In order to minimize the maneuvering capability of delta V and maximize the launch frequency and tolerance, the angle from the ascending node of the Moon orbital plane to the intersection of the parking orbit,  $i_d$ , is measured at -65 degrees. According to NASA studies, an optimum trajectory can be achieved at injection with a prior parking orbit. As such, the LTV will perform its TLI burn with a maneuver from the initial parking orbit altitude of 425 km (255 miles). In order to satisfy certain mission constraints such as flight time, missed distance, and Lunar approach orbital orientation, an optimum configuration for the propulsion system will have to be determined to meet the mission statement. This will be discussed in the next section.

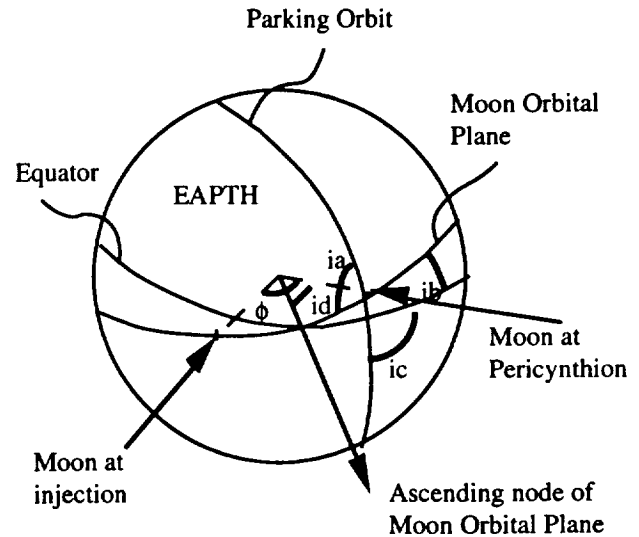


Figure 4.1 Earth Departure

##### 4.3.1.2 Propulsion System Requirements

To determine the propulsion system requirements for Earth departure, it is necessary to optimize a set of parameters: injection velocity,  $V$ ; injection position,  $j$ ; flight path angle,  $g$ ; and change in injection position,  $\Delta j$ . The injection position is achieved by an initial parking orbit. To minimize energy requirements for departure, the flight path angle has to be in the range from 2 degrees to 7 degrees. Within this range of operation, the delta V requirement is also minimized. For a maneuver at which the initial parking altitude begins at 425 km (255 miles), an optimum configuration includes a thrust-to-weight ratio of 0.15, and a specific impulse of 915 seconds. With the above figures, the total flight time is minimized at approximately 68 hours, and a required delta V of 3.1 km/s to escape the Earth's gravitational attraction.

#### 4.3.2 Earth-Moon Transfer

##### 4.3.2.1 Trans-Lunar Injection Conditions

Trans-Lunar trajectory depicts the passage from the Earth to the Moon. Figure 4.2 shows the configuration for the TLI phase of the mission. The Earth-Moon distance is assumed to be 56 Earth radii, and the injection altitude,  $h$ , is measured at 250km (150 miles). For most piloted Lunar missions, circumlunar trajectories generally describe the outbound passage and the return passage trajectories. Upon TLI phase, the LTV is injected with a velocity of 10.9 km/s, and flight path angle,  $g$ , of 5 degrees. The injection position is defined by  $j$  equal to 20 degrees, with a Moon lead angle,  $f$ , of 37 degrees.  $\Delta j$  denotes the magnitude of the change in injection position prior to injection.

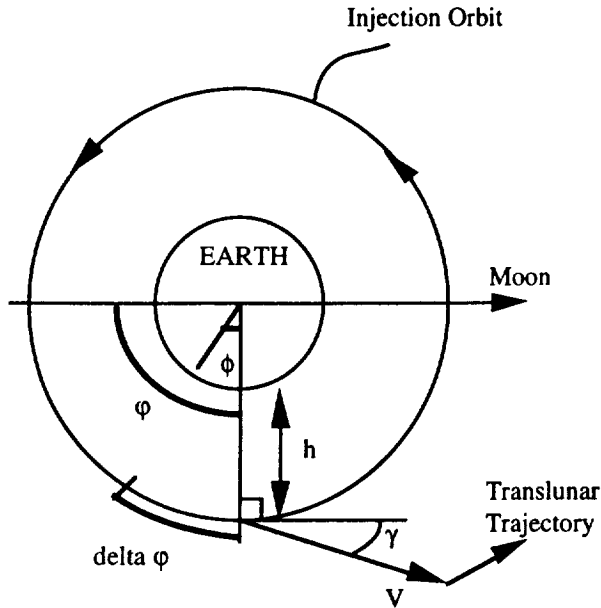


**Figure 4.2** Trans-Lunar Injection

The angle between the Lunar orbit and the Moon orbital plane,  $i_e$ , is 5 degrees, and the inclination of the Earth-Moon line and the descending node of the Lunar orbit,  $i_f$ , is 60 degrees (see Figure 4.3). The Lunar plane orientation and the inclination of the trajectory plane at arrival time are determined by the measurements of  $i_e$  and  $i_f$ .

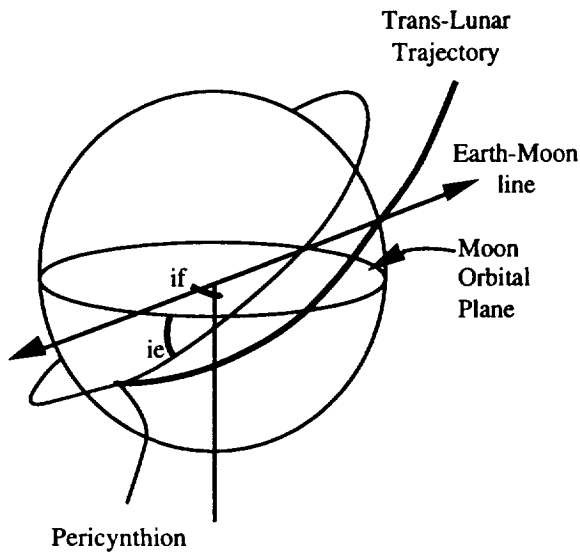


**Figure 4.3** Trans-Lunar Trajectory

The orientation of the trans-Lunar plane to the Moon orbital plane,  $i_g$ , is 60 degrees (see Figure 4.4). The pericyynthion altitude for trans-Lunar trajectory is 185km (111 miles), and

the time of flight from injection to pericynthion altitude is minimized at 68 hours. The TLI burn requires a delta V of 3.1 km/s to escape Earth's realm, and LOI requires a delta V of 1.1 km/s.

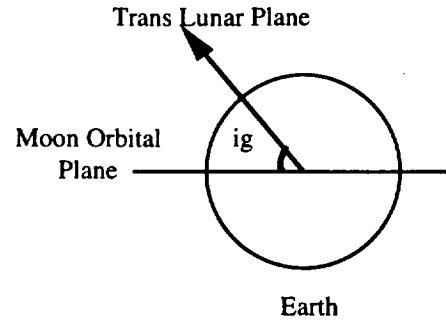


**Figure 4.4** Earth Departure

### 4.3.3 Lunar Orbit Determination

#### 4.3.3.1 Maneuvers between Lunar Orbits and Transfer Trajectories

In order to establish the delta V requirements for entry into Lunar orbits from trans-Lunar trajectories, and to inject into trans-Earth trajectories from Lunar orbits, it is necessary to look at entry and departure maneuvers between Lunar orbits and transfer trajectories. Figure 4.5 shows the maneuvers between Lunar orbits and transfer trajectories. The LTS mission requires a complicated and variable thrust schedule. As such, the orbital mechanics aspect of the transfer trajectories is based on the assumption that the entire transfer maneuver is conducted on the trans-Lunar trajectory plane and the trans-Earth trajectory plane, and that the propulsive thrust vector is constantly parallel to the velocity vector. For a Lunar orbital entry at a Lunar orbital altitude of 185km (111 miles), the delta V requirement is 1.1 km/s. Similarly for a Lunar orbital departure from the same Lunar orbital altitude, the delta V requirement is also 1.1 km/s. In these calculations, the off-nominal effects during entry maneuver are neglected.

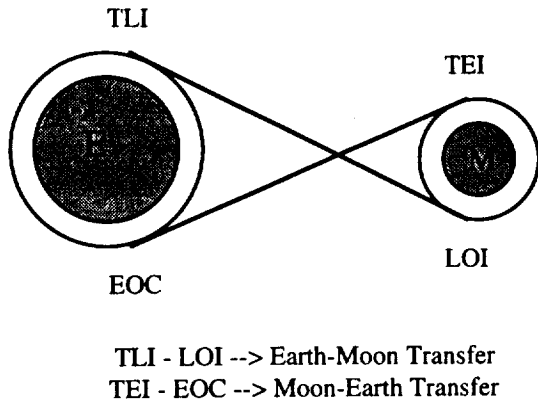


Figure 4.5 Maneuvers between Orbits

### 4.3.4 Moon-Earth Transfer

#### 4.3.4.1 Trans-Earth Injection Conditions

Figure 4.6 shows the configuration for the trans-Earth trajectory phase of the mission. After ascending from the Lunar surface, the LTV is placed into a circular parking orbit around the Moon. The Lunar orbit altitude for TEI trajectory is 185km (111 miles), with a flight path angle,  $\gamma$ , of zero degrees. The inclination of the parking orbit to the Moon orbital plane,  $i_j$ , is 5 degrees. The angle between the parking orbit plane and the Moon orbital plane,  $i_k$ , is 60 degrees, measured positively eastward from the Earth-Moon line to the descending node of the parking orbit. The central angle for the injection into the trans-Earth trajectory,  $i_l$ , is 50 degrees and is measured toward north from the descending node of the parking orbit. Both  $i_j$  and  $i_k$  determine the orientation of the circular Lunar orbit, and the position of the LTV is specified by the radius of the Lunar orbit and the measurement of the central angle. The injection position,  $\psi$ , is measured at -10 degrees, with an injection velocity of 1.2 km/s.

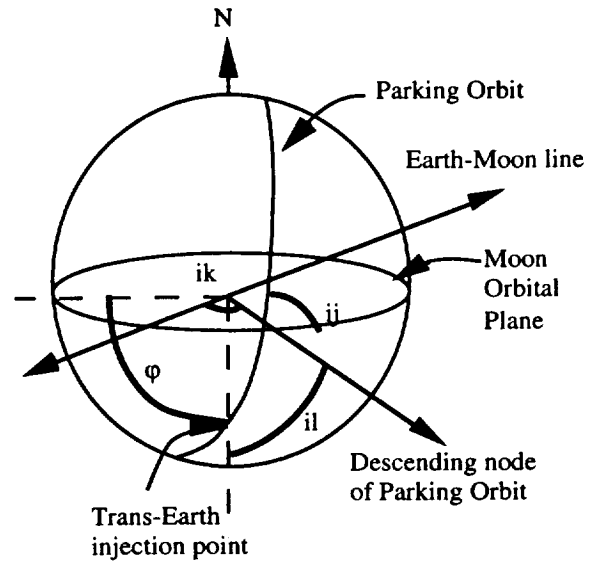


Figure 4.6 Lunar Departure

The return inclination of the trans-Earth trajectory to the Moon orbital plane,  $i_h$ , is defined at 180 degrees (see Figure 4.7). The delta V requirement for the Earth return leg is 1.1 km/s, and flight time for the trans-Earth trajectory is approximately 50 hours. The decrease in these values from the trans-Lunar trajectory reflects the lesser gravitational effect of the Moon compared to the Earth. These values are minimized for the Moon-Earth transfer profile.

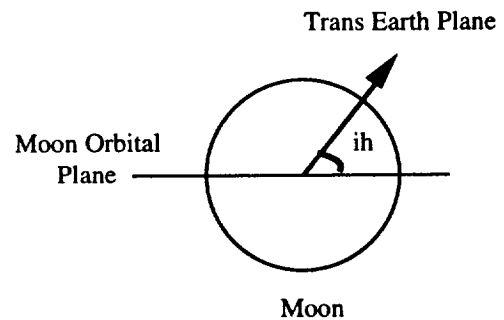


Figure 4.7 Trans-Earth Injection

### 4.3.5 Earth Return

#### 4.3.5.1 Earth Orbit Capture

For Earth return, the mission statement requires arrival in LEO from the trans-Earth trajectory for rendezvous with SSF. Upon entering the EOC phase, the kinetic energy of the LTV must be reduced to that of a circular Earth orbit by application of NTR thrust. The NTR deceleration technique

involves a direct reduction of the speed of the approaching LEV to that of an Earth orbital speed, along with a propulsive burn. Fuel requirements for EOC can be obtained by assuming the trans-Earth trajectory of the LTV as that of a hyperbolic profile, and that the required velocity reduction occurs impulsively. In the above configuration, the delta V requirement for the EOC phase is minimized at 3 km/s.

#### 4.3.5.2 Orbital Circularization

After executing the EOC phase, the orbital mechanics aspect of the mission calls for an orbital circularization phase. The LTV subsequently performs an orbital circularization in a low Earth satellite orbit, with a delta V of 310 m/s. In order for the LTV to execute a phasing with SSF to an orbit within 25km (15 miles), a delta V of 10 m/s is required. The final phase of the mission entails a docking of the LEV with SSF.

#### 4.4 Lunar Ascent / Descent Trajectories

While the LTV is in orbit around the Moon, the LEV must be able to descend to the Lunar surface to deliver the crew or cargo. A piloted mission also requires the LEV to ascend from the Lunar surface to return the crew to the orbiting LTV.

##### 4.4.1 Descent to the Lunar Surface

Once the LTV is in Lunar orbit at 185km (111 miles) from the Lunar surface, preparations are made for descent to the Moon's surface. Lunar descent is performed in two stages, a braking from the translunar hyperbolic trajectory to circular or elliptical Lunar orbits, and a subsequent descent to the Lunar surface by the LEV. Figure 4.8 depicts a Lunar descent profile. After separation from the LTV, the LEV experiences a retrothrust and enters the deorbit phase. Delta V required in deorbit is approximately 10 m/s. The LEV follows the deorbit coast, and performs orbital braking at an altitude of 20km (12 miles). When the LEV is 300 meters from the Lunar surface, the lateral velocity is reduced to zero, and the lander rotates such that the thrust vector is pitched over for hovering. The final descent phase entails a maneuvering capability of hovering and translation. Maximum vertical landing velocity on the Lunar surface is 3.1 m/s (10.2 ft/s); maximum horizontal velocity is 1.2 m/s (3.94 ft/s). Delta V required for Lunar descent is 2 km/s. Considering a thrust-to-weight ratio of 1.2, orbital braking at 20km (12 miles), terminal altitude at 300 meters, and a specific impulse of 450 seconds, the descent range is 90 degrees. Descent time to the Lunar surface is approximately 17 minutes.

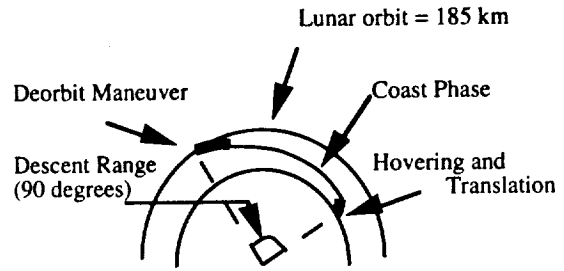


Figure 4.8 Lunar Descent

##### 4.4.2 Hovering and Translation

This section considers the propellant requirements and the optimum conditions for translation, vertical descent from hover, and hovering. After the final descent phase, the LEV is capable of hovering and translation. In order to achieve its mission, the LEV propulsion system must provide a constant acceleration of propulsive flow. Small mass ratio requirements for hovering and simplicity in analysis are the two most important reasons for a constant acceleration analysis of propulsive flow. In the motion profile of translation, vertical descent from hover, and hovering, a constant engine thrust with steady propellant flow rate is required. Vertical landing on the Lunar surface is 3.1 m/s, and horizontal maneuvering velocity is approximately 1.2 m/s.

##### 4.4.3 Ascent from the Lunar Surface

Ascent from the surface of the Moon to Lunar orbit requires three phases: ascent, coast, and injection. Figure 4.9 shows the profile of a Lunar ascent, which is very similar to the descent profile. The ascent phase burnout altitude is 20km (12 miles). Following that is a transfer coast phase to the Lunar orbit. The lunar ascent phase is completed with a propulsive injection into the Lunar parking orbit at an altitude of 185km (111 miles), where the LEV performs a rendezvous with the orbiting LTV. Delta V required for Lunar ascent is 1.9 km/s. Considering the thrust-to-weight ratio, burnout altitude, and specific impulse, the ascent range is found to be 180 degrees. Ascent time from the Lunar surface is approximately 10 minutes.

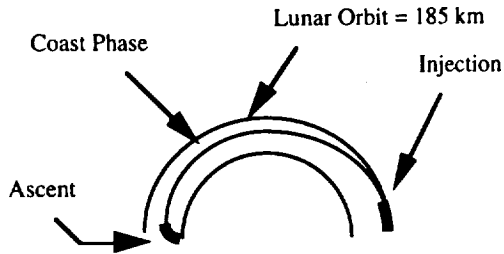


Figure 4.9 Lunar Ascent

## 4.5 Earth Orbit Activities

### 4.5.1 Orbit Options

While the LTV is in orbit around the Earth, it will be necessary to dock with SSF for such purposes as transferring crew and cargo, or for maintenance. Since safety limitations require the LTV to maintain a distance of at least 10km (6 miles) from SSF during all other times while in orbit, it is necessary to find an adequate orbit and accompanying docking procedure for when rendezvous with SSF is performed. Three different options were considered.

The first option places the LTV in the same orbit as SSF, but at a different orbital position. This would give the effect of the LTV "following" SSF around the Earth. One major disadvantage of this option is the fact that it would require the LTV to perform two in-plane orbit changes to dock with SSF, one to put it at a different orbital radius to "catch up" with SSF, and one to bring it back to SSF. Plus, this would cause SSF to pass through the trail of radioactive matter left by the NTR.

A second option is to place the LTV in an orbit at the same altitude as SSF, but in a different orbital plane. One of the biggest disadvantages is the high delta V required to change planes. For example, a one degree plane change at the orbital radius of SSF would require a delta V of about 135 m/s. The other disadvantage is that it would either require precise timing upon EOC to synchronize the LTV with SSF, or two in-plane orbit changes would still be required to align the two orbiting bodies.

The last option is to place the LTV in a slightly higher orbit than SSF, but in the same orbital plane. This eliminates one of the in-plane orbit changes, requiring only one in order to rendezvous with SSF. However, difficulties in timing arise due to the difference in orbital periods at different orbital radii.

### 4.5.2 LTV and SSF Orbits

After considering all three options, the last one was chosen. In order to analyze this option in more detail, the following parameters were used.

Space Station Freedom:

Orbital altitude = 400km (240 miles)

Orbital period = 92.56 minutes

LTV Parking Orbit:

Orbital altitude = 425km (255 miles)

Orbital period = 93.07 minutes

LTV Hohmann Transfer between orbits:

Delta V = 14.1 m/s

Transfer time = 46.4 minutes

Possible every 11.7 days

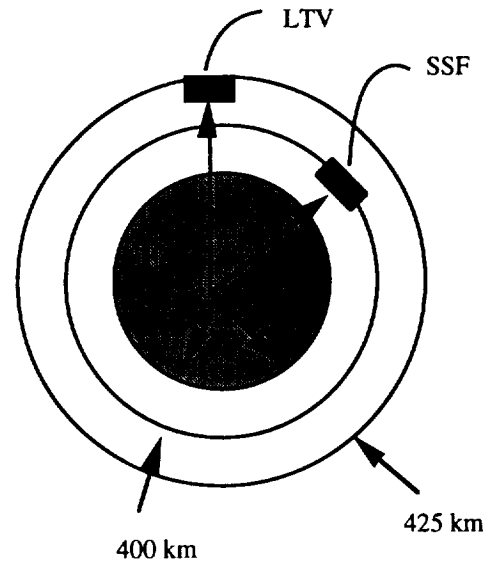


Figure 4.10 Earth Orbits

The altitude of the LTV parking orbit was chosen to insure the safety factor of at least 10km (6 miles) separation between the LTV and SSF. A slightly larger margin, 25km (15 miles), was used to increase the difference in orbital periods, since a larger difference improves the frequency of performing a Hohmann transfer. At this altitude, a Hohmann transfer could be performed approximately once every 11.7 days. This would require starting the transfer when the angle between the two orbits is approximately zero. If a transfer is needed to be done at some other time, it would still be possible, however a higher delta V would be required to achieve the maneuver.



## 4.6 Abort Scenarios

In the case of an NTR failure, several scenarios had to be studied to plan for an abort. Figure 4.11 illustrates the four cases considered.

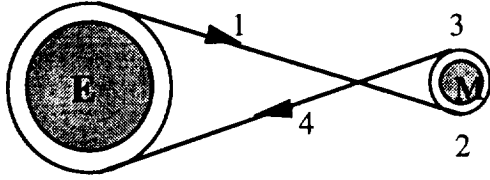


Figure 4.11 Abort Scenarios

1. Post-TLI / Pre-LOI stage. This case occurs after the trans-Lunar injection burn has been performed, but before the Lunar orbit insertion. The preferred abort scenario for this case is to disconnect the LEV from the LTV, orbit around the Moon utilizing Lunar gravity assist, and return to Earth. Upon arrival at Earth, the propulsive burn necessary to achieve LEO would be performed using the LEV.
2. Post-LOI / Pre-Ascent stage. This case is after the LTV has been placed in LLO, or after the LEV has descended to the Lunar surface, but before the ascent stage. If the crew has not yet descended, the abort scenario includes descent. Once on the Lunar surface, the crew can complete their mission, and then return to Earth in the LAM that will be available on the Moon.
3. Post-Ascent / Pre-TEI stage. Once the LEV has ascended in order to rendezvous with the LTV, it no longer is capable of landing on the Lunar surface again during that mission. If the TEI stage has not yet been completed, the LAM is remotely controlled to rendezvous with the LEV, and the crew transfer to the LAM to return to Earth.
4. Post-TEI / Pre-EOC stage. The last abort scenario case considered occurs after the LTV has performed the TEI burn but before insertion into Earth orbit. There is no alternate plan for this case in the event of an abort; it is considered an acceptable risk of the mission.

For the fourth case, three options were considered: acceptable risk, aerobrake the LEV to the Earth's surface, and equip the LTV with a ballistic capsule to return the crew to Earth. For either the case of the aerobrake or the ballistic capsule, a delta V would be required to change the trajectory of the vehicle from a hyperbolic orbit past the Earth to a trajectory that would send it to the Earth's surface. This delta V is approximately 3 km/s, which would result in a mass penalty of over 100 metric tons in fuel. Upon examining the factors involved, the only realistic option was

to consider an NTR failure at this stage an acceptable risk for the crew.

## 4.7 Delta V Requirements

Table 4.1 shows a summary of the delta Vs required for each stage of the LTS mission. The total mission delta V required is approximately 12.5 km/s, and may vary slightly depending on such details as how many times the LTV docks with SSF while in LEO and if a Hohmann transfer is used or not.

Phase	Delta V (m/s)
Trans-Lunar injection	3100
Mid-course correction (Earth-Moon)	10
Lunar orbit insertion	1100
Lunar descent	2000
Lunar ascent	1900
Trans-Earth injection	1100
Mid-course correction (Moon-Earth)	10
Earth orbit capture	3000
Circularization	300
Docking with SSF (minimum)	14
<b>Total</b>	<b>12,534</b>

Table 4.1 Delta V Table

## 4.8 Conclusion

According to mission constraints and parameters, the orbital mechanics of the LTS mission have been determined in order to maximize efficiency, minimize cost, and ensure the safety of each mission. The scenarios are based on pre-established assumptions and priorities for the given mission.

## 5.0 PROPULSION

### 5.1 Introduction

The responsibilities of the propulsion group include the selection of primary propulsion and Reaction Control Systems (RCS) for the LTV and LEV, as well as the determination of fuel requirements for the various mission stages. The evaluation of these systems took place over the course of one academic year and involved research and analysis of many competing propulsion systems. Several iterations and design changes occurred before the final propulsion configurations were obtained.

The following sections detail the selection of the LTV and LEV primary propulsion and Reaction Control Systems. Throughout the design process an effort was made by the propulsion discipline to justify its design selections through quantitative comparisons with other existing propulsion options. Final selection of the various LTS propulsive systems was made by judging the extent to which each system was compatible with the design group's mission statement. The members of the discipline feel that their efforts resulted in LTS propulsive systems which are indeed safe, reusable, economical and practical to interface with the rest of the LTS hardware.

## 5.2 LTV Primary Propulsion

The primary propulsion system for the LTV is a Nuclear Thermal Rocket (NTR). The decision to pursue the development of an NTR was made after determining that the fuel requirements of an all cryogenic LTV were too massive. By using an NTR, the LTV was able to be designed to fulfill the original mission goal of providing a robust transportation system, capable of supporting a permanent Lunar outpost.

### 5.2.1 Nuclear Thermal Rockets

The use of a nuclear thermal rocket for space vehicle propulsion is certainly not a new concept. In fact, NTR propulsion has a history spanning the past 38 years. In 1955, the U.S. Air Force and the Atomic Energy Commission (AEC) began the Rover Project. Rover was directed towards the research and initial development of nuclear reactor technology for single stage Intercontinental Ballistic Missile propulsion.<sup>5.1</sup> Several reactors were built and tested during this program in a series of designs denoted Kiwi. In 1958, the newly formed National Aeronautics and Space Administration (NASA) replaced the Air Force as partners with the AEC as primary developer of the nuclear propulsion effort. Then, in 1959, a new program began that was to expand on the successes of the Rover Project. This new program was known as the Nuclear Engine for Rocket Vehicle Application, or more succinctly, NERVA.

The NERVA program was directed towards the design and testing of a complete nuclear flight engine. By building upon the knowledge acquired through the Rover Project research, NERVA strove to develop the necessary components of an NTR and validate the concept through extensive component and full scale engine testing. In 1961, contracts were negotiated with Westinghouse and Aerojet General to build the reactor and system components, respectively. Component testing took place at Los Alamos

Scientific Laboratory with complete system testing at the nuclear test facility at Jackass Flats, Nevada.

Originally, the NERVA engine was a candidate for the upper stage of the Apollo program,<sup>5.2</sup> but the successes of an all chemical system relegated the nuclear rocket to the nonspecific role of a propulsion system for interplanetary travel. Work towards this goal continued until 1973, when the changing post-Apollo priorities of the nation shifted away from space exploration and the NERVA program was canceled. At its close, the combined Rover and NERVA programs had overseen the construction and testing of twenty reactors and two complete flight engines.<sup>5.1</sup> More importantly, these programs generated a data base that is again being reviewed by NASA, as the agency and the nation once again look towards the future of space exploration.

### 5.2.2 NTR Fundamentals

A nuclear thermal rocket uses a single propellant rather than the fuel-oxidizer combination of traditional chemical propulsion. An NTR replaces the combustion cycle of a chemical rocket with a simple heat transfer process between the reactor core and the propellant. This is accomplished by passing the propellant through a hot nuclear core, where it is heated to temperatures in excess of 2500 °K. Following this heat transfer, the propellant is expanded through the rocket nozzle which accelerates the flow to supersonic exit velocities. It is this expansion process which provides the thrust generated by an NTR.

Since specific impulse (Isp) is inversely proportional to molecular weight, fuel selection for the NTR is critical. For optimum performance, hydrogen was chosen as the propellant for the NERVA flight engine due to its low molecular weight and high specific heat. It is the use of hydrogen as the single propellant which allows an NTR to surpass the Isp of chemical rockets by a factor of two. To compare, a conventional liquid hydrogen/liquid oxygen chemical system has an average Isp of less than 500 seconds, while the NERVA flight engines demonstrated Isp values in excess of 800 seconds with a thrust of 333,600N (75,000 lbf).<sup>5.1</sup> Dr. S.K. Borowski, of the Nuclear Propulsion Office at NASA Lewis Research Center, estimates that with the inclusion of current technology, the Isp values of a NERVA derived NTR will reach 925 seconds.<sup>5.3</sup>

### 5.2.3 NTR versus Cryogenic Systems

It is the two-fold advantage in Isp which enables an NTR to use substantially less fuel than a chemical system. This is

due to the fact that the fuel mass flow rate at a specified thrust level is inversely proportional to  $I_{sp}$  as evident in equation 5.1.

$$\dot{m} = \frac{T}{g_0 I_{sp}} \quad (5.1)$$

Thus, the fuel mass flow rate required to generate a specific level of thrust is much less for an NTR than it is for a chemical system. This results in a significant reduction in the fuel required for the LTV to perform a round trip mission to the Moon. A comparison of the piloted LTV scenario is displayed in Figure 5.1.

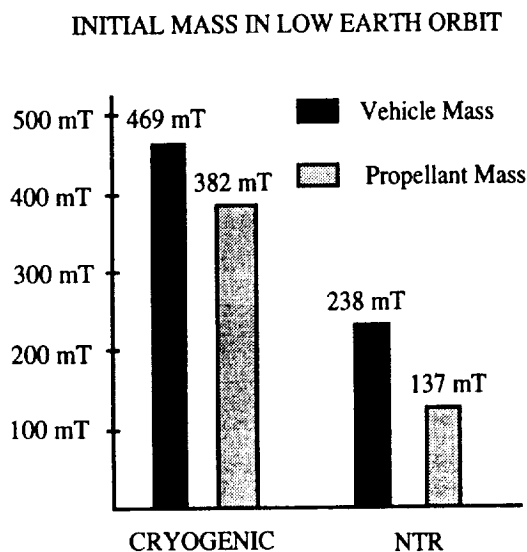


**Figure 5.1**  
Comparison of Vehicle & Fuel Masses.

As can be seen in Figure 5.1, the use of the NTR results in a 50.7% reduction in the total vehicle mass. This translates to a 64% reduction in the propellant mass, a savings of 245 t. In steady state operation, this represents significant savings with respect to mission costs. If one estimates the launch costs for the proposed Heavy Lift Launch Vehicle at \$1000 per kilogram, the monetary savings generated through the use of the NTR surpass \$230 million dollars per launch over a comparable chemical system. The reduction of propellant mass requirements as well as mission costs are the driving forces behind the decision to employ a nuclear propulsion system for the LTV.

#### 5.2.4 NTR Specifications

Several proposals for nuclear thermal rocket engines exist. These include such conceptual designs as liquid core, plasma

core, and particle bed reactors. However, these designs are conceptual in nature with no prototype flight engines ever tested. As such, the development of a flight ready engine in time to meet mission initiation in the year 2005 would be difficult to achieve. For this reason, a modified version of the solid core NERVA flight engine is selected as the primary propulsion system for the LTV. It is estimated that a flight rated engine based on the NERVA design can be ready within six years.<sup>5.1</sup>

The NTR to be used on the LTV is an updated version of the NERVA flight engine that will be capable of an  $I_{sp}$  of 925 seconds and 333,600 N (75,000 lbf) of thrust. The engine components consist of the nuclear reactor, turbomachinery, fuel pumps and lines, exhaust nozzle, and internal shield. The total mass of the reactor and its subsystems is approximately 8.5t. A 4.5t external radiation shield is also included to attenuate the radiation dose that the crew module will experience. This brings the NTR component mass to 13t.<sup>5.4</sup> The internal and external radiation shielding are constructed of borated-aluminum-titanium-hydride (BATH). This shielding attenuates the neutron and gamma radiation emitted from the reactor. Hydrogen is the single propellant and is thermodynamically expanded in an Expander cycle, as represented in Figure 5.2.

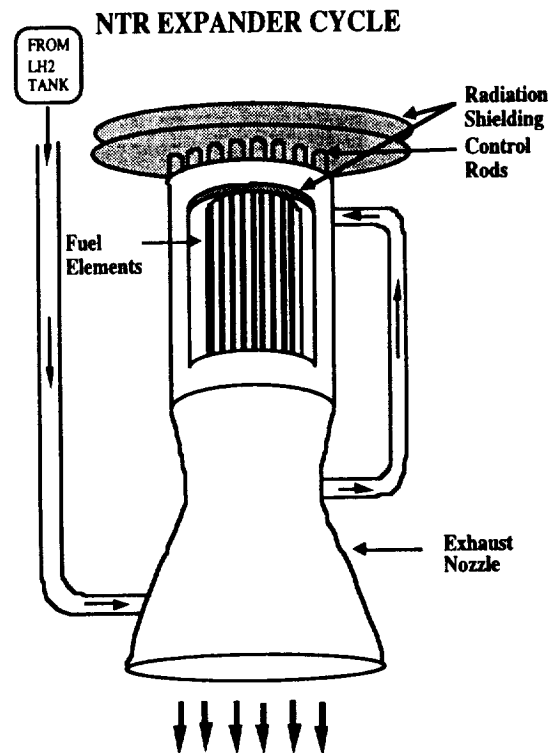


**Figure 5.2** NTR Operating Cycle

In the Expander cycle, LH2 is pumped from the fuel tanks down into the nozzle extension as indicated in Figure 5.2. It then passes through channels in the nozzle to cool the nozzle structure. Next, the hydrogen passes through coolant channels in the pressure vessel walls and into the upper portion of the reactor. Here, the LH2 cools the internal shield before being drawn off and routed through turbines which provide the work energy to operate the fuel pumps. By using the heated hydrogen propellant to run the turbomachinery, the NTR requires no external power source to maintain full power operation. Next, the LH2 is passed through the reactor core, where it is heated to 2500 °K (4500 °R). Finally, the hydrogen exits the exhaust nozzle at velocities in excess of 9,000 m/s, generating 333.600 N (75,000 lbf) of thrust.

A fully redundant system with dual turbopumps, fuel lines, and valves is incorporated into the design of the NTR. This full redundancy was found to increase the mass of the NTR by a mere 171 kg.<sup>5.4</sup> This modest mass penalty is deemed acceptable, in view of the criticality of engine restart with respect to the mission abort scenario, as defined by Mission Analysis.

### 5.2.5 NTR Operational Cycle

The operational cycle of the NTR begins with the rotation of the 16 actuator control drums indicated in Figure 5.2. The purpose of these control drums is to moderate the level of the reaction. This is accomplished by coating one half of a drum with a neutron absorbing material such as boron carbide, and the other side with a neutron reflective coating of beryllium. The reaction is begun by rotating the beryllium side toward the core, thus increasing the rate of the nuclear reaction. There exists a modest start-up transient of approximately 30 seconds. This is based on the original NERVA design criteria that the reactor be able to withstand the thermal loads associated with a transient of 85 °K/s.<sup>5.1</sup> The propulsive burn is terminated by rotating the control drums such that the boron carbide side once again faces the core and absorbs the neutrons emitted from the fuel elements.

Following the main burn, a cool-down burn must be performed to bring the reactor temperatures down to adequate levels. The cool-down transient is more difficult to define than the main burn transient. The cool-down consists of flushing hydrogen through the NTR to remove the heat that is built up during the burn. The removal of the latent heat built up within the NTR structure takes place within a few minutes at an approximate thrust level of 25,000 N (5600 lbf). However, there continues to be radiation heating due to the longer time required for the nuclear reaction to come

to a stop. To dissipate this radiation heating, the NTR must send short bursts of hydrogen into the engine, repeated over the span of a few hours. The thrust generated by these bursts is nominal, only 58 N (13 lbf) and is experienced for only brief periods.<sup>5.6</sup>

### 5.2.6 Nuclear Fuel Elements

The reactor core itself is composed of a cluster of hexagonal fuel rods. Each of these fuel rods has 19 coolant channels, 2.5 mm in diameter, through which the LH2 flows.<sup>5.1</sup> The fuel rods themselves are composed of fine particles of the fissionable element uranium ( $U^{235}$ ) suspended in a carbide compound. In the original NERVA engine, the uranium-carbide (UC) fuel was shaped into pellets and then suspended in a matrix material. A carbon-based matrix material is used because of its low neutron absorption as well as its high melting point, low density, and high strength at high temperatures.<sup>5.5</sup>

However, carbon reacts with hot hydrogen to corrode the fuel matrix and form methane and other hydrocarbons. This corrosion can seriously degrade the reactor's performance as well as shorten the operational lifetime due to the carbon loss from the matrix. This process can be attenuated by coating the matrix with a non-reactive material such as zirconium-carbide (ZrC). Eventually, cracks will form in the ZrC coating due to the repeated thermal cycling between shutdown and full power operation, at which time carbon mass loss will begin. With this inevitability in mind, a UC-ZrC composite fuel element was designed in which the reactive fuel is mixed with ZrC and dispersed throughout the carbon matrix in layers. In this design, once the outer ZrC coating is cracked, carbon will only be lost until the next layer of ZrC is reached. This is in contrast to the fuel particle design in which carbon loss would be indefinite due to the continuous carbon matrix. The two different fuel element concepts are illustrated in Figure 5.3.<sup>5.5</sup>

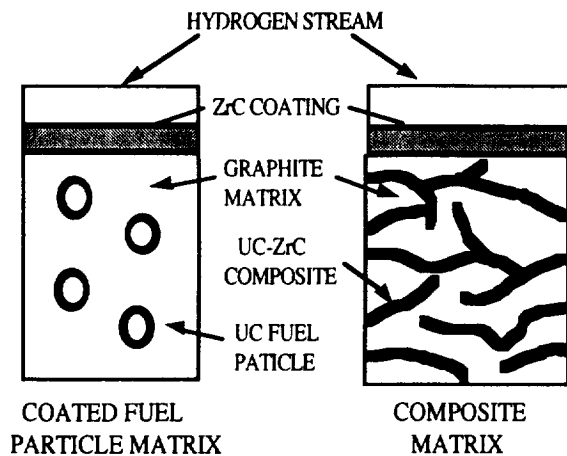


**Figure 5.3** Diagram of Two Fuel Elements

It is this composite matrix fuel element which is incorporated into the NTR flight engine due to its potential for increased resistance to hydrogen degradation and thus a longer NTR service life.

### 5.2.7 NTR Service Life

The dominant factor in the service life of the NTR is the burn endurance. Burn endurance is defined as the cumulative time that the NTR is engaged during any mission. The burn times for all primary propulsive burns have been calculated and are included in Table 5.1.

Mission Phase	Piloted Mission	Unpiloted Mission
TLI	35.16min	39.88min
LOI	9.05min	10.26min
TEI	5.15min	3.66min
EOI	10.82min	7.78min

**Table 5.1**  
Burn Times for Piloted & Unpiloted Missions

All calculations were done by relating total impulse ( $I_T$ ) to the thrust generated. Total impulse is defined as the integral of thrust with respect to time. If thrust can be assumed constant then  $I_T$  can be expressed as thrust times time. A second expression for total impulse is  $I_T = (I_{sp}) \cdot (m_p) \cdot (g_0)$ , where  $m_p$  is the mass of the propellant to be burned during that stage and  $g_0$  is the relative acceleration of gravity at Earth. Upon substitution, an expression for burn time can be obtained as follows:

$$t = \frac{I_{sp} m_p g_0}{T} \quad (5.2)$$

As was previously mentioned, there are transients in the thrust generation of the NTR. However, they are relatively small and can be neglected. Thus, the assumption of constant thrust for the NTR is a useful approximation for calculating burn times which can further be compared to those published in other baseline configurations. In this way, the analysis of the propellant requirements of the LTV can be further validated by comparing results with those of other independent sources. The values indicated in table 5.1 were compared with those of a baseline configuration for a fully reusable Lunar NTR proposed by Dr. Borowski.<sup>5.6</sup> The NTR burn times compare favorably with those of Dr. Borowski and thus justify the assumption of constant thrust.

The cumulative burn endurance of the NTR is approximately 60 minutes for both the piloted and unpiloted missions. Fuel element tests conducted under the NERVA program demonstrated a maximum burn endurance of 10 hours and 40 minutes before fuel element degradation becomes such that the NTR is no longer serviceable.<sup>5.3</sup> Based on this figure, the expected service life of the NTR will be on the order of five years (10 missions) before the effects of uranium mass loss and hydrogen degradation will require that the reactor be replaced.

### 5.2.8 End of Life NTR Disposal

The end of life disposal scenario is defined with two primary considerations in mind. First, the projected service life of the LTV crew module will exceed that of the NTR. As such, any disposal scenario will have to initiate in LEO, so that the LTV crew module can be removed. Second, it is undesirable to store the NTR in any sort of near-Earth disposal location such as a high Earth orbit. For these reasons, the most likely disposal scenario consists of placing the NTR in a long-term, stable, Solar circular orbit. Additionally, the NTR could be used as the primary propulsion system for either a Mars precursor mission or a deep space science probe.

At the end of the defined NTR service life of five years, the NTR will still be capable of producing useful amounts of thrust. This is based on the fact that the actual reactor life is 5.33 years, based on the NERVA test data. As such, the NTR will have enough fissionable uranium remaining in its fuel elements to provide the thrust necessary to propel itself to the final disposal orbit. The Solar circular orbit defined for the NTR is at 1.19 times the Earth-Sun radius at an angle of inclination of 2 degrees. This orbit is a non-Earth crossing orbit that is stable for well beyond one million

years and which can be obtained for the modest delta V requirement of 1250 seconds.<sup>5.6</sup>

Another unique alternative for NTR disposal is to use it as the primary propulsion system for a Mars precursor mission or a deep space probe. This is a particularly attractive disposal scenario as it can meet the propulsive requirements of a future science mission while removing the NTR from Earth orbit. This represents a best case disposal scenario.

### 5.3 LEV Primary Propulsion

While the NTR system on the LTV does an excellent job of shuttling between Earth orbit and Lunar orbit, a second vehicle, the LEV, is required to actually send people and material to the Lunar surface. Therefore, a primary propulsion system for the LEV must also be defined. Careful consideration of the primary propulsion system for the LEV is an important factor in controlling the initial mass in low earth orbit (IMLEO) of the LTS. This is due to the large extent to which Lunar ascent and descent fuel requirements, as well as LEV hardware masses, affect IMLEO. Fuel requirement analysis, aided by the use of a spreadsheet, see Appendix C, reveals that the addition of one kilogram in hardware to the piloted LEV increases IMLEO by six kilograms.

#### 5.3.1 System Requirements

Due to the difference in requirements between the landers of the piloted and unpiloted missions, the same primary propulsion system can not be used for both vehicles. In the piloted scenario, the propulsion system must be capable of landing 18.7 metric tons of dry mass and 12.7 metric tons of ascent fuel on the Lunar surface. The propulsion system will then be required to lift 18 metric tons of dry mass during Lunar ascent. The unpiloted mission descends with 58 metric tons of dry mass and requires no ascent propellant. Upon touchdown the difference in mass between the two missions is a full 27.3 metric tons, requiring the placement of a more robust main propulsion system on the unpiloted LEV.

#### 5.3.2 Engine Selection

RL10A-4 engines will be used as the primary propulsion system on both the piloted and cargo versions of the LEV. The other propulsion options available for use on the LEV are quite limited. Among these options are one other cryogenic system, several storable systems and a hybrid storable/cryogenic system.

Storable systems lend themselves well to two-stage LEV designs. In most scenarios currently under consideration, the descent stage utilizes a conventional cryogenic system, while the ascent stage relies on storable propellants. This is advantageous because a storable ascent stage has no boil-off.<sup>5.8</sup> Furthermore, the ascent stage fuel requirements are relatively small, and the lower Isp's of the storable system usually do not have a large impact on the overall LEV mass. The design under discussion here, however, utilizes a single stage LEV. For this reason, storable system options are eliminated on the basis of their Isp values. The use of storable systems on the LEV would increase the LEV fuel requirement by 60% over a comparable cryogenic system. This increased LEV fuel requirement would also have a large affect on the fuel requirement of the LTV.

Another option for the LEV primary propulsion system is a hybrid LOX/CH<sub>4</sub> system. This system does not fit the LTS mission scenario. Although it is capable of 1.5 times the thrust of the new generation RL10, a LOX/CH<sub>4</sub> engine masses 100 kg more than an RL10 engine. Furthermore, the Isp values of the hybrid LOX/CH<sub>4</sub> system are considerably less than that of the RL10.<sup>5.9</sup> Although the RL10 and the hybrid system are both capable of delivering the crewed mission to the Lunar surface with one engine, it is thought necessary that the crewed LEV have two thrusters in case of an engine-out occurrence. However, placing two massive hybrid thrusters on the LEV would be an unnecessary mass penalty when the lighter RL10's are capable of satisfying the performance requirements.

A final option for the LEV main propulsions system is the Advanced Space Engine (ASE). The Isp values of the ASE are greater than those of the RL10, but like the aforementioned hybrid system, the ASE is a more massive engine. The ASE is capable of approximately the same thrust levels as that of its RL10 counterpart, so it is presumed that the extra mass is a result of the high throttle ratio of the ASE. The throttle ratio of the ASE is given as 20:1, twice that of the RL10. However, the RL10 throttle ratio is more than sufficient for the scenario under consideration. Lastly, the RL10 is a proven design whereas the ASE is not presently in use.<sup>5.10</sup> The RL10 thrusters have been used extensively on the Centaur upper stages.<sup>5.11</sup> Therefore, the ASE is not an optimum choice for the LEV.

#### 5.3.3 Functional Aspects

Like other conventional cryogenic systems, the RL10 is a pump-fed engine. The engine uses hydrogen fuel at cryogenic temperatures to cool the thrust chamber. The engine is unique in that it then uses this expanded hydrogen to run the turbines for the pump-feed. This gaseous

hydrogen is then pumped directly into the combustion chamber.<sup>5.11</sup>

One factor contributing to the RL10's relatively high efficiency can be found in the aforementioned utilization of expanded hydrogen for turbine power. Utilizing expanded hydrogen to run the engine's turbines is novel in that most conventional systems use a gas generator cycle for this purpose. In this gas generator concept, the main propellant is tapped into directly, and portions of the main propellant are burned in a separate combustion chamber to power the turbines. This more conventional method, also known as the "bootstrap" concept, is less efficient because it fails to utilize turbine exhaust gas which has some bulk kinetic energy.<sup>5.11</sup>

• Total Mass	159 kg (350 lbm)
• Thrust	91180N (20500 lbf)
• Mixture Ratio	5:1.
• Specific Impulse	450 sec
• Throttle Ratio	10:1.
• Length	2.22m (90in)
• Nozzle Diameter	1.18m (46in)

**Table 5.2** RL10A-4 Engine Specifications

### 5.3.4 Provisions for Engine-Out

Two RL10 thrusters will be used on the piloted LEV. Two of these engines provide a thrust to Lunar weight ratio (T/W) greater than one for the entire duration of the Lunar descent in both the piloted and unpiloted case. Complications arise, however, when one considers the possibility of loosing the functionality of one of the RL10 thrusters.

For the piloted case, one engine will provide a Lunar T/W of greater than one for the entire descent, therefore enabling a successful touchdown even in the case of engine-out. However, due to the significantly larger mass of the cargo mission, the possibility of engine-out for this mission poses a more complicated problem. One RL10 engine would require the majority of the descent burn time to reach a T/W of unity, as it burns off LEV fuel at a rate of 20 kg/sec. This would leave too little time and too little fuel to decelerate the craft to a safe touchdown. This added complication to the engine-out scenario is due to the fact that the mass of the unpiloted LEV is 33 metric tons greater at the very beginning of the descent stage than that of the piloted LEV. Thus, four RL10 thrusters will be used on the unpiloted LEV. In the event of an engine-out, the

remaining thrusters are capable of maintaining a T/W of greater than one throughout the entire descent.

### 5.3.5 Engine and Fuel Line Placement

The RL10 thrusters are to be mounted on the lower tier of the LEV truss structure, using the structure itself as the hard point. The upper portion of the nozzle as well as the turbomachinery will then be positioned between the lower and middle tiers of the truss.

One concern in the use of a fuel line network as extensive as that found on the LEV, is the possibility of line rupture. Although a slim possibility, a ruptured line could result in fire if it occurred during operation of the RL10 or RCS thrusters. This would be most likely to occur during the various LEV docking maneuvers with the LTV or SSF. In an attempt to minimize the chances of rupture at any point in the mission, the fuel lines will always be mounted to the inside of the truss structure.

### 5.4 RCS

Like the primary propulsion system on the LEV, propulsive options for both the LTV and the LEV reaction control systems are limited strictly to chemical propellants. As with all chemically propelled rockets, a choice between cryogenic propellants and storable propellants must be made. Along with these considerations, the LTV and LEV RCS must be capable of performing both large and small maneuvers in a reasonable amount of time.

#### 5.4.1 Cryogenic RCS

While no cryogenic RCS's have yet been built, projected specifications for one concept of such a system are listed in Table 5.3.

Mass	14.1 kg (31 lbm)
Thrust	5560N (1250 lbf)
Specific Impulse	427 seconds
Mixture Ratio	4.5:1

**Table 5.3** LOX/LH2 RCS Engine

While this system is a LOX/LH2 fed engine, it is reasonable to expect comparable performance from a gaseous, boil-off fed system. Not surprisingly, this engine exhibits a high specific impulse. However, this benefit is somewhat negated by the nature of an RCS system. Since this system will not be called upon to produce long burns or large delta-V's, the total amount of system propellant will be quite small. Thus, the full benefits of a high specific impulse

will not be nearly as significant as was the case with the LEV primary propulsion system. Another benefit of using a cryogenic system is the utilization of the main tank boiloff which would otherwise simply be vented. However, this type of system requires an additional expander system to siphon off liquid fuel from the main tanks, since the boiloff rate will not provide enough fuel by itself.<sup>5.12</sup> A further benefit of cryogenic propellants is their non-toxic nature. Unlike storable propellants, oxygen and hydrogen have virtually no significant poisonous effects. This lack of toxicity simplifies servicing by human operators.

In addition to having two major advantages, cryogenic engines also have two major disadvantages. The largest disadvantage of cryogenic systems is the lack of any existing engine designs or well-detailed engine proposals. Unlike storable systems which have over 30 years of proven operation, no cryogenic RCS exists. Additionally, if a cryogenic system is to use main tank boiloff, then fuel line and system complexity increases dramatically. On the other hand, if a separate set of fuel tanks are dedicated to the RCS, then boiloff becomes a concern. In steady state operations, the LTV will be required to stay in orbit for approximately six months. During this period significant amounts, possibly as much as 5%, of the cryogenic propellants will be lost to boiloff.

#### 5.4.2 Storable RCS

Since the space shuttle RCS utilizes storable propellants, this system serves as a good reference point for evaluating storable systems in general. Specifically, the shuttle system is fueled by monomethylhydrazine (MMH) and uses nitrogen tetroxide (N<sub>2</sub>O<sub>4</sub>) as an oxidizer. Caution must be taken to distinguish this system from the OMS system, which produces a higher thrust level than that required of the either the LTV or LEV RCS. The shuttle system is composed of 38 primary thrusters and 6 vernier thrusters. Because the shuttle utilizes its RCS system for stability and control during reentry into the atmosphere, it is much more complex than that needed on the LTV or LEV.<sup>5.13</sup> Specifications for the shuttle primary thrusters are given in Table 5.4.<sup>5.14</sup>

Manufacturer	Marquardt Company
System Mass	500kg (1100 lbm)
Thrust	3870N (870 lbf)
Specific Impulse	280 seconds
Fuel/Oxidizer	MMH/N <sub>2</sub> O <sub>4</sub>

**Table 5.4** Shuttle Primary Thrusters

In comparing a storable system to the cryogenic system previously described, the most notable difference is in engine specific impulse. Storable systems have significantly lower Isp's than their cryogenic counterparts. This is the major disadvantage of storable systems. An additional disadvantage of storable RCS thrusters is the toxicity of their propellants. While these propellants are not fatal on contact, added care must be taken whenever human operators service these thrusters.

As expected, the major benefit of a storable RCS thruster is its lack of boiloff. Unlike cryogenic thrusters, storable thrusters experience no loss in fuel regardless of the mission duration. This means no insulation mass is required and no extra fuel margin needs to be added. Additionally, storable systems use propellants with relatively high densities. Thus, the fuel tanks for storable systems are much smaller than for a comparable cryogenic system. These small fuel tanks permit individual thrusters or entire clusters of engines to be assembled as a complete module containing both fuel and engine. These modules can then be placed exactly where needed on the vehicle. A modular design of this type reduces the amount of extra fuel line plumbing required and adds an inherent redundancy to the entire RCS.

#### 5.4.3 LTV RCS

##### 5.4.3.1 Engine Selection

Based on the relative benefits and disadvantages of the two RCS options discussed earlier, the most likely candidate for use on the LTV is a storable RCS. The modularity of a storable RCS greatly reduces the complexity of the entire system and, as mentioned previously, a modular system lends added redundancy.

One type of RCS which is readily adaptable to the LTV is the previously discussed shuttle RCS. This system produces thrust at levels deemed necessary for operation of the LTS. The RCS will be needed for several different vehicle maneuvers. The system will be expected to impart a 10 m/s midrange correction to the vehicle on both the outbound and inbound trajectories as well as a small trajectory correction to facilitate disposal of the TL/LOI main tanks. Furthermore, the RCS will have to provide enough thrust to swing the vehicle around 180 degrees to change the direction of the NTR thrust vector. The vehicle will also be rotated about its axis of symmetry. In the current configuration, the LTV RCS is responsible for imparting a 70 m/s total delta V to the LTS during the mission. Due to the large delta V required for the final circularization burn, the LTV RCS will not be used. Instead, the NTR system will be used for this 300 m/s burn.



This significantly reduces the thrust requirement for the LTV RCS.

The reader is asked to refer to Table 5.4 for technical data on the Marquardt thrusters to be used on the LTV.

#### 5.4.3.2 Engine, Tank, and Fuel Line Placement

It is necessary that the LTV vehicle be able to maneuver freely in all six degrees of freedom. This will be accomplished by strategic placement of eight, quad-directional pods on the LTV. To improve rotational maneuvering time of the LTV, the RCS pods will be located as far from the LTV center of mass as is practical. Thus, the pods will have the longest possible moment arms over which to act on the LTV. The pods will be placed on each face of the truss, forming two rings of thrusters at each end of the vehicle.

The fuel mass requirements for the RCS total 2.3 mT. This results in the placement of eight spherical Nitrogen Tetroxide tanks each having a diameter of .59 meters and eight monomethylhydrazine tanks each having a diameter of .68 meters. The LTV RCS tanks may be conveniently placed to the inside of the main truss, with each pair of propellant tanks in close proximity to their respective thruster pod. This arrangement is suitable in terms of space as well as conducive to simple fuel line placement.

#### 5.4.4 LEV RCS

##### 5.4.4.1 Engine Selection

The earlier decision to use only two RL10 engines for the LEV primary propulsion simplifies the truss design by eliminating the use of a force distribution manifold. However, use of only two RL10 engines requires the placement of a substantial RCS system on the LEV to control the craft during ascent and descent in the event of engine-out.

As was the case with the LTV RCS, both storable and cryogenic propellants presented themselves as options for the LEV RCS. To date, no gaseous oxygen/hydrogen RCS has ever been employed in Lunar lander operations. Conversely, many landers have flown with storable RCS systems. Historically, the Apollo missions utilized a storable RCS fueled with Aerozine-50 and used nitrogen tetroxide as an oxidizer. Each of the various Apollo missions consumed between 300 and 600 lbm of RCS fuel.<sup>5.15</sup> Because the mission scenario currently under consideration utilizes a considerably larger lander than Apollo, the mass of required LEV RCS fuel will be greater.

This fuel mass requirement will be somewhat reduced through the use of next generation RCS thrusters with higher Isp's. The RCS for use on the LEV is a storable thruster and is specified in Table 5.5.<sup>5.16</sup>

Manufacturer	Hamilton Standard
Total System Mass w/Tanks	73.1 kg (160.8 lbm)
Thrust	622N (140 lbf)
Fuel	Hydrazine
Number of Thrusters	16 (4 per quad)
Mass Per Thruster	2kg (4.4 lbm)

**Table 5.5** Storable Lander RCS Engine

As was the case with the LTV RCS, the modularity and redundancy of storable systems is simply too valuable to neglect. Also, the total vehicle mass penalty incurred by using a lower Isp storable system is less than one ton.

##### 5.4.4.2 Engine, Tank and Fuel Line Placement

The best location for the lander RCS is on the lander legs themselves. This removes the nozzle exhaust from any sensitive lander components and utilizes long moment arms to help in craft rotational maneuvering. The thruster fuel tank can be located inside the structure of the landing leg.

Currently, both the piloted and unpiloted LEV's are allowed only 30 seconds of hovering. This limitation makes the use of moderately powerful RCS thrusters necessary because the vehicle must be able to rotate and translate quickly enough to insure achievement of correct orientation within the 30 second time limit.

In the 30 second hovering window, the RCS system is capable of accelerating the piloted LEV to a velocity of 1.2 m/s, allowing the vehicle to translate 14 meters within this time frame.

The hydrazine fuel tank arrangement for the RCS will consist of four equally sized spherical tanks. Each tank will measure .68 meters in diameter, and will be mounted on the inside of the landing gear structure. This placement should afford considerably more protection for the tanks that if they were mounted externally, and lends simplicity to placement of fuel lines because of the proximity of each tank to the RCS thruster pods.

## 5.5 Fuel Requirements

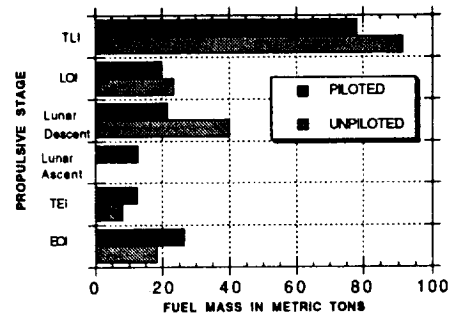
### 5.5.1 Propulsion Spreadsheet: Appendix C

To accommodate the continually changing design configurations as well as mass revisions, a spreadsheet capable of continually recalculating fuel masses is utilized. To meet the needs of the design group as it undergoes the critical task of trial configuration analyses, the spreadsheet is designed to accommodate changes in every major component of the mission scenario. In this way, the trial configuration can be modified to provide for best fuel efficiency. The spreadsheet lends itself well to determining the feasibility of various abort options. It also provides a secondary specification sheet which can be used for mission scenario clarification. The current spreadsheet provides for up to 12 modestly differing trial configurations to be compared at any given time. It also provides short descriptions of the trial configuration and brief comments on trial configuration feasibility. As well as calculating the fuel requirements for the six major propulsive stages of the mission, the spreadsheet also calculates RCS fuel requirements for the LEV and LTV in every RCS burn stage.

### 5.5.2 Fuel Requirement Breakdown

The LTS fuel mass requirements are shown Figure 5.4. The fuel requirements for both missions are separated into the six major propulsive phases.

FUEL REQUIREMENTS FOR PROPULSIVE STAGES



Mission Phase	Piloted	Unpiloted
TLI	78.2	91.5
LOI	20.0	23.4
Lunar Descent	21.6	40
Lunar Ascent	12.7	0
TEI	12.4	8.2
EOI	26.6	18.5

**Figure 5.4**  
Fuel Requirements for Mission Phases

Figure 5.4 clearly shows that the unpiloted mission consumes more fuel in TLI, TEI, and Lunar descent, while the piloted mission consumes more fuel during all return stages. This result is intuitive when one considers the large amount of mass which the unpiloted mission leaves on the Lunar surface. The total fuel requirement for the piloted and unpiloted missions are 137.2 and 141.5 metric tons respectively.

The fuel requirement analysis also shows effects of mass additions on IMLEO. Mass increases on permanent parts of the LTV increases LTS IMLEO by a factor of three. Mass increases on permanent parts of the LEV increases LTS IMLEO by a factor of six.

## 5.6 Conclusion

An important part the mission statement which drove the design of the Lunar Transportation System was that part which stressed economy in design and function. One important factor in mission cost is the IMLEO estimate, which is very much a function of fuel requirements. The propulsion discipline has chosen high efficiency propulsion systems in an attempt to reduce IMLEO. At the same time, the discipline's design efforts have stressed utility, reliability, and safety as key to successful LTS missions.

## 6.0 STRUCTURAL AND THERMAL ANALYSIS OF LTS

### 6.1 Structural Developments

#### 6.1.1 Lunar Excursion Vehicle

The focus of the Structures discipline has been the design and analysis of truss structures to provide support to the components of both the Lunar Transportation Vehicle (LTV) and the Lunar Excursion Vehicle (LEV). The design process consisted of laying out truss structures to maintain separation of the components of the vehicles as well as defining material and geometric properties for the trusses. The analysis consisted of developing finite element models of each truss including specification of proper boundary conditions and interpretation of the results from the model, and testing of a physical scale model of the landing gear to provide closure to the design by verifying the computer results by direct comparison with physical test results.

##### 6.1.1.1 Specification and Modeling of Operating Conditions for LEV

The function of the LEV truss is to provide support to the crew module, fuel tanks and engines of the LEV during transport to the Moon and descent to the Lunar surface.

The most critical loading condition for the LEV truss was established to be the landing. The analysis of the landing was considered to include an examination of the LEV's rigid body lateral stability in tipping at touchdown, modeling of the spring/damper system in the landing gear to predict the acceleration input to the vehicle at touchdown and an analysis of the load distribution in the truss structure to allow for mass reduction in the truss through removal of non-load-bearing members.

The lateral tipping stability model of the vehicle was developed using conventions established for the Apollo missions. These missions assumed a worst case landing scenario with a 12 degree surface incline at the landing site and a maximum vehicle horizontal velocity at impact of 1.2 m/s (3.94 ft/s). A schematic representation of the model of the LEV at touchdown is presented in Figure 6.1:

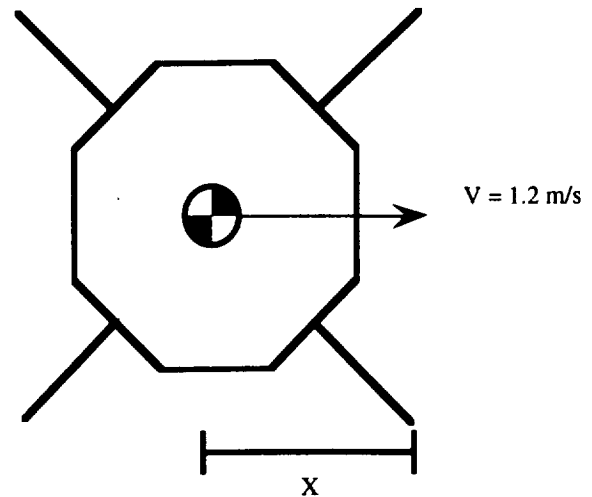


Figure 6.1 Worst-Case Landing Orientation

From consideration of Figure 6.1, it is evident that model reflects the most severe orientation for the lander with the velocity vector oriented between two of the landing gear. This condition presents the shortest distance from the support base of the vehicle to its center of gravity. In addition to the orientation of the velocity vector relative to the vehicle, the velocity was also considered oriented for a down the slope of the landing site. With these assumptions, the stability tipping analysis was reduced to equating the horizontal kinetic energy of the vehicle at touchdown with the gravitational potential energy change of the center of mass required to rotate the vehicle up onto two legs, into an unstable equilibrium. This is shown schematically in Figure 6.2.

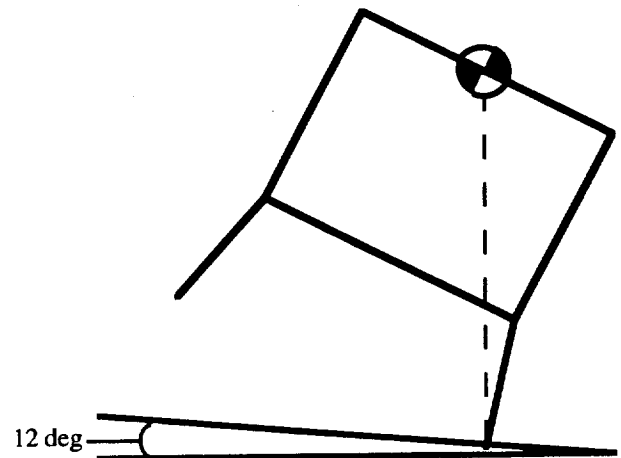


Figure 6.2 Unstable Equilibrium Point

For the initial lateral stability analysis, the center of gravity was assumed to be at the top of the lander, 8m (26.25 ft) above the surface. Assuming this location of the center of

gravity, the lander was found to reach the unstable lateral tipping equilibrium point when the critical distance X, shown in Figure 6.1, was 4.6m (15.1 ft). This critical distance was used to define the current diagonal length between landing gear from foot to foot of 13.02 m (47.72 ft). Further specification of the LEV configuration indicated that the true center of mass of the vehicle at approximately 2m above the bottom tier of the truss. Assuming this location for the center of mass, the critical distance X is found to be 1.665 m (5.075 ft). With the new critical distance, the diagonal length between landing gear would be reduced to 11.21 m (34.17 ft). This is a change that would be incorporated in the next revision of the design.

In addition to achieving lateral tipping stability, it was also identified as necessary to limit the accelerations experienced by the components supported by the truss. A specific acceleration requirement was established by the Crew Systems Discipline such that the astronauts not exceed an acceleration equal to 1.7 times that of Earth's gravity during landing. For specification of the landing gear, a safety factor of 1.5 was assumed, establishing a maximum allowable design acceleration of less than 1.13 g's.

A separate model of the LEV was developed for analysis of the acceleration input to the vehicle at touchdown. At touchdown, the kinetic and potential energy of the LEV must be completely dissipated. This dissipation was assumed to occur entirely in the landing gear of the truss. An additional constraint to the landing was that the landing gear deflect less than 1 meter (3.28 ft) in length during landing to reduce the possibility of bending and warping of connected truss members. The dissipation device in the landing gear was modeled as a spring-mass-damper system, and differential equations describing the response were formulated. The exact solution to the differential equations was found to be impractical. Hence, an approximate numerical solution was formulated by integrating finite difference equations with a spreadsheet. For the finite difference analysis, a time step of 0.001 seconds was selected for a step increment two orders of magnitude smaller than the total duration of the impact, estimated at approximately 0.3 seconds. This time step was selected to provide adequate resolution of the solution. At each time step, the position of the vehicle was calculated from the velocity during the previous step. The difference between the downward kinetic energy of the vehicle from the previous time step and the change in energy lost to the damper and spring through the change in position was used to establish the current kinetic energy. The new kinetic energy was then converted into the velocity at that time step.

Initially, values were assigned to the spring constant (k) and the damping coefficient (b) such that these values provided

the maximum individual accelerations of 1.13g. Hence, when the velocity was at a maximum, the damper would provide maximum acceleration; where the displacement is maximum, the spring provides maximum acceleration. Assuming the maximum vertical landing velocity of 3.1 m/s (10.2 ft/s), and defining the maximum displacement at 1 meter (3.28 ft), the initial estimates were  $4K = 650 \text{ kN/m}$  and  $4b = 200 \text{ kN/m/s}$ . The constants (k) and (b) were considered multiplied by four (4) to allow for the four landing gear which each have a spring damper system. A plot of the acceleration and velocity of the lander after touchdown assuming these values is provided as Figure 6.3.

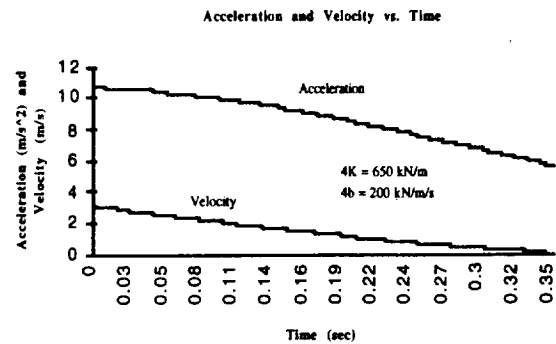


**Figure 6.3**  
Initial Values of Spring Constants

This analysis revealed that the entire kinetic energy of the lander was absorbed into the spring-damper system with a displacement of 0.6 meters (1.97 ft). However, as evident from Figure 6.3, the impact at landing was at a level that was considered too rigorous for the astronauts, with an instantaneous accelerational increment of  $10 \text{ m/sec}^2$ . Since the lander was found to come to rest in a displacement of less than one meter, it was possible to increase the spring constant and decrease the damping coefficient to reduce the instantaneous acceleration to the astronauts. Figure 6.4 shows results from the analysis using  $4K = 800 \text{ kN/m}$  and  $4b = 150 \text{ kN/m/s}$ . The instantaneous acceleration for this model is found to be  $8.9 \text{ m/sec}^2$ . While the instantaneous accelerational increment is still large, it is less than that at the Earth's surface.

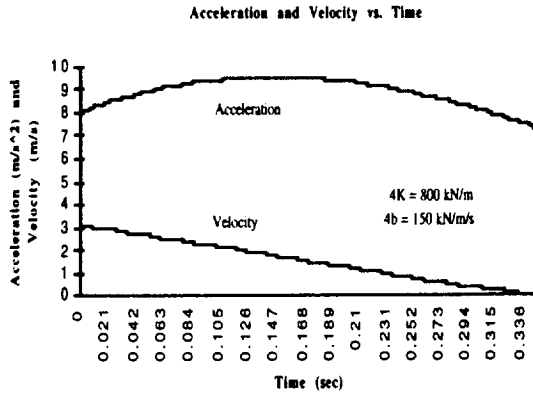


Figure 6.4 Modified Spring Constants

### 6.1.1.2 Vehicle Configurational Layout with Structural Justification

The third analysis on the LEV was of the distribution of forces, under loading, in the truss structure. Several potential configurations were considered for this analysis. The optimum shape was chosen based on the factors established by the lateral tipping stability analysis and acceleration models described above as well as configurational issues such as fuel tanks, engine and crew module support as described below.

An vertical octagonal truss shape was derived to provide support for the crew module during descent to the Lunar surface. The crew module was approximated as a cylinder with a diameter of 4.42m (14.5 ft) and 5m (16.4 ft) high. A second factor considered in the truss design was the layout of the landing gear, fuel tanks, and the cargo on the truss. It was decided to attach these components to the truss at the intersection of truss members, called "hardpoints", for maximum structural support. The third factor considered in the truss design was the failure mode of the truss under loading. The second concentric ring in each tier was included outside of the first to provide in-plane rigidity to the structure as well as increased support in the vertical direction.

Another factor considered in the truss design was the failure modes of the truss members themselves. The most relevant of these failure modes was identified as buckling. Buckling is most evident in long, slender truss members. To avoid this failure mode, the configuration was designed to minimize the number of "long" members involved. Thus, a three tier configuration was established. This three tier configuration provided the necessary hardpoints to mount components, while simultaneously increasing the overall

rigidity of the structure by reducing the likelihood of buckling in any member.

Finally, the members of the truss structure were set for first analysis as having a tubular cross-section of 10 cm (3.92 in) outer diameter and wall thickness of 2 cm (0.79 in). The final conceptual design configuration for the LEV truss is shown in Figure 6.5.

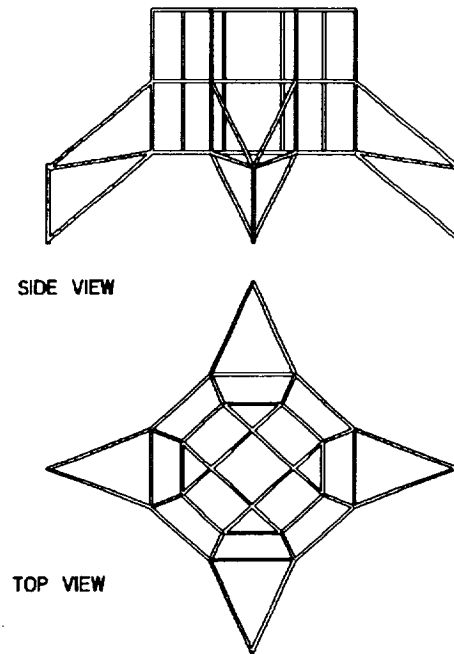


Figure 6.5 LEV Truss Configuration

The final design factor considered was the placement and mounting of the engines to the truss structure. The RL-10 engines have a height of 2.3m (7.55 ft) and a minimum required clearance between the bottom of the engine and the Lunar surface at touchdown of 1.5m (4.92 ft). The distance from the bottom tier of the LEV truss to the ground was set at 3m (9.84 ft) to allow the astronauts to easily maneuver beneath the vehicle. These constraints dictated that the engines be mounted within the truss itself. Hence, the engines were mounted on the middle tier of the truss and approximately 1 m above the bottom tier. The engine mounts attached both to the inner and outer octagons of the middle tier with the thrust force supported at the top of the RL-10 engines.

The material chosen for the members of the LEV truss structure was an Aluminum Lithium (AlLi) alloy, in particular, Weldalite 049 because of the weight consideration

of the vehicle. Titanium alloys were also considered to provide increased strength where necessary.

For comparison, Table 6.1 presents the mechanical properties of several high-strength alloys.<sup>6.1</sup> From Figure 6.1, it is evident that Weldalite has strength comparable to steel with a density as low as Aluminum.

The fuel tanks were considered as being constructed of Weldalite at minimum gage thickness. The Hydrogen tanks were considered as cylindrical with a diameter of 2.5 m (7.62 ft). The oxygen tanks were modeled as spherical. Each of the tanks is connected to the four nearest nodes on the truss.

Material	Modulus (GPa)	Strength (MPa)	Density (kg/m <sup>3</sup> )
AlLi	77	700	2700
Ti alloy	117	910	4960
Steel	207	703	7770
Al	68	100	2700

Table 6.1 Material Properties

### 6.1.1.3 I-DEAS Model Description

Structural analysis of the defined LEV truss configuration was attempted with the I-DEAS finite element analysis software. The first step of the analysis was the specification of a model geometry within the I-DEAS program. The geometric model was then meshed into a finite element model automatically by I-DEAS. The mesh was constructed from linear beam elements. A global element size of 1 meter was used to allow for better resolution of the deformation. Linear beam elements were selected to provide accurate modeling of the rigid connections assumed for the welded construction of the truss. The finite element model developed for structural analysis with I-DEAS is shown in Figure 6.6.

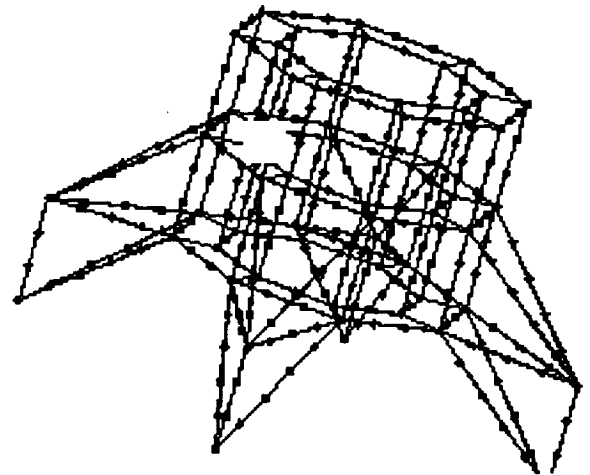


Figure 6.6 I-DEAS Finite Element Model of LEV

Before implementation of the I-DEAS structural analysis, it was necessary to establish proper boundary conditions for the model. Proper constraint of a modeled structure for analysis in I-DEAS involves elimination of all rigid body rotations and translations from the model, while ensuring that the model is not over constrained in a manner that is not physically accurate. Constraining all four landing gear feet on the lander from movement in any direction was deemed inaccurate. It was reasoned that in actual application, the legs of the lander would tend to spread out away from the center of the truss when loaded vertically. The landing gear were constrained from motion vertically, based on the assumption that each leg would support load and be employed on a planar surface. However, the vertical constraint on the landing gear was not sufficient for analysis of the truss since it allows for the model to rotate about its axis and translate in the horizontal plane. To eliminate the translational freedom of the model, one landing gear foot was constrained from translational motion in all three directions. To eliminate the rotation of the model about the truss axis, the foot diagonally opposite the completely constrained foot was restrained from translational motion in a direction perpendicular to the diagonal connecting the two feet.

For purposes of loading the truss model, the restraint that the lander should not exceed an acceleration of 1.7 times the Earth's gravity was used. Again, a safety factor of 1.5 was assumed to ensure that the structure would withstand loads due to an acceleration 2.55 times that of Earth's gravity.

In order to properly load the model it was necessary to determine the loads that various components that comprise the LEV will impart to the truss. The most significant of

these loads came from the fuel tanks, particularly the oxygen fuel tanks, and crew module on the lander. The loads due to the fuel tanks were modeled as follows: Each of the eight fuel tanks were attached at one face of the octagonal truss between two tiers of the truss. The tanks were supported by connection to the tiers above and below it. Thus, each tank was supported by four nodal connections. The spherical oxygen tanks were located on the lower half of the truss, between the landing gear, while the cylindrical hydrogen tanks were connected at the upper half of the truss, above the landing gear. Each tank was modeled as distributing the support load equally over the four nodes on the local face of the truss. Hence, each tank was modeled as exerting a vertical support force equal to one-quarter its weight on the four nodes supporting it. In addition, because the center of gravity of the tank was necessarily away from the structure because of the geometry, the tank also caused inward and outward forces on the truss. The complete loading scheme for a typical fuel tank is presented in Figure 6.7.

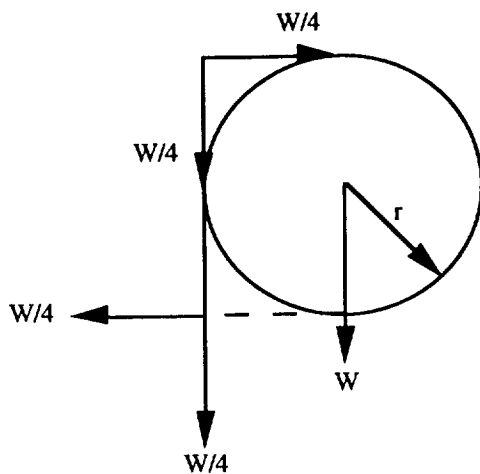


**Figure 6.7**  
Tank Loads on the Four Nearest Nodes

This configuration also served to simplify the moment calculation: the weight of the tank acted on a moment arm of the same length as the reaction forces. Thus, the inward and outward tank forces divided the moment equally. Hence, the inward and outward forces were also one fourth the weight of the tank.

The other loads on the truss structure were less difficult to model. The weight of the crew module in the center of the truss was modeled as distributed evenly over the interior ring nodes of each tier and the four support nodes across the bottom of the truss. The weight of the engines was applied at the engine mounts. With the loads to the LEV truss defined, the model was then analyzed.

#### 6.1.1.4 Description of and Results from I-DEAS Analysis

The I-DEAS analysis provided the displacements of the truss at the nodes, and the complete stress state in each beam. Unfortunately, I-DEAS provided output for the stress state of the beams in terms of the individual maximum stress components, but did not give a single numerical value for the combined stress state. Hence, it was necessary to input the individual stress components in a spreadsheet to combine them. As a convention, the maximum shear stress was assumed to always occur at the location of maximum bending stress for purposes of combining the stress state. This was a conservative assumption.

With this assumption, it was necessary to convert the stress components from the local Cartesian coordinates of the bar to local cylindrical coordinates. The conversion was for ease of calculation. In cylindrical coordinates,  $s_{rr}$  must be zero, since there was no load against the side of the bar. Since the inside of the bar is not pressurized,  $s_{tt}$  also had to be zero. Correspondingly, the shear stress between these two directions must also be zero.

The assumption that the maximum stress in the beam occurs at the same location as the maximum bending stress required the determination of the location of this point. The magnitude and direction of the maximum bending stress were calculated from the maximum bending stresses in the X and Y direction by vector addition. Once that angle was calculated, 90 degrees were added or subtracted from it to locate the point of maximum compressive or tensile stress. If the axial force on that beam was compressive, then the side of the beam that was in compression from the bending moment had the greatest axial load. The location of that point was taken at 90 degrees clockwise from the direction of the combined bending stress. Likewise, if the axial stress on the beam was tensile, the maximum axial load was taken on the tensile side of the bending moment. Thus the point of maximum stress was at 90 degrees counter-clockwise from the angle of maximum stress. Once that angle was determined, the maximum shear stress was converted from x-y coordinates to r-t coordinates. Because the stress state was considered in cylindrical coordinates, the torsional stress was  $T_{zt}$ .

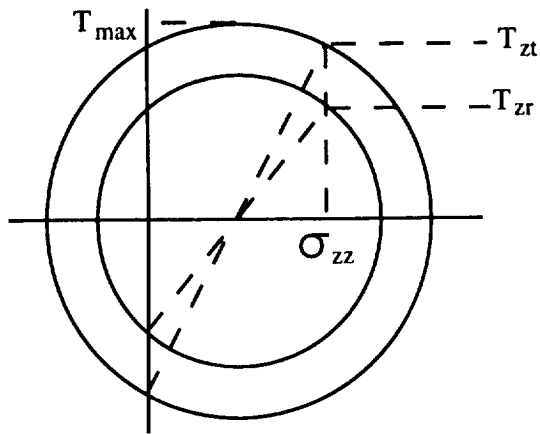


**Figure 6.8** Mohr's Circle of Stress

Using the three stresses in cylindrical coordinates, Mohr's circle was used to provide information about the combined stress state in the bar. Figure 6.7 shows an application of Mohr's circle to this particular problem. The maximum stress state was taken as the combination of  $\sigma_{zz}$  with whichever shear stress is larger-- in this instance  $T_{zt}$ . The Tresca shear criterion was used for failure. Hence, if the maximum shear stress exceeded half of the yield stress, the member was considered to have failed.

Using the configuration described above, with the member described above, I-DEAS indicated a maximum stress state for the entire truss structure of  $6.38E7$  Pa (9256 psi), compared to Tresca failure value of  $3.5E8$  Pa (50776 psi). Hence, even the conservative estimate was only 18% of the yield strength of the material.

Since the safety factor was included in the loading scenario, the goal was to make the truss as light as possible while maintaining the maximum stress in the members less than the specified maximum. For purposes of mass reduction, two new tubular cross sections were created: the first section has an outer diameter of 8cm (3.15 in) and the second has an outer diameter of 6cm (2.36 in). Both sections were set with a wall thickness of 1cm (0.39 in). The horizontal members forming the inner and outer rings on all three tiers were reduced to the 6cm (2.36 in) diameter section members, and the connections between the inner and outer rings were reduced to 8cm (3.15 in) diameter sections. The analysis was performed on the reduced truss model, and I-DEAS predicted a maximum stress of  $1.08E8$  Pa (15668 psi) while the spreadsheet calculated  $1.23E8$  Pa (17844 psi). These values were still roughly one-third of the allowed maximum.

## 6.1.2 Lunar Transportation Vehicle

### 6.1.2.1 Specification and Modeling of Operating Conditions for LTV

The operating environment for the LTV was identified to be significantly different than that for the LEV since the LTV does not maintain contact with a grounded body, but rather is accelerated by the NTR engine. The acceleration of the LTV produces loading in the truss structure through the masses which are attached to the truss and must be accelerated with it. The most crucial loading condition for the LTV was identified to be the TLI burn, when the vehicle is accelerated with its maximum fuel. As a worst case scenario, the vehicle was modeled to experience its maximum mission acceleration with its maximum fuel mass. The maximum acceleration to be experienced by the LTV was specified by the Propulsion Discipline to be 0.6 earth g's. Hence, this is the acceleration from which the analysis was pursued.

### 6.1.2.2 Vehicle Configurational Layout with Structural Justification.

The purpose of the LTV truss is to maintain the LEV and LTV crew module 33m (108.3 ft) from the Nuclear Thermal Rocket to maintain the radiation exposure to the crew within acceptable limits. The truss was modeled with rectangular sections spaced at three meter intervals. At the end of the truss where the fuel tanks are attached, the truss sectional dimensions were established at 4m (13.1 ft) by 4m (13.1 ft) to allow for attachment of fuel tanks to the truss without interference between them. At the mid-point of the truss, the sectional dimensions were reduced to 3m (9.144 ft) by 3m (9.144 ft) to minimize the weight of the truss while maintaining its rigidity. Finally, at the end of the truss where the crew module is located, the truss assumes an octagonal shape identical to the inner rings of the LEV to provide support to the LTV crew module and to provide for a favorable mating to the LEV truss. In addition to the rectangular members in the truss, diagonal members are also included to provide rigidity against torsion and bending. These members were located such that no more than six members connect at any node to reduce the complexity of the truss structure. For preliminary analysis, the truss was considered to be constructed of Weldalite members of the heavy cross-section defined for the LEV with 10cm (3.94 in) outer diameter and 2cm (.79 in) wall thickness. The final conceptual design for the LTV truss is shown in Figure 6.8.



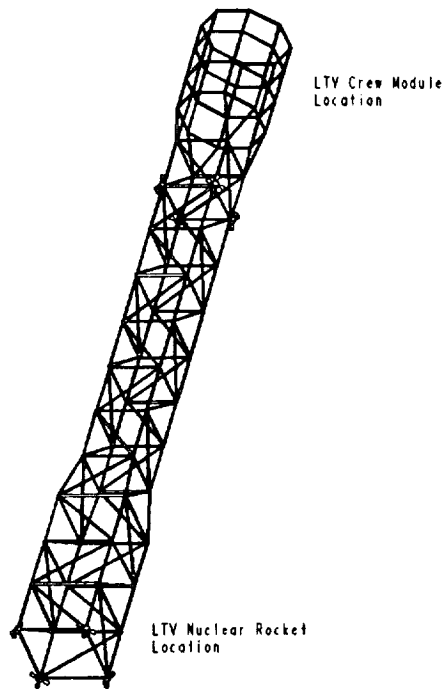


**Figure 6.9** LTV Truss Configuration

The fuel tanks were assumed to mount to the truss at the corner nodes nearest to them. The tanks were modeled as constructed of Weldalite at minimum gage wall thickness. It is assumed that the tanks would include some soft of baffling within them to minimize shifting of the fuel mass during acceleration of the vehicle. The details of the baffling structure within the tanks were not resolved at this stage of the design.

### 6.1.2.3 I-DEAS Model Description

An I-DEAS model of the LTV truss structure was developed. The LTV truss was also modeled with linear beam elements similarly to the LEV, again with a global element size of one meter for an adequate resolution of the stress distribution in the model. The I-DEAS model of the LTV truss is shown in Figure 6.10.

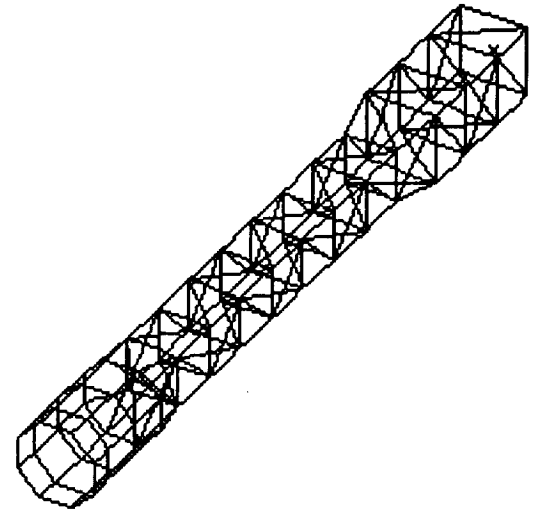


**Figure 6.10** I-DEAS Model of LTV Truss

Although, the loading of the LTV truss is due to acceleration, the deformation of the truss was analyzed with linear statics nonetheless by applying the loads that would be imparted to the truss if the fully loaded vehicle (all fuel tanks full) were accelerated at its maximum acceleration in the lightest configuration, 0.6 earth g's. These assumptions create a worst-case loading scenario for the vehicle. The loads to the truss were assumed to be distributed as follows: The LEV is attached to the LTV truss at the forward-most octagonal ring of the truss. Hence, the acceleration load due to the LEV on the LTV was modeled as distributed over the eight corner nodes of the forward ring. The crew module acceleration load was assumed to be distributed over the two middle tiers of the octagonal section of the truss. Hence, the crew module acceleration load was applied over the sixteen nodes of the middle two octagonal sections of the truss. The large (TLI) fuel tanks were considered to each distribute axial load to the truss over the nearest eight nodes. In addition, to the axial loads, these tanks were considered to impart moment loads on the truss outward at the front two pairs of nodes and inward to the truss at the two rear pairs of nodes. The small (TEI) fuel tanks were modeled as distributing load at the large section of the truss at the two middle sets of the nodes in the larger section of the truss. Similarly to the TLI tanks, the TEI tanks were assumed to impart moment loads as well, with the outward forces at the front pair of nodes and inward forces at the rear pair of nodes.

#### 6.1.2.4 Description of and Results from I-DEAS Analysis

The analysis of the LTV truss was not completed at the time of this report. However, initial buckling analysis performed indicated that additional members were necessary, particularly in the region of the truss where the octagonal section joins to the square sections, to withstand the loads on the truss. The deformed geometry predicted by this analysis is shown in Figure 6.11.

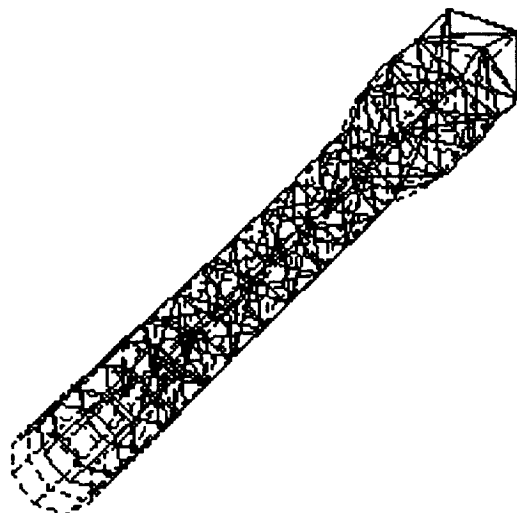


Figure 6.11 I-DEAS Predicted Deformed Geometry For LTV Truss

#### 6.2 Physical Testing of LTS Systems

As described above, the analysis of the LTS systems was performed with the I-DEAS structural finite element analysis software. Both trusses were modeled with linear beam finite elements to reflect the welded construction assumed for the truss structure. In order to gain increased insight into the validity of this modeling method, it was proposed to perform a physical test for comparison to the I-DEAS prediction. The scope of the test was restricted to involve the landing gear of the LEV, rather than either truss in entirety to reduce the labor required to construct the test fixture. In addition, since the scope of the test was to provide verification of the modeling method only, the I-DEAS model of the landing gear was constructed to reflect the physical test article, rather than the actual LEV landing gear. The physical test article was constructed from Aluminum 6061 tubing with 0.500" outer diameter and 0.0625" wall thickness to approximate the landing gear structure roughly to 1/8 scale. Again, since the I-DEAS model was constructed to model the test article, it was not significant for the test article to exactly replicate the truss

landing gear. A diagram of the test article is shown in Figure 6.12.

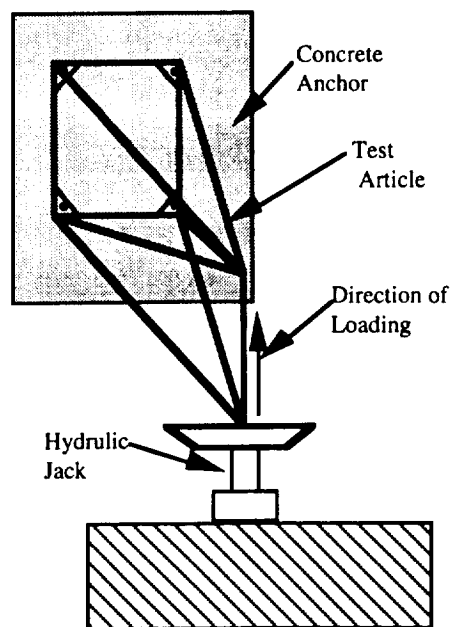


Figure 6.12 Physical Test Article Geometry

#### 6.3 Thermal Analysis Developments

The primary focus of the Thermal Analysis Discipline was thermal control of the LTS systems. Thermal control is defined by establishing acceptable temperature ranges for all components on the vehicle and then designing thermal systems to maintain the components within the specified temperature limits while operating in the surrounding environment. Two primary types of thermal control systems are typically considered: active and passive.<sup>6.2</sup> Active thermal control systems involve some energy input to operate such as a compressor or pump. Passive thermal control devices make use of natural phenomenon to transfer heat.

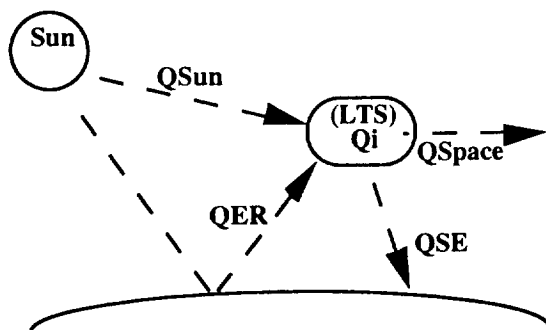
Two heat transfer mechanisms have been identified for space travel: radiation and conduction.<sup>6.2</sup> Radiation heat transfer is considered to occur primarily on a macroscopic scale between the vehicle and other bodies surrounding it. Conduction is modeled as occurring locally between components on the vehicle. These modes of heat transfer can cause numerous undesirable effects to the vehicle. In particular, they are responsible for boil-off of the cryogenic fuels in the tanks. Effective thermal design minimizes the effects of heat transfer.

### 6.3.1 Lunar Transportation Vehicle

#### 6.3.1.1 Specification of Design Thermal Conditions / Constraints

Three primary thermal loading environments have been defined for the LTV corresponding to the three phases of its mission. These include heat loads experienced while in Low Earth Orbit, during transit to and from the Moon, and while in Low Lunar Orbit.<sup>6.2</sup> Figures 6.13, 6.14 and 6.15 summarize schematically the thermal loads on the LTV in each environment.

#### Thermal Loads in Low Earth Orbit (LEO)



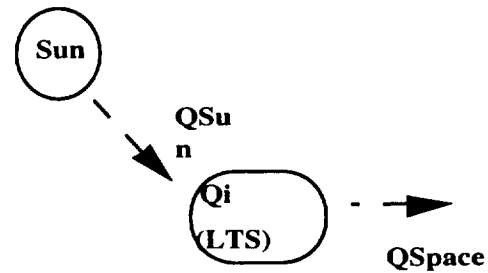
Energy Balance @ Steady State:

$$Q_{Sun} + Q_{ER} + Q_i = Q_{Space} + Q_{SE}$$

**Figure 6.13**  
Thermal Loads in Low Earth Orbit

Figure 6.13 describes the thermal loads to the vehicle while in Low Earth Orbit. These are defined as follows:  $Q_{Sun}$  represents the radiant energy from the sun that is directly incident upon the vehicle.  $Q_{space}$  represents the radiant heat transfer from the vehicle to the surrounding environment.  $Q_i$  allows for possible internal thermal energy generation by the spacecraft.  $Q_{se}$  represents the radiation between the spacecraft and the Earth and  $Q_{er}$  represents solar radiation which is reflected off of the Earth's atmosphere. At steady state the energy balance on the spacecraft is that shown in Figure 6.13.

#### Thermal Loads in Transit (TLI or TED)



Energy Balance @ Steady State:

$$Q_{Sun} + Q_i = Q_{Space}$$

**Figure 6.14** Thermal Loads in Transit

The heat load environment while the vehicle is in transit between the Earth and Moon is described in Figure 6.14. Only two heat transfer terms were identified for this environment, namely  $Q_{sun}$  and  $Q_{space}$ , defined as above. Again, a thermal energy balance was defined as shown in the figure.

The final heat load environment identified for the LTV occurs during occupancy in Low Lunar Orbit. This environment was identified as similar to that in Low Earth Orbit except that the reflected radiation from the sun is not evident. Figure 6.15 summarizes the thermal loads on the LTS during this phase of the mission.

### Thermal Loads in Low Lunar Orbit (LLO)

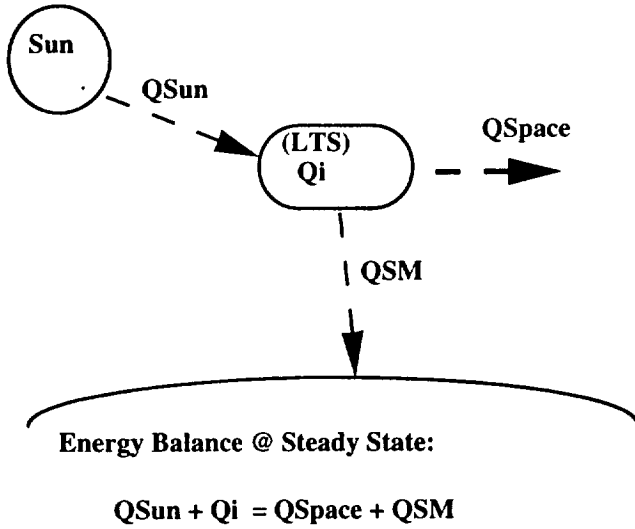


**Figure 6.15**  
Thermal Loads in Low Lunar Orbit

Expanded representation of each of the heat transfer mechanisms described above are presented in Figure 6.12:

$$Q_{sun} = \alpha_s A_{\perp} I_s$$

$$Q_{space} = \sigma \epsilon_s F_{s,s} A_s (T_s^4 - T_{space}^4)$$

$$Q_{ER} = a \alpha_s F_{S,E} A_s I_s$$

$$Q_{SE} = \sigma A_s F_{S,E} (\epsilon_s T_s^4 - \epsilon_E T_E^4)$$

$$Q_{SM} = \sigma A_s F_{S,M} (\epsilon_s T_s^4 - \epsilon_M T_M^4)$$

$$Q_{ENG} = \sigma A_s F_{S,ENG} (\epsilon_{ENG} T_{ENG}^4 - \epsilon_s T_s^4)$$

- $\alpha \Rightarrow$  Absorptivity (typical)
- $\epsilon \Rightarrow$  Emissivity (typical)
- $F_{X,Y} \Rightarrow$  View Factor between Body X and Body Y

**Figure 6.16**  
Definition of Heat Transfer Terms

The values of alpha and epsilon vary with position on the vehicle.

### 6.3.1.2 Thermal Analysis of LTV

For purposes of thermal analysis of the LTV truss, the following assumptions were held. First, the incident radiation from the sun ( $Q_{sun}$ ) was taken at a constant value of  $1400 \text{ W/m}^2$  rather than a difference in fourth order temperatures for radiation heat transfer. The truss was assumed to be such that shading of members onto others could be ignored. Hence, all elements of the truss, except those covered by the fuel tanks and the louvers around the crew module were assumed to be radiated equally by sunlight. No method to determine the sun radiation input to the other areas of the truss was developed at this stage of the design. Resolution of the view factors for concealed and/or shaded areas of the truss would be included in the next level of design of the truss.

With the assumption that the members of the truss are at all times illuminated by sunlight, there was found to be no development of a "hot" and "cold" side of the truss. However, it was still necessary to consider the possibility that each individual member on the truss might develop hot and cold sides which would introduce unfavorable thermal stresses into the LTV truss. Hence, a computer finite element code was developed to examine the temperature gradient which might result in the members radiated in this manner. This model simulated the effect of solar flux on a cross section of a typical truss member. A complete listing of the program, including comments, is included in Appendix D.

The model breaks the beam cross section into 60 wedges or elements. A schematic representation of a model element is shown in Figure 6.17. Heat transfer to and from elements is accomplished by two mechanisms: radiation and conduction.

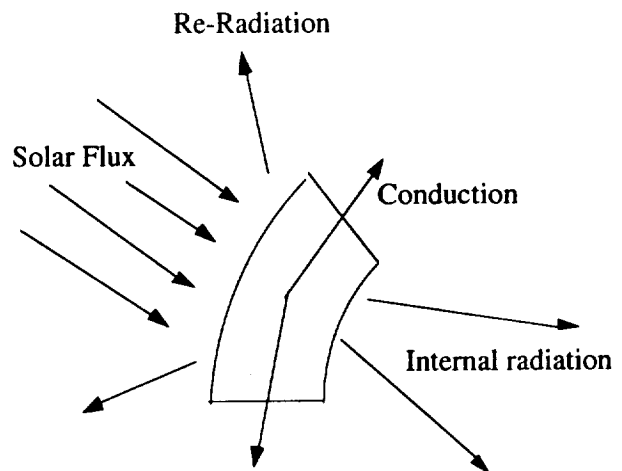


**Figure 6.17**  
Single Model Element and Heat Transfer Modes

As is shown in the figure, each element radiates out to space through its outer surface and also radiates to each other element in the cross section except for its four nearest neighbors. All surfaces are considered to have the same view factors and absorptivity and emissivity characteristics. In addition, all elements are treated as black bodies. The assumption of uniform view factors is not the most accurate assumption that can be made. However, the results of the program demonstrate that the effects of this view factor error are negligible.

Conduction is considered to occur between adjacent elements only and uses a forward difference method. The characteristic length is taken as the average of the inner and outer arc lengths of each wedge section. The flux area is taken as the wall thickness of the member. All heat transfer operations are defined per unit length and can be scaled to any member length.

Minimum and maximum temperatures in the cross section are plotted in Figure 6.18. It can be clearly seen that the temperatures trend toward 265K. It is also important to note the small difference in minimum and maximum temperatures. Essentially what is occurring is the conduction terms are dominating the radiation terms. The total solar flux into the cross section is quite small compared to the ability of the material to conduct heat away from the hot areas. This translates into small thermal gradients in the truss cross section and hence low thermal stresses.

The reason for the small transient and the rapid onset of steady state temperatures is found in the selection of initial conditions. After iterating the program for a few cycles, trends in the minimum and maximum temperatures were observed. The initial conditions were modified based on these trends which reduced the total computation time by orders of magnitude.

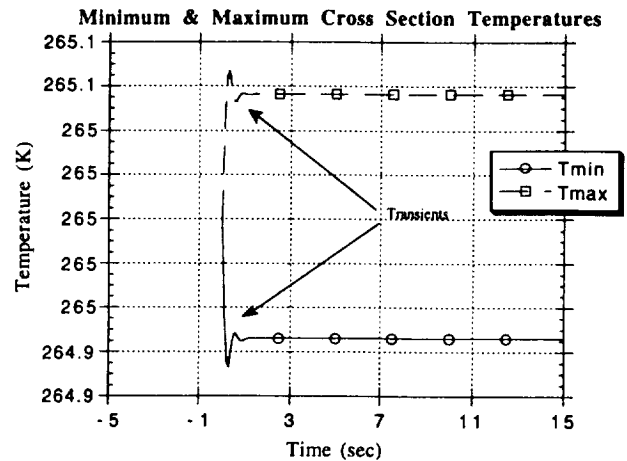


**Figure 6.18**  
Minimum and Maximum Element Temperatures

### 6.3.1.3 Configurational Layout with Thermal Justification

The coating for the LTV truss is white paint. The paint was assumed for analysis to be degraded with emissivity  $\epsilon = 0.90$  and absorptivity  $\alpha = 0.36$ , respectively. The crew module is also assumed covered with the white paint. The fuel tanks were considered as covered with MLI insulation. These are discussed separately due to the unique importance of heat transfer to them.

Three concepts were considered to effect thermal control on the LTV crew module.<sup>6.2</sup> Two are presented in Figures 6.19 and 6.20 below. As shown in Figure 6.19, radiant heat transfer to and from the LTV crew module is regulated with a series of louvers, which are mounted on the octagonal truss structure around the crew module. The louvers consist of flat plates mounted on rods which rotate about a centerline. The louvers are covered with solar cells for power production. The heat transfer to the solar cells on the louvers was not analyzed in detail at this stage of the design. By rotating the louvers open and closed, the effective view factor and absorptivity of the crew module is controlled. The configuration of the louvers during operation of the LTV is such that the louvers on the side of the vehicle upon which sunlight is incident are closed completely to take advantage of the maximum area for solar power collection. On the opposite side of the vehicle, the louvers were assumed to be left open completely to allow for the crew module to radiate to space. By proper implementation of an automatic thermal control system on the vehicle, the louvers would be oriented such that the steady state temperature of the vehicle is constant.<sup>6.2</sup>

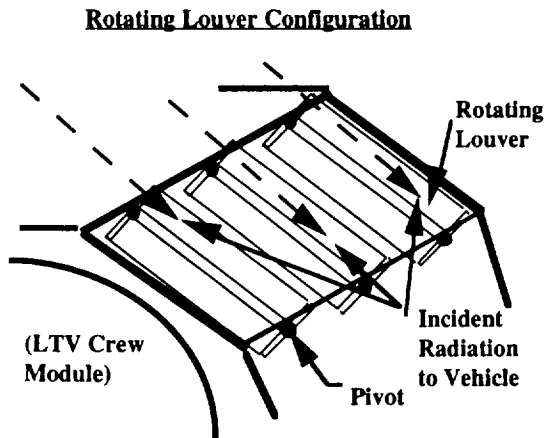


**Figure 6.19**  
Rotating Louvers Configuration

While the louvers allow for a net balance of the thermal energy input to and output from the vehicle, there is no provision for the asymmetric thermal stresses which result from this loading. Two additional concepts were considered to deal with this issue. The first concept is taken from a technique employed during the Apollo missions, which involves axial rotation of the vehicle during transit between the Earth and Moon. The rotation allow for a more distributed thermal loading of the vehicle.

The second concept considered for alleviating the asymmetric thermal loading of the LTV was to include a heat pipe on the crew module.<sup>6.2</sup> Figure 6.20 shows a concept developed for spacecraft to effectively distribute heat around the vehicle surface.

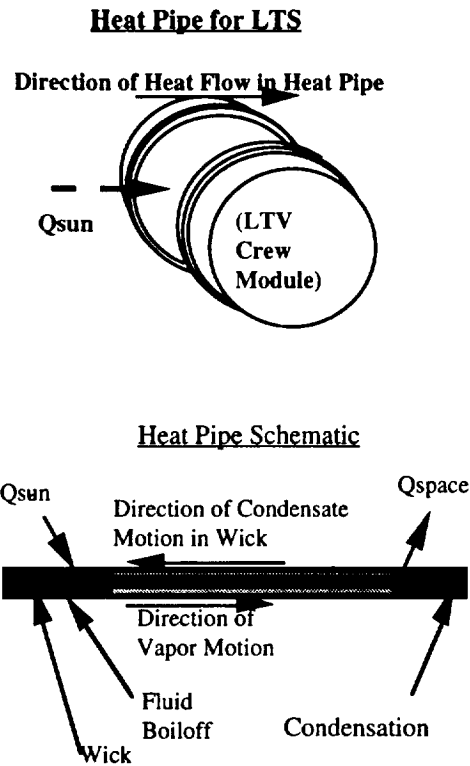


**Figure 6.20** Heat pipe for LTS

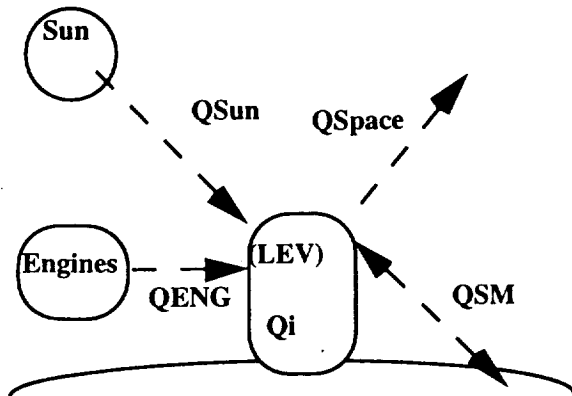
The heat pipe consists of a wick mounted within a tube which is then wrapped around the vehicle surface. The pipe functions when incident radiation to the tube on the thermally loading side of the vehicle boils off the thermal fluid (typically ammonia or some other refrigerant). The vapor expands and travels in the tube around the hull of the vehicle. When it reaches the opposite side of the vehicle, there is a net heat transfer from the pipe to space and hence the fluid condenses. The condensate is then returned to the input side of the vehicle through capillary action due to the wick. The most useful aspect of the heat pipe is that over appropriate temperature ranges, it functions passively; no pumps or compressors are required. The combination of the heat pipe system and rotation of the vehicle was used to provide thermal control for the LTV.

### 6.3.2 Lunar Excursion Vehicle

#### 6.3.2.1 Specification of Design Thermal Conditions / Constraints

In addition to the thermal loads described above for the LTV, the LEV experiences the heat loading environment present on the surface of the Moon. This loading environment is presented in Figure 6.21.<sup>6.2</sup>

### Thermal Loads in Low Lunar Orbit (LLO)



Energy Balance @ Steady State:

$$Q_{Sun} + Q_i + Q_{ENG} = Q_{Space} + Q_{SM}$$

**Figure 6.21**  
Thermal Environment on Lunar Surface

As shown in Figure 6.21, the heat transfer loads to the vehicle in this environment include heat transfer between the vehicle and the sun, between the vehicle and the surface and between the vehicle and the radiating engines after descent.

### 6.3.2 Thermal Analysis of LEV

Thermal analysis of the LEV, other than the analysis of the cryogenic boiloff from the fuel tanks was not completed at the time of this report.

### 6.3.3 Cryogenic Boiloff

Since the LEV requires the use of cryogenic propellants, an investigation of thermal effects on these propellants is required. Several issues arise when transporting cryogenic liquid fuels in the harsh space environment. The boiling temperatures of LH<sub>2</sub> and LOX are approximately 21°K (-252°C) and 92°K (-181°C), respectively. While the average temperature in space is 3°K (-270° C), the intense thermal energy from the sun, radiation reflecting from the earth's surface and radiation reflecting from the moons surface working together, bring the temperature of the cryogenes to their boiling point.<sup>6.3</sup> When this occurs, the fuels inside the tanks evaporate. This evaporation is known as boiloff. If the boiloff is not effectively controlled, it can jeopardize the mission by a reduction in fuel mass and a pressure increase inside the tanks. The increase in pressure is resolved with pressure release valves on the tanks that vent the boiloff vapor to space or redirect it to the fuel cells or

the engines. The loss of fuel mass is critical and is the primary reason for examining boiloff phenomenon.

In considering boiloff rates for the LTS, each tank set is placed into one of four mission phase categories depending on the duration of exposure to thermal energy. These phases are summarized in Table 6.2 below:

Mission Phase	Duration (days)
(1) LTV TLI	7
(2) LEV DESC	10
(3) LEV ASC	24
(4) LTV TEI	27

**Table 6.2** Duration of Tank Exposure

An allowable boiloff percentage for each tank, depending on the duration of exposure to thermal energy, was defined as 1% for the LTV TLI and LEV descent tanks and 5% for LEV ascent and LTV TEI tanks.

### 6.3.2.1 Multi-layer Insulation

The goal for each tank for each mission phase is to minimize the heat leak into the cryogen tanks, since heat leakage is directly related to boiloff. This is accomplished through the use of Multi-layer Insulation or MLI. MLI is a thermal blanket that surrounds each tank. It is assumed that one blanket surrounds each tank and is attached to the tank with velcro straps and Lexan pins.<sup>6.3</sup> An outer jacket surrounds the MLI to protect the tanks from dust and meteoroids. Figure 6.22 depicts the tank configuration incorporating the MLI blanket.

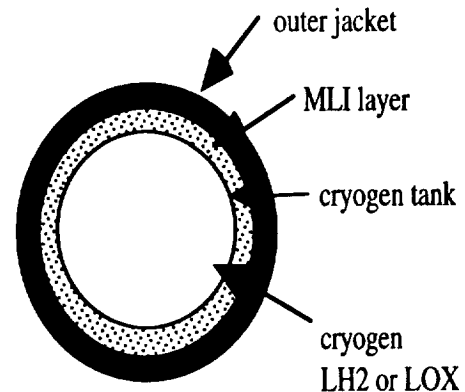


**Figure 6.22** Tank Configuration

The MLI consists of aluminized Kapton shields which are separated by Dacron spacers. The Kapton shields exhibit excellent reflective properties, while the Dacron spacers

serve to minimize conduction between the Kapton shields.<sup>6.3</sup> One Kapton shield and one Dacron spacer comprise one layer of MLI. There are 24 layers per centimeter. This is shown in Figure 6.23.

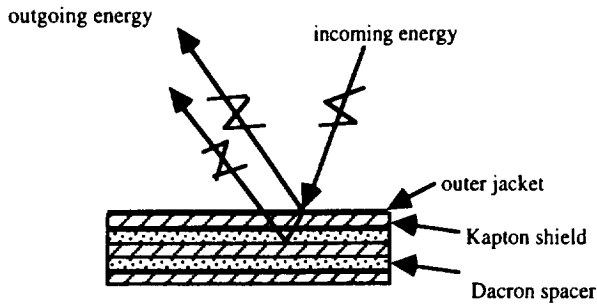


Figure 6.23 MLI layers

The MLI functions as follows: Incoming radiation enters the MLI layers. A good portion of this energy is reflected into space by the aluminized Kapton shield. The remaining energy penetrates deeper into the MLI until it reaches the second Kapton shield, where a significant portion of this energy is reflected into space. The process continues until some of the original energy finally reaches the cryogen.<sup>6.3</sup>

The amount of MLI applied to each tank becomes important when considering the associated weight penalties. Therefore, it is desirable to find an optimum MLI thickness for each tank. The approach to minimize heat leak and therefore minimize boiloff is to determine an optimum multi-layer insulation thickness for each mission phase. The "optimum point" is that MLI thickness at which the "total mass" is a minimum.<sup>6.4</sup> The "total mass" is the sum of the MLI and propellant boiloff masses.<sup>6.4</sup>

### 6.3.3.2 Thermal Analysis of Cryogenic Tanks

The following thermal analysis is adopted from a report by Sverdrup<sup>6.3</sup>. The analysis takes advantage of a computer code, modified to meet the LTS mission specific criteria, that iteratively solves for MLI masses, boiloff masses and total masses in increasing increments of MLI thicknesses. With this data, plots of masses versus thickness are made to determine the optimum thickness for each tank. When considering the thermal analysis, a few factors are important.<sup>6.3</sup>

- (1) radiation from the sun, earth and moon
- (2) radiation between MLI layers
- (3) radiation through seams between layers
- (4) conduction through spacer material
- (5) conduction through pins holding layers together

Major factors influencing boiloff rates need to be considered also. These are:

- (1) boiling point temperature
- (2) tank surface area
- (3) heat of vaporization

A detailed analytical approach of this thermal analysis along with the modified computer code is included in Appendix E.

### 6.3.3.3 Results

MLI thicknesses were determined for each mission phase. The LH2 tanks were assumed to be cylindrical. The LOX tanks were assumed to be spherical. The dimensions, volumes and surface areas used in this analysis are given in the Table 6.3.

LEV LOX DESC	LEV LOX ASC
$r = 1.31 \text{ m}$	$r = 1.07 \text{ m}$
$\text{vol} = 9.5 \text{ m}^3$	$\text{vol} = 5.15 \text{ m}^3$
$\text{s.a.} = 21.57 \text{ m}^2$	$\text{s.a.} = 14.39 \text{ m}^2$
LEV LH2 DESC	LEV LH2 ASC
$l = 6.24 \text{ m}$	$l = 3.37 \text{ m}$
$r = 1.25 \text{ m}$	$r = 1.25 \text{ m}$
$\text{vol} = 30.61 \text{ m}^3$	$\text{vol} = 16.56 \text{ m}^3$
$\text{s.a.} = 58.83 \text{ m}^2$	$\text{s.a.} = 36.29 \text{ m}^2$
LTV TLI	LTV TEI
$l = 9.58 \text{ m}$	$l = 1.42 \text{ m}$
$r = 4.2 \text{ m}$	$r = 4.2 \text{ m}$
$\text{vol} = 531 \text{ m}^3$	$\text{vol} = 78.24 \text{ m}^3$
$\text{s.a.} = 363.65 \text{ m}^2$	$\text{s.a.} = 148.31 \text{ m}^2$

Table 6.3 Physical Properties of Tanks

The optimum MLI thicknesses for each tank are shown in the plots located in Appendix E. The graphs plot mass versus thickness. There are three curves: a MLI mass curve, a boiloff mass curve and a total mass curve. As noted earlier, the "optimum point" is that MLI thickness at which the "total mass" is a minimum. This occurs at the intersection of the MLI mass curve and the boiloff mass curve. At this point, the propellant boiloff savings balance the MLI weight penalty. It is shown from these plots that as the exposure to thermal energy (i.e. trip duration) increases, the boiloff for a given MLI thickness increases, therefore the "optimum thickness" increases. This can be seen by the movement of the "cup shape" of the total mass curve to the right as the trip duration increases. This suggests that optimum MLI thickness is dependent on mission duration.



The resulting MLI thicknesses and corresponding masses for each tank are summarized in tabular form below:

Tank	Thickness	Mass
LTV TLI	1.524 cm	161.9 kg
LEV LH2 des	2.54 cm	49.41 kg
LEV LOX asc	12.7 cm	71.75 kg
LEV LH2 asc	10.16 cm	118.1 kg
LEV LOX des	3.05 cm	33.72 kg
LTV TEI	4.57 cm	167.25 kg

**Table 6.4** MLI Thicknesses and Masses

For each mission, there are two of each of the tanks listed above. Therefore, the total MLI mass is:

Total MLI Mass (12 tanks) = 1024.26 kg (2258.5 lbm)

It should be noted this analysis is a first approach to determine optimum MLI thicknesses. The values for thicknesses and therefore masses are subject to change as fuel masses and tank sizing changes.

## 7.0 CREW SYSTEMS, AVIONICS, AND POWER

### 7.1 Crew Systems Introduction

The crew systems group defines the crew needs and develops the appropriate systems to meet those needs. Crew systems is responsible for the crew module sizing and design, the life support systems and environmental control, radiation protection and the crew functions.

#### 7.1.1 Environmental Control and Life Support System (ECLSS)

The purpose of the environmental control and life support system is to provide the basic functions needed to support life. These functions include atmosphere revitalization, control and supply; temperature and humidity control; water recovery and management; waste management; fire detection and suppression; food storage and preparation; radiation protection; and external dust removal.

##### 7.1.1.1 ECLSS Design Considerations

When designing an ECLS system, there are several factors which determine the systems that will be placed on the spacecraft. The crew size and mission duration affect a number of systems. The amount of consumables needed, the power requirements, hardware design and vehicle mass

are all areas that depend on these parameters. The mission location determines the availability of resupply and the degree of spacecraft self-sufficiency. It also determines the degree of mass loop closure needed. Finally, to satisfy the mission requirements, the system must be designed to have component commonalty, reusability and cost efficiency.

#### 7.1.1.2 Mass Loop Closure

Mass loop closure deals with water and oxygen (O<sub>2</sub>) recovery. The degree of closure depends on the crew size, mission duration and the availability of resupply. Table 7.1 compares several levels of closure and the mission duration supported for the type of closure.

Level of Closure	Type of Closure	Mission Duration
Closed	closed except for losses (e.g. leaks)	permanent bases
Partially Closed	utilizes regeneration techniques to reduce expendables	weeks
Open	all masses brought along or resupplied (no reuse)	days

**Table 7.1**  
Mass loop closure comparison

Closing the loop reduces the amount of consumables that must be brought along; however, reclaiming water and O<sub>2</sub> from waste products requires special equipment. Closing the loop only becomes cost effective when weight savings can be accomplished with the closure.

Both the LEV and LTV will utilize a open loop system for several reasons. The mission length is on the order of six days for the LTV and a matter of hours for the LEV in normal operations. A crew of six requires a relatively small amount of consumables for these mission durations. The LEV and LTV will undergo servicing and resupply at SSF between each mission.

#### 7.1.1.3 Crew Consumable Requirements

For the crew to survive in the space environment, certain needs must be met. Oxygen, water and food must be supplied. A human can survive for only 4 minutes without

oxygen, 3 days without water and 30 days without food. A list of the required consumables<sup>7.1</sup> is given in Table 7.2. The values are based on an average metabolic rate of 136.7 W/person (11,200 BTU/person/day) and a respiration quotient of 0.87.

Consumable	Requirements per Earth Day
Oxygen	0.84 kg (1.84 lbm)
Food Solids	0.62 kg (1.36 lbm)
Water in Food	1.15 kg (2.54 lbm)
Food Prep Water	0.76 kg (1.67 lbm)
Drink	1.62 kg (3.56 lbm)
Metabolized Water	0.35 kg (0.76 lbm)
Hand / Face Wash Water	4.09 kg (9 lbm)
Urinal Flush	0.49 kg (1.09 lbm)
<b>Total</b>	<b>9.92 kg (21.87 lbm)</b>

**Table 7.2**  
Human Daily Consumable Requirements

### 7.1.2 ECLSS Subsystems and Functions

The ECLSS is comprised of several subsystems each of which play an integral part in maintaining ECLS system. The systems that are included in the ECLSS are the Temperature and Humidity Control (THC), Atmosphere Control and Supply (ACS), Atmosphere Revitalization (AR), Waste Management System (WMS) and the Fire Detection and Suppression (FDS).

#### 7.1.2.1 Temperature and Humidity Control (THC)

The THC has several functions. Specifically these functions are air temperature and humidity control, ventilation, equipment cooling, thermally conditioned storage, and particulate and microbial control.

Current THC use a condensing heat exchanger (CHX) to regulate the temperature and humidity of the air (Figure 7.1).

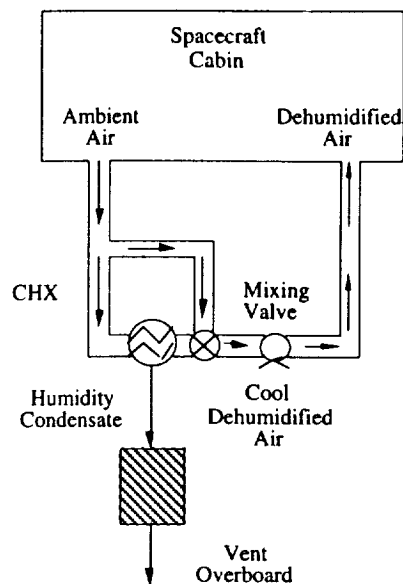


**Figure 7.1** THC Schematic

Temperature is controlled by adjusting the air flow through the CHX. The cabin air loop is separate from the avionics air loop.

#### 7.1.2.2 Atmosphere Control and Supply (ACS)

The ACS primarily controls the O<sub>2</sub> and N<sub>2</sub> storage and distribution, as well as maintain air pressure. Both O<sub>2</sub> and N<sub>2</sub> are stored in high pressure tanks, at supercritical temperatures, external to the LEVCM and LTVCM. On the LEV, oxygen from the power system supply will be used for the cabin air supply to reduce the storage tank masses. The LTV, however; must have its own oxygen tanks since the power is supplied by solar arrays. Nitrogen, however, will have dedicated storage tanks for crew use. Sensors in the ACS will maintain the cabin air in the needed O<sub>2</sub>/N<sub>2</sub> mass and partial pressure ratios.

#### 7.1.2.3 Atmosphere Revitalization (AR)

The AR system is responsible for the removal of CO<sub>2</sub> from the air supply and Trace Contaminate and Control (TCC) monitoring. Both the LEV and LTV will utilize 2 Lithium Hydroxide (LiOH) canisters for the removal of excess CO<sub>2</sub> from the air. For a crew of 4, the LiOH canisters must be replaced every 12 hours and every 8 hours for a crew of six<sup>7.1</sup>. Activated charcoal removes odors and trace contaminants. Screens and High Particulate Atmosphere (HEPA) filters located in the ventilation system aid in the removal of dust particles.

#### 7.1.2.4 Waste Management System

The waste management system encompasses four types of waste products. The metabolic wastes consist of moist solids, i.e. feces and vomitus, and urine. Other solid wastes are generally paper and plastic products. The sources include fax machines and food containers. Liquid wastes are produced by water processors, perspiration and hygiene water. Gaseous wastes are generally produced by respiration. These gases include CH<sub>4</sub>, H<sub>2</sub>S, H<sub>2</sub>, CO, and CO<sub>2</sub>.

Several systems are needed to remove the different waste products from the environment. A Waste Management Facility (WMF) or commode can be used to collect, dehydrate and store feces until the system can be serviced. The commode also collects urine which is vented overboard. The commode can be unreliable; therefore, fecal bags are used as a backup. The waste products in the used bags are mixed with a biocide to prevent the growth of microorganisms. The bags are then stored and disposed of at the end of the mission. The LTVCM will have a commode, similar to the space shuttle's (Figure 7.2), as the primary metabolic waste disposal system, with fecal bags as the backup. The weight constraints on the LEVCM prevent the use of a commode. However, stay times on the LEVCM will be on the order of a few hours in normal operations. The crew pressure suits are capable of collecting the waste products. In abort scenarios, the primary system of waste collection on the LEVCM will be fecal bags.

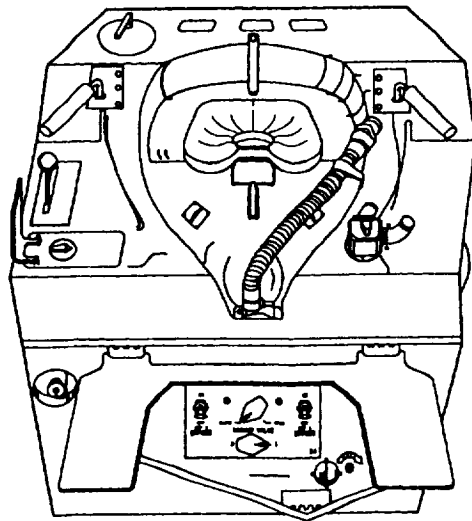


Figure 7.2 Space Shuttle WMF<sup>7.5</sup>

On both the LEVCM and LTVCM, other solid wastes will be collected, packaged and stored onboard. The waste

products are easily removed from the vehicles when they are serviced in LEO.

There are several options for the disposal of liquid wastes. Water residues from perspiration that enter the air can be removed by the Temperature and Humidity Control (THC) system. Depending on the amount of hygiene water, the waste can be vented overboard if the amount is small, or collected and removed during servicing for larger amounts. Other liquid wastes will be stored and removed at servicing. Several processes can be used to remove gaseous wastes from the air. For short missions, CO<sub>2</sub> is commonly removed from the air by lithium hydroxide (LiOH) canisters. The process is non-reversible and the canisters must be replaced periodically. Other gaseous wastes be removed by the Trace Contaminate Control Assembly (TCCA).

#### 7.1.2.5 Fire Detection and Suppression (FDS)

The FDS system uses sensors located in the cabin and avionics air return lines to detect smoke particulate. If a fire is detected, the FDS releases stored CO<sub>2</sub> to suppress the fire.

#### 7.1.2.6 Atmosphere Composition

Historically, spacecraft atmospheres have consisted either of 100% oxygen (i.e. Mercury, Gemini and Apollo) or an oxygen and nitrogen mixture (i.e. Skylab and the Shuttle). The most important air constituent in determining air content is oxygen (O<sub>2</sub>).

There are several requirements for determining the O<sub>2</sub> levels. For long durations, the partial pressure of O<sub>2</sub> must be maintained above 3.0 psi, and the total pressure above 8 psi for normal functioning crew members. A pure oxygen environment can be tolerated at low total pressures (3.75 to 7.3 psia). However, there is a considerable fire hazard in these conditions. To reduce the risk of fire, a physiologically inert gas is combined with the oxygen to increase the cabin total pressure while maintaining the partial pressure of oxygen around 3 psia.

The partial pressure of oxygen is crucial to the crew's health. Table 7.3 indicates the effects of reduced O<sub>2</sub> partial pressures.

Oxygen Partial Pressure (psia)	Effect
3.1	Normal sea level atmosphere level
2.7	Accepted limit of alertness. Loss of night vision. Earliest symptoms of dilation of the pupils.
2.2	Performance seriously impaired. Hallucinations, excitation, apathy.
1.9	Physical coordination impaired. Emotionally upset, paralysis, loss of memory.
1.6	Eventual irreversible unconsciousness.
0-0.89	Anoxia. Near-immediate unconsciousness, convulsions, paralysis. Death in 90 to 180 seconds.

**Table 7.3**  
Effects of Reduced O<sub>2</sub> Partial Pressure

Oxygen partial pressures between 3.1 psia (normal sea level) and 6 psia can also be undesirable. In this partial pressure range, a oxygen toxicity (hyperoxia) occurs. The symptoms are generally respiratory (inflammation of lungs, various heart symptoms). At P<sub>O<sub>2</sub></sub> around 5 psia changes in red blood cell fragility and permeability have been reported at long periods of exposure<sup>7.3</sup>.

Other considerations in the design of the spacecraft atmosphere are the carbon dioxide (CO<sub>2</sub>) and carbon monoxide (CO) levels in the air. Excess CO<sub>2</sub> concentrations (3% and higher) can cause chronic CO<sub>2</sub> toxicity which is characterized by changes in blood pressure, pulse or temperature. The characteristics generally normalize after about a month of breathing normal air. Carbon monoxide is particularly dangerous because it is odorless, colorless, and the symptoms of CO toxicity are not readily noticeable. The ECLSS maintains CO concentrations at acceptable levels.

The current design approach for manned spacecraft atmospheres is the use of a standard sea level atmosphere. This is done for several reasons. The combined O<sub>2</sub>-N<sub>2</sub> atmosphere significantly reduces the risk of a fire. Also,

the higher internal pressure of 14.7 psia reduces the mass of the power system by improving the convection characteristics. Finally, experiments do not have the added complication of nonstandard pressure or atmospheric composition.

Both the LEVCM and the LTVCM will have a standard atmosphere for most on-orbit operations. Table 7.4 indicates the standard partial pressures of a sea level atmosphere.

Parameter	Standard Sea Level Values	
	kPa	psia
Total Pressure	101.36	14.7
Oxygen Partial Pressure	21.37	3.04
Nitrogen Partial Pressure	78.6	11.44
Water Vapor Partial Pressure	1.38	0.2
Carbon Dioxide Partial Pressure	0.04	0.0058

**Table 7.4**  
Standard Sea Level Partial Pressures

It will be necessary to introduce a 100% O<sub>2</sub> and approximately 5 psia environment on the LEVCM for pre-EVA operations to prevent decompression sickness (see section 7.1.7). The reduced pressure environment will be initiated after the LEV landing and will continue through EVA suit donning and vehicle exit.

#### 7.1.2 Crew Module Design Considerations

When designing a crew module, several factors must be considered to make the module and the crew functional in its environment. The modules purpose and functionality, the user and the environment it is operated in must all be taken into account during the design process.

The primary consideration is modules purpose. The primary purpose of the LTVCM is to transport the crew from LEO to LLO and return. The LEVCM has several functions. First, it serves as a transport vehicle between SSF and the LTV. Second, it transports the crew between LLO and the Lunar surface. Finally, in an abort situation, it must be capable of providing life support to the crew until the Lunar surface can be reached.

The user population of the module needs to be considered in the initial design phases. Because of the international cooperation (Japanese to Europeans and Americans) that will be necessary to support a Lunar base and be wide range of people (scientists to pilots) that are likely to travel there, the modules must be designed to accommodate a variety of people. Design limits are based on the 5th percentile to the 95th percentile of the user population. For the purposes of defining limiting sizes of the population, NASA provides information<sup>7.3</sup> on the body sizes of the 5th percentile of Asian Japanese to the 95th percentile of the American male.

Another consideration is the environment the module will be operating in. The LTV operates only in a microgravity environment; while the LEV operates in the microgravity of space, as well as, the 1/6th gravity environment of the Lunar surface. On the LTV, placement of stowage and equipment are not limited by the crew members reach. However, the body assumes a neutral body position (joints bend slightly) in a microgravity environment. A workstation positioned at a comfortable waist level in a gravity environment is not necessarily in a comfortable to work at in a microgravity environment.

### 7.1.3 LTV Crew Module

The LTVCM is designed to support a crew of 6 for the transit between LEO and LLO. All life support systems on the LTVCM are independent of the LEVCM. In the event of a system failure, the LEV can take over life support functions.

#### 7.1.3.1 Dimensions and Structural Mass

A Space Station Common Module (SSCM) is used for the LTVCM. By using a module that is already in production, costs are minimized. Also, much of the hardware used on future Lunar missions (i.e. FLO) scenarios is developed for the SSCM.

The external dimensions of the LTVCM are shown in Figure 7.3. The modules outside diameter of 4.42 m (14.5 ft) is determined by the maximum diameter that the Space Shuttle payload bay is capable holding (SSF modules will be deployed by the shuttle). A length of 5 m (16.4 ft) was determined to be adequate for the mission. The 5 m length gives ample room to carry out in transit experiments and provides relatively comfortable living space.

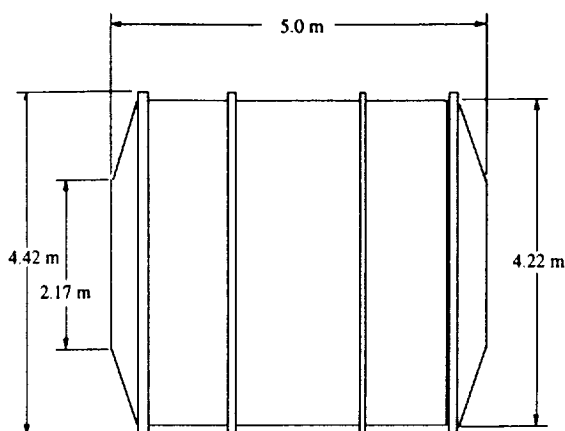


Figure 7.3 LTVCM External Dimensions

The structural mass of the module was determined from SSCM data<sup>7.4</sup>. The mass of the primary structure is 3712 kg (8184 lb) and the mass of the secondary structure is 1657 kg (3653 lb). Appendix F gives a breakdown of the primary and secondary structural components and masses.

#### 7.1.3.2 Internal Layout

The usable internal dimensions of the module are given in Figure 7.4. All four sides of the module contain racks 1.016 m (40 in) deep. The racks provide structural support to the module cylinder and contain the systems which will be used in the module (i.e. galley, science station, ECLSS). A 0.1016 m (4 in) space is provided between the racks and the module wall for plumbing. The usable width and length of the module are 2.19 m (7.19 ft) and 4 m (13.12 ft), respectively.

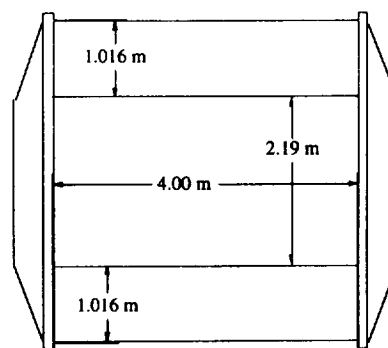
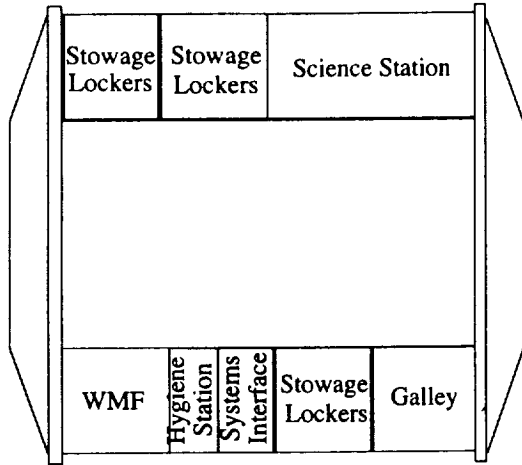


Figure 7.4 LTVCM Internal Dimensions

The placement of internal components is shown in Figure 7.5. The science station was placed opposite the galley and WMF to better distribute the weights along the x-axis of the module. The WMF was placed on the module end opposite of the galley to reduce the chance of bacteria spreading. The personal hygiene station was placed next to the WMF for

the same reason. A systems interface panel was added to allow the crew members to control certain functions of the module (i.e. temperature) and to display systems status to the crew. Stowage is provided in several locations throughout the module.



**Figure 7.5** LTVCM Component Layout

The science station will carry crew oriented and autonomous experiments that will be carried out throughout the mission. Several hours of the crews schedule is set aside for performing experiments during the transit. The autonomous experiments can be run in transit and also in LLO while the crew is on the surface. These experiments offer an advantage over SSF since the LTV will provide a stable platform in microgravity, free of crew disturbances. The science station experiments will be a modular design so that they can be readily swapped for other experiments during LTS servicing in LEO

The galley serves as a food preparation facility. It contains areas to store the food, meal accessories, tray and food related trash. The oven can heat meals for up to seven persons in approximately 90 minutes. A diagram of the galley is given in Figure 7.6.<sup>7.5</sup>

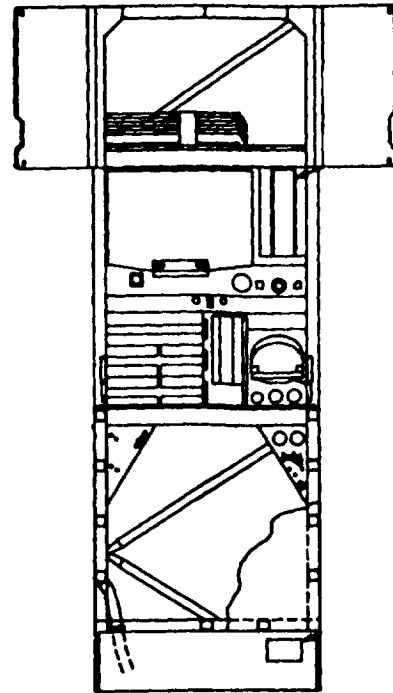


**Figure 7.6** Space Shuttle Galley<sup>7.5</sup>

### 7.1.3.3 LTV Consumable Requirements

The consumables for the LTVCM include food, water, O<sub>2</sub> and N<sub>2</sub>. The mass of the consumables depends on trip duration and crew size. Trip time is considered to be 6 days with a 48 hour contingency. The number of crew members is assumed to be 6 (for steady state operation).

Each crew member requires 0.62 kg (1.36 lb) of food per day which is provided in snacks and three meals for each normal day in transit. The food consists of individually packaged re-hydratable items.

The water requirements for the crew members are 15 kg (33.1 lb) per person per day. The water will be used for food preparation (rehydration), drink, hand and face wash water and urinal flush. Water for the LTV must be brought along from LEO since the power system utilizes a solar array instead of fuel cells which create water. The water will be stored in tanks external to the crew module. The crews water requirements are 720 kg (1587 lb) for normal operations and contingency. The science station may also require a water supply; therefore, 280 kg (617 lb) has been included in the mass estimates. The total LTV water requirements are 1000 kg (2204 lb).

Oxygen and nitrogen requirements are not only based on the amount needed for metabolic purposes, but also on the

internal volume and number of repressurizations. For the analysis it was assumed that the LTVCM would undergo 6 repressurizations. This gives a total O<sub>2</sub> mass of 200 kg (441 lb) and N<sub>2</sub> mass of 650 kg (1433 lb).

### 7.1.3.4 LTVCM Power Requirements and Vehicle Total Mass

The average power required for the ECLSS and internal components is 3.1 kW. The total wet mass of the LTVCM is 9809 kg (21625 lb). A detailed breakdown is given in Appendix G.

### 7.1.4 LEV Crew Module

The LEVCM supports a crew of six for both descent and ascent operations to the Moon. It also serves as a transfer vehicle between SSF and the LTV during normal operations. In the event of an LTV ECLSS failure or an abort due to the NTR, the LEVCM is capable of providing primary life support to the crew.

#### 7.1.4.1 Dimensions and Structural Mass

Like the LTVCM, the LEVCM also utilizes the SSCM. The exterior dimensions (diameter and length) of the module are the same as the LTVCM (see Figure 7.3). The mass of the primary structure is 4278 kg (9431 lb). The mass of the secondary structure is 1657 kg (3653 lb). Appendix H gives a detailed breakdown of the structural masses.

#### 7.1.4.2 Internal Layout

The dimensions of the internal usable space on the flight deck and dust containment deck (DCD) are 2.2m by 2.2m (7.22 ft by 7.22 ft). These dimensions were determined from the internal diameter of the module (4.22 m) and the rack depth (1.016 m). The usable length of the module is 4 m (13.1 ft). The height of the dust containment deck was chosen to be 2.10 m (6.9 ft) so that a crew member would be able to comfortably stand in the DCD while donning an EVA suit. The height of the flight deck is 1.75 m (5.74 ft). This was deemed adequate since crew will be in a microgravity environment or seated for the majority of the time they occupy the flight deck. Once on the Lunar surface, the crew can move into the DCD.

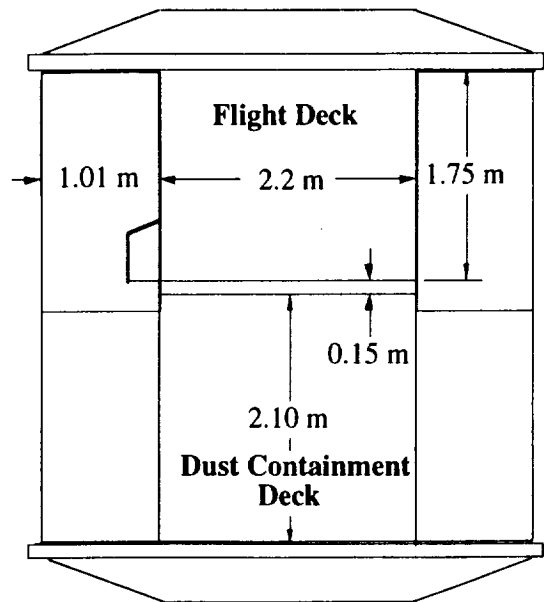


Figure 7.7 LEVCM Internal Dimensions

Figure 7.8 depicts the layout of the flight deck. The Commander (CDR) and Pilot (PLT) each have a side panel containing system interfaces. The side panels give both the CDR and PLT access to system function controls with minimal movement. The side panels are also less likely to be bumped, inadvertently changing switch positions, when crew members are entering or exiting their seats. The panels directly in front of the CDR and PLT contain the CRTs for monitoring the functioning of various systems, as well as, screens which will display images from the externally mounted video cameras.

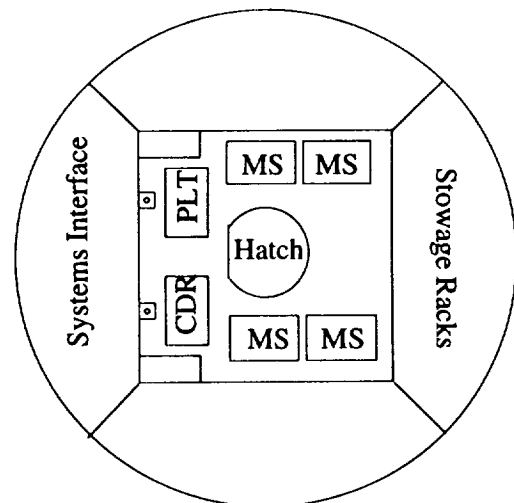


Figure 7.8 LEVCM Flight Deck Layout

The Mission Specialists' (MS) seats (Figure 7.9) were rotated 90 degrees to allow for more leg room and easier mobility in the 1/6 g environment of the Moon. The MS seats are removable and can be folded to a height of 0.28 m (11 in) for stowage (Figure 7.10). The seats can easily be stored in lockers while on orbit to give more room in the LEVCM. Before undocking from the LTV, the seats can be secured in place for the Lunar descent. On the surface, it may be desirable to remove the same seats from the flight deck and place them in the airlock area for use in the EVA suit donning.

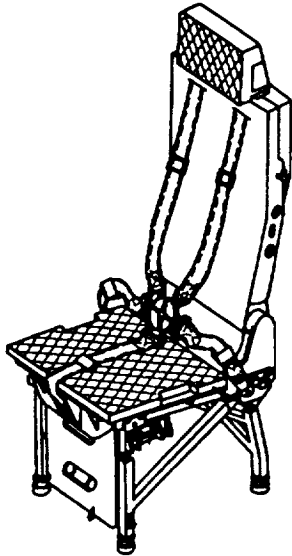


Figure 7.9 Mission Specialist Seat<sup>7.5</sup>

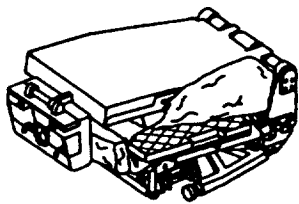


Figure 7.10 Mission Specialist Seat in Stowed Position<sup>7.5</sup>

The pilots seats (Figure 7.11) are permanently mounted to the LEVCM floor. The Rotational Hand Controller (RHC) used to fly the vehicle is mounted onto the seat frame. For both the MS and PLT, a portable life support system can be attached to the seat. This life support system is used by the crew members while in pressure suits.

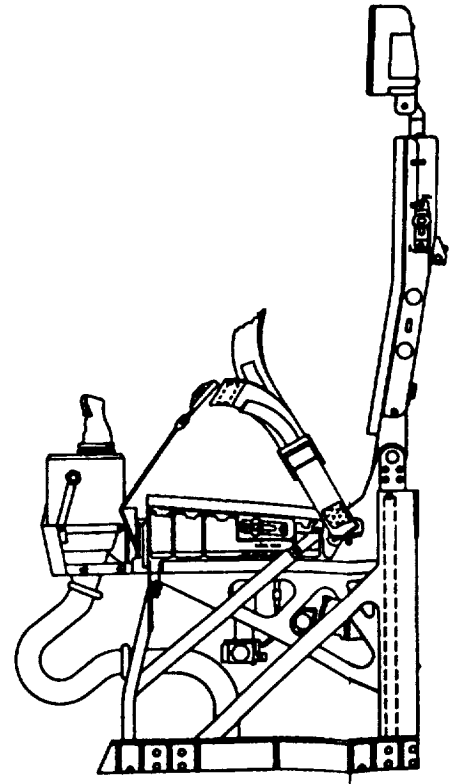


Figure 7.11 Pilot Seat<sup>7.5</sup>

#### 7.1.4.3 LEV Consumable Requirements

Consumables for the LEVCM are considerably less than the LTVCM in normal operations. In the event of an abort from the LTV, the LEVCM must be able to sustain a crew of 6 for up to 3 days. The LEVCM will carry 7.44 kg (16.4 lbm) of food, enough for one meal per crew member. The meals can be rehydrated with a small water dispenser (Figure 7.12) located on the flight deck. The water dispenser will draw water from a storage tank used to collect the fuel cell water.



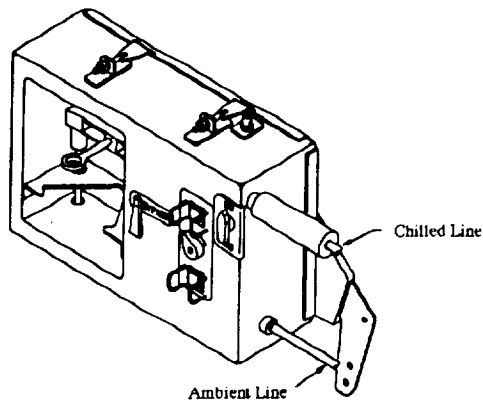


Figure 7.12 Water Dispenser<sup>7.5</sup>

The O<sub>2</sub> and N<sub>2</sub> supplies allow for 3 days of normal use with 24 hours as a contingency and 6 repressurizations. The total mass of consumables for the LEVCM is 943.5 kg (2081 lb). A breakdown of consumable masses is given in Appendix H.

#### 7.1.4.5 Power Requirements and Total Vehicle Mass

The LEVCM power requirements are considerably less than those of the LTVCM. The ECLSS system consumes most of the LEVCM power needs. A vacuum located in the DCD used during EVA activities and a water dispenser located on the flight deck for aborts and Lunar activities both use a small amount of power. The average power requirement for these systems is 2.8 kW. The total wet mass of the LEVCM is 9360 kg (20635 lb). A breakdown of the power requirements and masses are given in Appendix G.

### 7.1.5 Radiation

The two types of radiation that the crew will be exposed to in space flight are Ionizing and Non-Ionizing Radiation. Non-Ionizing Radiation (NIR) is generally not energetic enough to break molecular bonds. Most of the NIR that the crew would be exposed to comes from within the spacecraft from sources such as communications and electronic equipment, lasers etc. Ionizing radiation breaks chemical bonds within biological systems. The effects are dependent on the radiation type (e.g. gamma, X-ray, electron) and magnitude as well as the tissue effected. Sources of ionizing radiation are naturally and artificially generated. The three main sources of natural radiation are geomagnetically trapped radiation; galactic cosmic radiation (GCR); and solar particle event radiation (SPE). Artificial sources occur from on-board electric power sources such as radioisotopes and nuclear reactors, small radiation sources and induced radioactivity.

#### 7.1.5.1 Definition of Terms

##### Dose (D):

- The amount of radiation energy absorbed by the tissue.
- Common unit of measure is the rad (1 rad = 100 ergs/g of material)
- SI unit is the gray (Gy); 1 Gy = 100 rads

##### Linear Energy Transfer (LET):

- The rate of energy dissipation along the path of a charged particle.
- Units are keV/μm

##### Quality Factor (Q):

- An artificial factor dependent on the LET of which biological effects from absorbed doses may be related to x- and gamma radiation (how much biological damage) having units which are non-dimensionalized

- Values are based on the most detrimental biological effects from continuous low dose exposure. Values for many high rate exposures may be considerably lower

##### Dose Equivalent (DE)

- The amount of biologically damaging ionizing radiation
- Common units of measure are rem (roentgen equivalent man)
- SI unit is sievert (Sv) where 1 Sv = 100 rem
- DE = D X Q (dose times quality)

##### Relative Biological Effectiveness (RBE)

- Nondimensional parameter related to but different from Q.
- Based on experimentally determined effects of different types of radiation on biological systems

#### 7.1.5.2 Radiation Exposure Limits

Radiation exposure guidelines have been established to define how much ionizing radiation a person can be exposed to. Tables 7.5 and 7.6 describe the short term dose equivalent limits and career limits for protection against non-stochastic effects.

Time Period	BFO* (Sv)	Lens of Eye (Sv)	Skin (Sv)
30 day	0.25	1.0	1.5
Annual	0.50	2.0	3.0
Career	see Table 7.6	4.0	6.0

\*Blood Forming Organs (BFO) denotes the dose at a depth of 5 cm (1.97 in).

Table 7.5  
Short Term Dose Equivalent Limits

Age (years)	Female (Sv)	Male (Sv)
25	1.00	1.5
35	1.75	2.5
45	2.00	3.2
55	3.00	4.0

**Table 7.6**  
Career Whole Body Dose Equivalent Limits

The limits in Table 7.6 are based on a 3% lifetime excess risk of cancer mortality.

### 7.1.5.3 Radiation From NTR

To determine if any radiation shielding is necessary, the amount of radiation exposure must be estimated. It was determined that the crew can expect to receive 5.48 rems per mission (2.74 rems per transit leg) from the NTR.<sup>7.6</sup> This figure assumes that the center of the crew module is 46.8 m from the center of the reactor core and that the BATH radiation shield is in place. The amount of background radiation (GCR) at an altitude of above 38000 km with no shielding is 57 rems per year. This equates to approximately 1 rem per mission. The combined radiation levels due to the NTR and GCR for a 3 day transit to or from the Moon is 4 rems. This level of radiation exposure falls well within the NASA guidelines of 25 rems in a 30 day period.<sup>7.2</sup>

To reduce truss weight, it is desirable to decrease the distance between the crew module and the center of the core. It was determined that the radiation level is inversely proportional to the square of the distance. Using a separation distance of 46.8 m and radiation dosage of 5.48 rems, a multiplier of 12000 was calculated. This gives the following equation for the variation of radiation with distance for the LTS NTR:

$$Re\ ms = \frac{12000}{r^2}$$

This formula with a length of 33 m gives a mission radiation level of 11.02 rems. For the three day trip to the Moon, the total radiation level is approximately 6.5 rems. The combined radiation dosage due to the background radiation and the NTR radiation per mission is approximately 13 rems. Exposure levels on the lunar surface should be minimal since the habitation module will be buried in the regolith for radiation shielding. These radiation levels again fall within the NASA guidelines for both the 30 day and 1 year exposure limits.

### 7.1.5.4 Types of Radiation Shielding

To protect the crew from radiation overexposure, radiation shielding must be used. Electromagnetic shielding deflects the charged particles. This type of shielding is impractical due to its weight and power requirements. Chemical protectors involve injecting chemicals into the blood. These protectors have adverse side effects, only protect against low LET radiation and have only been successfully used on animals.

Mass shielding offers the best means of protecting the crew from radiation overexposure. With mass shielding, the structure provides protection from radiation. The outer skin of the spacecraft and associated structural elements can be used as a radiation shield. Strategically placing massive internal components can also increase radiation protection. However, this method only provides protection in certain directions.

There are a number of materials that provide radiation shielding. Aluminum provides good radiation protection for all types of radiation. Polyethylene has good protection for electron radiation and lead protects against bremsstrahlung or high power radiation.

### 7.1.5.5 Radiation Shielding Recommendations

The NTR has two radiation shields included in the design. The internal shield primarily protects the turbomachinery. The external shield, located between the NTR and the truss (Figure 7.13), provides radiation protection for the crew. The external shield is made of Borated Aluminum Titanium Hydride (BATH). The shield is 2.54m (8.3 ft) in diameter, 0.186m (7.3 in) thick and weighs 4t.

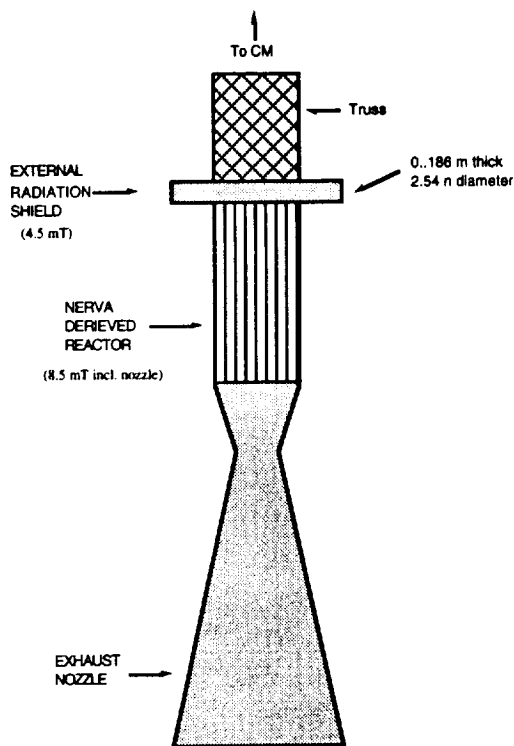


**Figure 7.13**  
BATH Radiation Shield Location

Additional radiation shielding is provided by massive objects placed between the radiation source and the crew member. The end cones and standoff structure of the LTVCM will provide some shielding from NTR radiation.

The LEVCM can serve as a storm shelter in the event of an in transit SPE. The pre-descent LEV is surrounded by LOX and LH<sub>2</sub>. This provides an ideal mass shield. The LTV could also be reoriented so that the X axis is aligned with the radiation source (the sun). This will allow the maximum amount of mass to absorb the radiation before it reaches the crew.

### 7.1.6 Lunar Dust

A special consideration in the design of the LEVCM were problems with the lunar dust. There are several characteristics of lunar dust that make it especially difficult to control. Electromagnetic potential causes the dust to levitate near the terminator and the dust has sharp edges which dig into the surfaces it comes into contact with, making it harder to remove.

Dust containment on the LEV is important for two reasons. First, unlike Apollo, the LTS is reusable. The internal components must be protected from contamination which may reduce their usable life span. Second, the LEV serves

as the transfer vehicle between the LTV and SSF. The integrity of the experiments on SSF could be jeopardized if Lunar dust were to enter the air supply.

To contain the dust from the surface, the LEVCM utilizes a Dust Containment Deck (DCD). The crew will don and doff the EVA suits in this area. Upon returning to the vehicle, the crew will doff their suits and remove as much dust as possible with a small vacuum located in the DCD. The crew will then enter the flight deck and seal the hatch between the two decks. The hatch will remain sealed until a more thorough cleaning can take place during servicing. Another method the crew will use to prevent LEV dust contamination is overalls worn over the EVA suit. The overalls will be removed and stored immediately prior to entering the LEV. The overalls will not only prevent dust from entering the vehicle, but will also help prevent excessive wear on the suits from the dust.

### 7.1.7 Decompression Sickness

Decompression sickness can result if the change in pressure (from cabin pressure to the EVA suit pressure) is rapid enough and has a large differential. The most common symptom of decompression sickness is the bends. The bends is characterized by extreme pain in the joints when it is being flexed. It usually begins in the tissue around the joints and extends along the bone shaft. The chokes is the next most common symptom. The chokes are characterized by chest pain, cough and respiratory distress. The chokes generally requires longer altitude exposure than required for the bend.

Decompression sickness is impossible to predict. However, if the supersaturation ratio (partial pressure of N<sub>2</sub>/total barometric pressure) exceeds 1.22 there is a risk of decompression sickness. Several factors can cause increased susceptibility to decompression sickness; obesity, very cold temperatures, exposure to compressed air breathing within 24 hours of decompression, age, physical exertion and injuries.

## 7.2 Avionics Introduction

In order to reach its destination, the LTS must have a system of avionics. This system will entail a set of subsystems that include communications, GN&C, and data management. Failure of any of these systems can lead to a major mission catastrophe.

### 7.2.1 Avionics Requirements

A primary requirement of the LTS avionics is that it be useful for both piloted and unpiloted missions. All

subsystems must be controllable by both pilots and ground controllers.

The avionics will also be required to be largely redundant. A failure will still permit the LTS to function smoothly. Too guard against faults, much of the avionics will have multiple redundancy.

Subsystem avionics will be nearly identical on each crew module. The LTV will contain the main avionics because that module will be the CM for steady-state operations. The LEV will only be used for the lunar descent and ascent and in case of LTV failure.

## **7.2.2 Communications**

Communications with the spacecraft are vital for mission success. Communication is more than just audio and visual interaction. It also includes commands to the crew, commands to the hardware on the spacecraft, and tracking.

### **7.2.2.1 Communication Bands**

Two communication bands will be used throughout these Lunar missions. The first will be the Ku-band. The frequencies of the Ku-band are between 12 and 14 GHz.<sup>7.7</sup> This will be the primary band used for all communication. The second band is the S-band. It operates near the 2 GHz<sup>7.7</sup> frequency range. Although the S-band will be used primarily as a back-up, it will also be used for some routine communication.

The Ku-band is selected as the primary communication band because of its high frequency. Signals sent on high frequencies have lower power requirements than those sent on lower bands. However, signals sent to Earth on high frequencies tend to dissipate in bad weather near ground stations. In severe weather, signals can be completely dissipated. Lower frequencies can withstand inclement weather. That is the reason for selecting the S-band as a communications backup. The disadvantage in these lower frequencies is the higher power requirements.<sup>7.7</sup>

### **7.2.2.2 Tracking and Data Relay Satellite System (TDRSS)**

The TDRSS is an existing system of satellites designed to track and relay data to and from vehicles in space. This also includes orbiting satellites. It can operate on most frequency bands, but mainly utilizes the Ku and S bands.<sup>7.8</sup> TDRSS uses three ground stations around the earth to assist in its operation. Their locations are in Goldstone, California; Canberra, Australia; and Madrid, Spain.<sup>7.9</sup>

### **7.2.2.3 Advanced Tracking and Data Relay Satellite (ATDRSS)**

The ATDRSS uses the same concept as the TDRSS only more advanced. The communication bands of the ATDRSS will remain the Ku and S bands. The specifics of the ATDRSS are still being studied. NASA does not know if it will merely add on to or create a whole new system to replace the existing TDRSS.<sup>7.10</sup> Nevertheless, at the time of these lunar missions, the ATDRSS is scheduled to be in place.

### **7.2.2.4 Antennae**

Several antennae will be used by the LTS. Two main antennae, in particular, will be utilized, one carrying Ku-band and the other S-band. Both steerable antennae will be attached to the LTV. The antennae will send and receive the bulk of the communications necessary for the LTS.

To assist the main antennae, several omnidirectional antennae will be placed on each crew module. These are not steerable. They are placed on the surface of the crew modules such that communications can be sent in any direction from each module.

On the lunar surface, erectable, or possibly semi-permanent, antennae will be in place. These can be erected by the first crew to the lunar surface. These type of antennae will be used for main communications while on the lunar surface.

### **7.2.2.5 Video Cameras**

Several video cameras will be placed on the LTS. Two will be placed on the LTV for docking assistance. Another pair will be placed on the LEV for lunar landing assistance. Additionally, there are six other cameras on the LTS. Each module has one internal camera similar to that carried on the shuttle. These cameras will show what is going on inside the crew modules. The remaining four cameras are on the LEV's lander truss. The truss mounted cameras will provide pictures of the landing area for the crew and ground stations. Each of these cameras have a pan/tilt unit. Thus, the cameras can be moved at will.

## **7.2.3 Guidance, Navigation, and Control (GN&C)**

Guidance of the spacecraft is necessary to ensure that it reaches its destination. Navigation accurate to within a small error is made easier with GN&C equipment, such as gyroscopes, accelerometers, and sensors.

### 7.2.3.1 Hexad Navigation Unit

Gyroscopes, accelerometers, and IMU's are normally used for GN&C. However, a new product has been created. It is the Hexad Inertial Navigation Unit, commonly referred to as just Hexad. It contains a set of laser-ring gyroscopes, accelerometers, and IMU's all in one unit.<sup>7.11</sup> This unit will provide improved navigation over individual pieces of equipment.

Gyroscopes measure the vehicle's angular rates of the about pre-designed axes. These measurements are then sent into an onboard computer for processing.<sup>7.11</sup> In the Hexad, laser ring gyros replace traditional gimbal gyros. A laser ring of light provides a closed path, or loop. Two counter-rotating laser beams circulate in this ring. When the gyro is rotated the path lengths for the beams change, one becomes longer while the other becomes shorter. This causes a phase shift in the beams. When the shifted beams are combined the phase difference describes the rate of rotation.<sup>7.7</sup>

Accelerometers measure normal and lateral acceleration. These are used for flight control calculations. These measurements are also sent to the flight computer.<sup>7.11</sup>

IMU's supply the vehicle with attitude and acceleration data. IMU's are normally installed on a rigid, structural beam.<sup>7.11</sup>

The Hexad is a new piece of equipment. It is not space rated at this time.<sup>7.11</sup> It is assumed to be space rated by the time these missions are ready to commence.

### 7.2.3.2 Star Trackers

Star Trackers are sensors that assist in navigation by aligning themselves with select stars. These sensors are supplied with a "star catalog" software program to determine where certain stars are and to identify them. They measure changes in the vehicle motion relative to these stars.<sup>7.7</sup>

Early Star Trackers had to select certain stars from all visible stars. This also required astronaut expertise of constellation and star recognition. Current Star Trackers block out distant stars or stars with small light output. They also have shielding to protect themselves from the intensity of the sun as it is too bright for this instrument.<sup>7.7</sup>

### 7.2.3.3 Sun Sensors

Sun Sensors are another type of sensor that assists navigation. They "see" where the sun is. These sensors measure angles that the sun makes in body coordinates. Sun

Sensors, along with Star Trackers, are used to calibrate the IMU's inside the Hexad.<sup>7.7</sup>

### 7.2.3.4 Landing and Docking

Landing and docking will be assisted by three items. The first two, radar and lighting, have been used extensively in the past. Radar works like a homing device and can tell how close a vehicle is to its intended target. Video cameras will also be used. These will assist a great deal in minimizing time and fuel consumed for landing and docking operations. With this equipment, automatic docking may be possible. Currently, only the former Soviets have accomplished automatic docking.

### 7.2.4 Data Management

Data management is a set of hardware which stores and retrieves data for any subsystem on a spacecraft. Most data used is by the GN&C. Data can be sent from anywhere via communication links, sensors, guidance equipment, crew commands, computer software, and other computer hardware.<sup>7.11</sup>

### 7.2.5 Crew Interface

Though the crew will have a large amount of electronics to work with, this design focuses only on what the pilots will use. The pilots will have a set of instruments that will include video displays of the landing area, video controllers, Rotational Hand Controllers (RHC), keyboards, and warning lights.

#### 7.2.5.1 Glass Cockpit

To make the flight as easy as possible, CRT screens will be installed on each flight deck. These screens will be used to show normal flight operations, display information entered from the keyboards, and to communicate with the crew in the event of audio blackout. The most important advantage will be the ability to instantly inform the crew in the case of a system failure or similar problem

#### 7.2.5.2 Video Control

Also available to the crew will be another set of screens which will be able to display any available camera angle. Ground stations will have similar control for unpiloted missions.

### 7.2.6 Avionics Summary

Lists of all the avionics for the LTS are contained in the Appendices. Appendix I details the LEV's avionics. Appendix J describes the LTV's avionics. Masses for each LTS avionics subsystem are listed in Table 7.7.

Subsystem	LEV Mass (kg)	LTV Mass (kg)
Communication	157.4	151.4
GN&C	213.2	200.0
Data Manage.	52.6	62.6
<b>Total</b>	<b>423.2</b>	<b>414.0</b>

**Table 7.7** Avionics Subsystem Masses

Thus, the total mass of the LTS avionics is 837.2 kilograms.

### 7.3. Power System Introduction

Electrical power generation, distribution, and control is another focus of Crew Systems, Avionics, and Power. Electrical power is a necessity for the systems on board the Lunar Transportation System.

The electrical power requirements of the LTS are comprised of the needs of the crew systems, avionics equipment, propulsion systems, and allowance for future growth. These power requirements are met by the electrical power production devices on the LTS and are delivered by means of the Electrical Power Distribution and Control (EPD&C) assemblies.

#### 7.3.1 Power Requirements

The power requirements for the LTS are best broken down into the primary mission occurrences with respect to power demanded. These four mission occurrences consist of the LTV and LEV docked and sharing power generation systems, the occupied LEV undocked from the LTV, the unoccupied LTV with the LEV undocked, and the unoccupied LEV under low power consumption during periods on the Lunar surface. The power requirements for these four mission occurrences are represented in Figure 7.14.

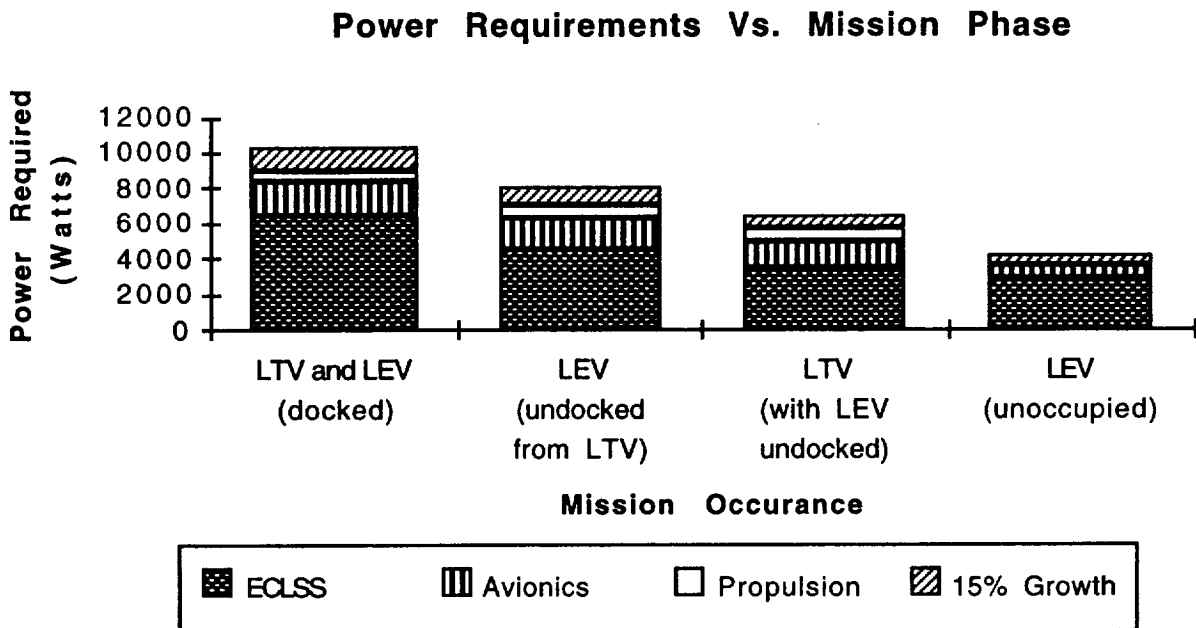


**Figure 7.14** Power Requirements vs. Mission Phase

The power number presented represents the peak load power requirement for the corresponding mission occurrence. System power requirements are a summation of the individual sub-system power requirements as obtained from documentation concerning the individual sub-systems. For more information on these system power requirements please reference relevant sections in this report along with Appendix G, Appendix I and Appendix J. The amount of power allotted for the propulsion systems of the LEV and LTV is representative of a cryogenic propulsion system.<sup>7.12</sup> A fifteen percent growth factor is added to the total of the operating power load to allow for the addition of other systems at a later date.

**7.3.1.1 LTV and LEV Docked**

The first of the mission occurrences affecting power requirements occurs while the LTV and the LEV are docked together. An example of this is situation occurs during TLI and TEI . During these times the total power demanded is slightly less than 10.3kWe. The power consumption of each system of the LTS while the LTV and LEV are docked is represented in Table 7.8.

System	Power (We)
LTS ECLSS	6373
LTS Avionics	1929
LTS Propulsion	650
15% Growth	1342
<b>Total</b>	<b>10294</b>

**Table 7.8**  
LTS Power Requirements (LEV and LTV Docked)

**7.3.1.2 Occupied LEV Undocked from LTV**

A separate mission occurrence is while the occupied LEV is undocked from the LTV. During such times the LEV is typically under one of the following conditions: ferrying the crew from SSF to the LTV, transporting the crew from LLO to the Moon's surface and back to LLO from the Moon's surface, ferrying the crew from the LTV to SSF, operating as part of an abort scenario, or performing as a temporary shelter on the Lunar surface. The power required by the LEV under these circumstances is presented in Table 7.9.

System	Power (We)
LEV ECLSS	4414
LEV Avionics	1929
LEV Propulsion	650
15% Growth	1048
<b>Total</b>	<b>8041</b>

**Table 7.9**  
LEV Power Requirements (undocked and occupied)

**7.3.1.3 Unoccupied LTV with LEV Undocked**

Another possible occurrence with respect to power consumption occurs when the LTV is unoccupied and the LEV detached and operating independently. The power requirements of the LTV while unoccupied is represented in Table 7.10.

System	Power (We)
LTV ECLSS	3410
LTV Avionics	1559
LTV Propulsion	650
15% Growth	842
<b>Total</b>	<b>6461</b>

**Table 7.10**  
LTV Power Requirements (unoccupied on orbit)

**7.3.1.4 LEV Unoccupied on Lunar Surface**

The LEV will achieve its lowest power requirement while on the Lunar surface. During this time the ECLSS system will be powered down to run at a reduced load primarily to control the temperature and humidity in the LEVCM. The avionics will be operating at minimal power levels; however, the avionics are expected to be able to provide some communication and data handling capabilities while the LEV is unoccupied on the Lunar surface. The propulsion system of the LEV will be entirely shutoff during this interval. While the LEV is on the Lunar surface the power demanded will be approximately 4.2kWe as shown in Table 7.3.4.

System	Power (We)
LEV ECLSS	2820
LEV Avionics	826
LEV Propulsion	0
15% Growth	546
<b>Total</b>	<b>4192</b>

**Table 7.11**  
LEV Power Requirements (unoccupied on surface)

### 7.3.2 Power Generation Systems

Several systems for meeting the power requirements of the LTS were examined. These included batteries, flywheel systems, photovoltaic arrays, open loop fuel cells, regenerative fuel cells, radioisotope thermoelectric generators, nuclear reactor power systems, and others. Of these systems the flywheel and radioisotope thermoelectric generators were eliminated due to lack of a space qualified system and poor efficiency, respectively. The power systems that have been designed for the LTS will incorporate the use of a photovoltaic arrays, fuel cells, and batteries.

#### 7.3.2.1 Battery Systems

Battery systems are and will continue to be the primary means of electric energy storage onboard spacecraft. Batteries are generally divided into two major categories: primary and secondary. Primary batteries typically have high power densities but are non-rechargeable. These batteries are especially well adapted to one-time events. Primary batteries have historically been silver-zinc batteries with a limited cycle life; however, more recently lithium batteries having greater power densities and capabilities for recharge have gained acceptance. Secondary batteries are strongly suited to continuous charging and discharging. Nickel-cadmium batteries are the predominant type; however, nickel-hydrogen batteries are becoming more prevalent due to their greater charge per unit mass and depth of discharge capabilities.<sup>7.7</sup>

Table 7.12 lists popular chemical battery types, their energy densities, and pros or cons.<sup>7.7</sup>

Battery Type	Energy Density	Pro/Con
Silver-zinc (Ag-Zn)	175 W-hr/kg	Limited life cycle
Nickel-cadmium (NiCd)	15-30 W-hr/kg	Low energy density Long life Deep discharge tolerant
Nickel-hydrogen (NiH <sub>2</sub> )	40 W-hr/kg <sup>7.13</sup>	High pressure Promise high energy densities
Lithium (LiSOCl <sub>2</sub> )	650 W-hr/kg	Very high energy density Higher Cell Voltage
Lithium (Li-V <sub>2</sub> O <sub>5</sub> )	250 W-hr/kg	High energy density Higher Cell Voltage
Lithium (LiSO <sub>2</sub> )	58-80 W-hr/kg	High energy density Higher Cell Voltage

**Table 7.12** Battery Chemical Types

#### 7.3.2.2 Photovoltaic Systems

Photovoltaic or solar arrays are the workhorse when it comes to spacecraft power systems. Photovoltaic arrays are comprised of a large number of individual cells arranged on an appropriate substrate. Each cell produces a relatively limited current and voltage. However, proper arrangement of series and parallel electrical connections can provide any desired current and voltage within physical limitations. Deployable photovoltaic arrays have been built with power outputs of 20 kWe and Space Station Freedom will use 56.25 kWe provided by six 34 by 12m (111.6 ft by 39.4 ft) solar panels.<sup>7.14</sup>

Various array systems exist including extendible panels and roll-up arrays. A problem with very large arrays and the attendant high voltage and power levels is that of conductor mass and insulation between circuit elements. This can be particularly detrimental in flexible arrays and represents one of the practical limits to the sizing of solar arrays. Additional problems concerning photovoltaic arrays include conversion efficiencies, tolerance to the natural charged-particle space irradiation environment, micrometeoroids,



artificial threats, temperature stability, pointing and tracking requirements, and ground test qualification of large-area solar arrays.<sup>7.14</sup> Photovoltaic arrays are most efficient when the array is normal to the impinging sun light. Therefore, positioning of a craft or directional control of a solar array may be necessary in order to meet the required power levels. Radiation has a detrimental effect on solar cells, and some degradation will occur with any mission. However, missions that take place or spend an appreciable amount of time in the van Allen belts will experience greater degradation rates.<sup>7.7</sup>

Table 7.13 details some of the currently available photovoltaic cells and their energy conversion efficiencies.<sup>7.14</sup>

Solar Cell Type	Conversion Efficiency (%)
Silicon (Si)	13 - 15
Gallium Arsenide (GaAs)	16 - 18
Gallium Arsenide / Germanium (GaAs/Ge)	19

**Table 7.13** Solar Cell Conversion Efficiencies

Table 7.14 shows present day silicon solar cells with rigid array technologies. This table shows the difference in specific power relative to the structure it is attached to. A panel consists of the solar cells, substrate, and wiring. An array consists of a panel plus a boom assembly and fittings.<sup>7.14</sup>

Criteria	Panel	Array
Specific Power (W/kg)	23.8 - 36.3	21.0 - 28.2
Areal Power Density (W/m <sup>2</sup> )	111.5 - 113.8	111.5 - 113.8
Areal Density (kg/m <sup>2</sup> )	3.14 -- 4.67	4.04 - 5.32

**Table 7.14**  
Silicon Solar Cells with Rigid Array Technologies

From Table 7.14 it is apparent that the addition of structural mass to support a solar panel is non-negligible.

### 7.3.2.3 Fuel Cell Systems

Fuel cells are devices which allow direct conversion of chemical energy into electricity. The fuel cell operates by injecting an oxidizer and fuel into a cell similar in internal arrangement to a battery where an internal oxidation reaction creates electricity. This process takes place without the high temperature and other complications associated with combustion.

Hydrogen and oxygen are the reactants used in currently operational fuel cells. The output from these cells is essentially pure water. In an open loop fuel cell this water may then be used for crew consumption and other uses with little or no treatment. For regenerative fuel cells this water is later disassociated into its constituents of hydrogen and oxygen, see Figure 7.15.<sup>7.15</sup> Fuel cells are a proven technology and have been used to power Gemini, Apollo, and Space Shuttle vehicles.<sup>7.7</sup>

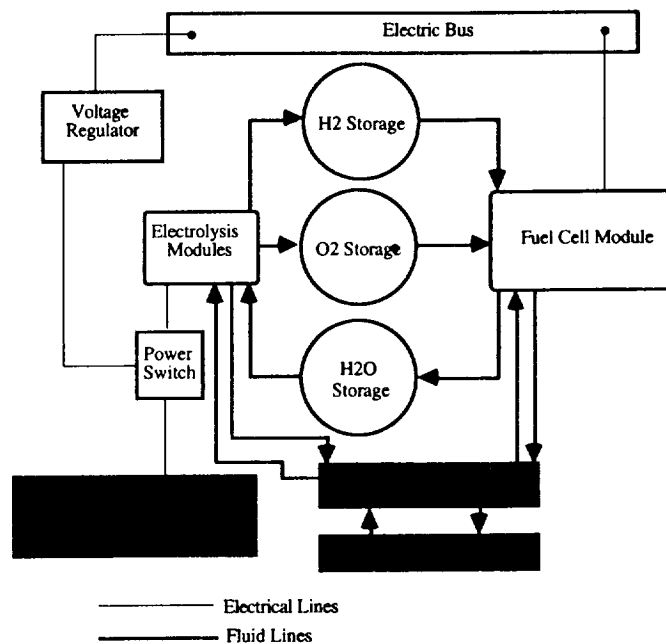


**Figure 7.15** Regenerative Fuel Cell Schematic

### 7.3.3 LTV Power Generation System

#### 7.3.3.1 LTV Photovoltaic Array System

The LTV primarily consists of a truss network which exists for the purpose radiation protection by keeping the crew a sufficient distance away from the nuclear thermal rocket. This structure provides a large surface on which to attach a solar panel. Placement of a solar panel on the truss network allows for a lighter solar array design since a

structural system is already in place. For this reason, a solar array is selected as the primary power generation source on the LTV.

The LTV truss network consists of two basic cross-sectional shapes: an octagonal portion of the truss that encloses the LTVCM and a square portion of the truss which is the structural member from the NTR to the octagonal section. Octagonal and square cross-sectional views of each of these sections are shown in Figure 7.16 and Figure 7.17, respectively.

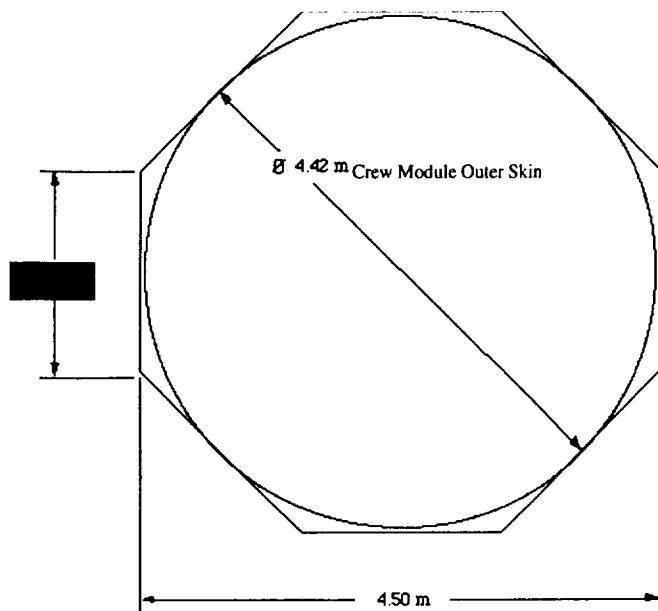


Figure 7.16 Octagonal Cross Section of Truss

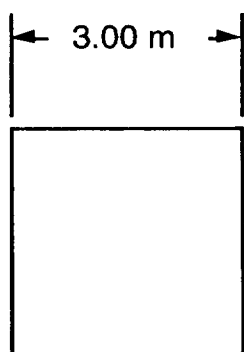


Figure 7.17 Square Cross Section of Truss

The shape of the cross section is important to the operation of a solar array because a solar array is most efficient when the collecting surface is normal to the incident solar

radiation which it converts to electricity. However, it will be necessary for the LTS to rotate about the axis normal to the cross-section (out of the page) in order to control solar heating of the LTS. Because of the need for the vehicle to rotate, each side of the truss will need to be covered with a solar array and the output of the solar array will depend on the angle that the LTS is rotating through.

In order to explore the effect of this rotation on power generation, it is first necessary to define a set of axes. Using the cross sections from Figure 7.16 and Figure 7.17 the axes are placed such that the positive x-direction starts from the center of each section and extends to the right, the positive y-direction starts from the center of each section and extends in the upward direction, and a positive angle is defined as starting from the positive x-axis and traversing in a counterclockwise direction. Since these figures are symmetric, an analysis of the power output of a solar array placed on one of their faces need only be performed for the interval of zero to ninety degrees (for the case where the z-axis is normal to the incident solar radiation). The incoming solar energy was assumed to be normal to the face having the positive x-direction normal and then the cross section is rotated about the z-axis through ninety degrees. The normalized values calculated for the output of the octagonal cross section, the square cross section, and the combination of these are shown in Figure 7.18.

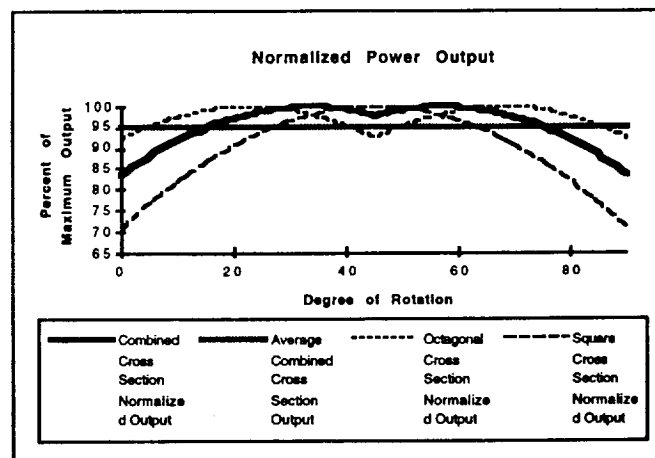


Figure 7.18 Normalized Solar Array Power Output

From this figure it can be seen that the octagonal cross section has a more continuous power output (average of 97% of maximum) than the square cross section (average of 89% of maximum). Also, the combined cross section power output does not drop below sixty percent of its maximum, and the average of the combined cross section power output is approximately ninety-five percent of the

maximum power output. This shows that a solar array would perform favorably if placed on the truss of the LTV.

Next a comparison needs to be made between the kinds of solar cells available. Table 7.15 shows a comparison between various solar cells with rigid array technologies.<sup>7.14</sup>

<b>Silicon Array</b>	
<b>Criteria</b>	<b>Result</b>
Efficiency (% AMO)	13
Specific Power (W/kg)	33.2
Areal Power Density (W/m <sup>2</sup> )	103.3
Areal Density (kg/m <sup>2</sup> )	3.1
Cell Thickness (mm)	0.2
<b>GaAs / GaAs Array</b>	
<b>Criteria</b>	<b>Result</b>
Efficiency (% AMO)	17
Specific Power (W/kg)	34.1
Areal Power Density (W/m <sup>2</sup> )	122.7
Areal Density (kg/m <sup>2</sup> )	3.6
Cell Thickness (mm)	0.25
<b>GaAs/Ge Array</b>	
<b>Criteria</b>	<b>Result</b>
Efficiency (% AMO)	19
Specific Power (W/kg)	44.0
Areal Power Density (W/m <sup>2</sup> )	137.8
Areal Density (kg/m <sup>2</sup> )	3.1
Cell Thickness (mm)	0.125

**Table 7.15**  
Performance of Solar Cells with Rigid Arrays

Table 7.15 clearly shows that the best choice for a solar array is GaAs/Ge solar cells. The next step is to determine the effective area of the octagonal section of the truss to determine the effective area for power output from the array. This is done by multiplying the average of the normalized output value by the amount of effective surface of the octagonal truss observing solar radiation. To get the electrical power output from the octagonal section of the solar array the area which has just been calculated is multiplied by the areal power density. To obtain the mass of this array the total array area, including parts of the array not producing power, is multiplied by the areal density and is referenced in Table 7.16

<b>GaAs/Ge Array on the Truss Octagonal Section</b>	
<b>Criteria (6.25 m Octagon)</b>	<b>Result</b>
Power Output (We)	4060
Array Mass (kg)	288

**Table 7.16**  
Power Parameters of the Octagonal Truss Section

Additional power is obtained by completing the same procedure for the square section of the truss. Table 7.17 gives these numbers as a function of array length.

<b>GaAs/Ge Array on the Truss Square Section</b>	
<b>Criteria</b>	<b>Result</b>
Power Output (We/m)	520
Array Mass (kg/m)	37.2

**Table 7.17**  
Power Parameters of the Square Truss Section

In order to meet the peak power requirement of the LTS of 10294 We, twelve meters of the square truss network in addition to the octagonal truss section will be covered with solar panels. This results in the total array mass and power given in Table 7.18.

<b>GaAs/Ge Array</b>	
<b>Criteria</b>	<b>Result</b>
Total Power Output (We)	10300
Total Array Mass (kg)	735

**Table 7.18**  
Array Output and Mass to Meet Peak Power Demand

### 7.3.3.2 LTV Battery System

The LTV will require the addition of a battery system in order to deal with the sudden variations in power that accompany the usage of a photovoltaic array and any sudden power loading on the LTV. This battery system will be comprised of Ag-Zn batteries due to their large energy density and ability to accommodate heavy power draws. Such a system would consist of 60kg (132 lbm) of batteries having a total storage capability of 16500 W-hr. The LTV running on the battery system alone at peak power would

exhaust the batteries in slightly more than one and one-half hours.

### 7.3.4 LEV Power Generation System

#### 7.3.4.1 LEV Fuel Cell System

The LEV has a lower power requirement than the LTV, and it is impractical to power by photovoltaic arrays due to the Lunar landing loads. Therefore, a power generation system consisting of fuel cells was determined to be the best choice. The peak load on the LEV is 8041 We. This load can be met for 6 days, using the reaction rates of the fuel cells given in Table 7.19<sup>7.16</sup>, and consists of the equipment listed in Table 7.20.<sup>7.14</sup>

Constituent	Reaction Rate
Hydrogen (consume)	0.051 kg/kW-hr
Oxygen (consume)	0.406 kg/kW-hr
Water (generate)	0.453 kg/kW-hr
Waste Heat (generate)	1978 J/kW-hr

Table 7.19 Fuel Cell Reaction Rates

Component	Quantity	Total Mass (kg)
Fuel Cell	4	351
O <sub>2</sub> Tank	3	254
H <sub>2</sub> Tank	3	271
H <sub>2</sub> O Tank	3	14
Support Equip.		120
O <sub>2</sub> Reactants		850
H <sub>2</sub> Reactants		101
<b>Totals</b>		<b>1961</b>

Table 7.20 Fuel Cell Power System

These tables show that mass of a fuel cell power system is not negligible. The quantity of fuel cells needed is based on a maximum generation of 2.6 kWe each.<sup>7.7</sup> Tankage and reactants account for 69% of the mass of the LEV power generation system. This system meets all of the design criteria except that there is not enough reactants available to accommodate the longest stay times on the Lunar surface. During such times, the LEV may be "plugged into" the power generation system for the Lunar Habitation Modules.

#### 7.3.4.2 LEV Battery System

The LEV will require the addition of a battery system in order to deal with the sudden variations in power that accompany the usage of a vacuum and other ECLSS items. This battery system will be comprised of Ag-Zn batteries due to their large energy density and ability to accommodate heavy loadings. Such a system will consist of 60kg (132 lbm) of batteries having a total storage capability of 16500 W-hr. Running on the batteries alone, the LEV can operate at peak power for only two hours.

#### 7.3.5 Electrical Power Distribution and Control (EPD&C)

The EPD&C system contains all of the sub-systems necessary to utilize the power systems on the LEV and LTV. The EPD&C consists of three redundant bus distribution systems, which transfer dc power to loads throughout. Inverters convert dc power to ac power. Three redundant ac bus systems transfer three-phase ac power to the crew module(s). Power is distributed and switched via assemblies for power control and load control assemblies. Power contactors connect battery modules to the power bus. A bus interface transfers power from the LTV to the LEV while the two are docked. Three battery voltage regulators maintain the battery supply within acceptable tolerances and a battery charge control trickle charges the Ag-Zn batteries. The LEV and LTV will each require their own individual EPD&C systems which can be connected while the two are docked together. The EPD&C for the LEV and LTV is estimated to be 550kg (1210 lbm) each.<sup>7.12</sup>

#### 7.3.6 Power System Mass Summary

Adding the contributions of the components of the power systems for the LTV and the LEV, their respective masses are presented in Table 7.21.

<b>LTV</b>	
<b>Component</b>	<b>Mass</b>
Solar Array	735
Battery System	60
EPD&C	550
<b>Total</b>	<b>1345</b>
<b>LEV</b>	
<b>Component</b>	<b>Mass</b>
Fuel Cell System	1136
Battery System	60
EPD&C	550
<b>Total</b>	<b>1746</b>

**Table 7.21**  
LEV and LTV Power System Mass Summary

## 8.0 CONCLUSION

Our once great lead in space has diminished. New powers like Japan and Europe stand ready to exploit the vast frontier. Losing to these powers will end the era of U.S. space domination which could finally lead to losing it all together. This report is dedicated to the exploration of space, the greatest adventure of all time.

*Space is truly the last great frontier. There are vast distances which must be crossed, hostile environments to overcome, and horizons which quite literally reach to eternity. These are the challenges, the callings to which humanity has always answered.*

*We have marveled at the birds, and learned to fly. We have gazed at the moon, and set foot upon it's surface.*

*Humanity has reached out to the four corners of the earth and now reaches to the stars. It is human nature, . . . it is human destiny.*

*-Mike Mecklenburg 1993*

# Appendix A

## Crew Activity Timeline

Daily Cycle	Mission Time	Activity
T - 00:18:00	T - 01:00:00	Crew transfers from SSF to LTV in LEV
T - 00:14:00	T - 00:20:00	LEV rendezvous with LTV
T - 00:12:00	T - 00:18:00	Doff suits and stowage complete, PR
T - 00:11:00	T - 00:17:00	Personal stowage, MS 1 prepares meal
T - 00:10:00	T - 00:16:00	Evening Meal
T - 00:09:00	T - 00:15:00	Prepare for Sleep Period
T - 00:08:00	T - 00:14:00	Begin Sleep Period
T + 00:00:00	T - 00:06:00	Wake -up, MS2 prepares meals
T + 00:01:00	T - 00:05:00	Breakfast
T + 00:02:00	T - 00:04:00	Don Suits
T + 00:04:00	T - 00:02:00	Systems Checkout
T + 00:05:30	T - 00:00:30	Crew enters LEV, prepares for TLI Burn
T + 00:06:00	T + 00:00:00	TLI burn initiates
T + 00:06:35	T + 00:00:35	TLI burn completed
T + 00:08:30	T + 00:02:30	Doff Suits, stowage complete, MS3 prepares meal
T + 00:09:30	T + 00:03:30	Lunch
T + 00:12:00	T + 00:06:00	Jettison TLI Tanks
T + 00:13:00	T + 00:07:00	MS4 prepares meal
T + 00:14:00	T + 00:08:00	Evening Meal
T + 00:15:00	T + 00:09:00	Prepare for Sleep Period
T + 00:16:00	T + 00:10:00	Begin Sleep Period
T + 01:00:00	T + 00:18:00	Wake -up, MS1 prepares breakfast
T + 01:01:00	T + 00:19:00	Breakfast
T + 01:02:00	T + 00:20:00	Begin Scientific Activities
T + 01:05:00	T + 00:23:00	MS2 prepares lunch
T + 01:06:00	T + 01:00:00	Lunch
T + 01:07:00	T + 01:01:00	Continue Scientific Activities
T + 01:10:00	T + 01:04:00	MS3 prepares dinner
T + 01:11:00	T + 01:05:00	Dinner

T + 01:12:00	T + 01:06:00	PR
T + 01:14:00	T + 01:08:00	Mid-Course Correction Burn
T + 01:15:00	T + 01:09:00	Prepare for sleep period
T + 01:16:00	T + 01:10:00	Sleep Period
T + 02:00:00	T + 01:18:00	Wake Up, MS4 prepares breakfast
T + 02:01:00	T + 01:19:00	Breakfast
T + 02:02:00	T + 01:20:00	Scientific Activities
T + 02:05:00	T + 01:23:00	MS1 prepares lunch
T + 02:06:00	T + 02:00:00	Lunch
T + 02:07:00	T + 02:01:00	Continue Scientific Activities
T + 02:10:00	T + 02:04:00	MS2 prepares dinner
T + 02:11:00	T + 02:05:00	Dinner
T + 02:12:00	T + 02:06:00	Relaxation, PR
T + 02:13:00	T + 02:07:00	Prepare for Sleep Period
T + 02:14:00	T + 02:08:00	Sleep Period
T + 02:22:00	T + 02:16:00	Wake up, MS3 Prepares Breakfast, Donn Suits
T + 02:23:00	T + 02:17:00	Breakfast, Continue Donn Suits
T + 03:00:00	T + 02:18:00	Systems checkout
T + 03:01:30	T + 02:19:30	Crew enters LEV, Prepares for LOI Burn
T + 03:02:00	T + 02:20:00	Lunar Orbit Insertion Burn
T + 03:02:09	T + 02:20:09	LOI Burn Complete
T + 03:03:00	T + 02:21:00	Begin Landing Sequence
T + 03:04:42	T + 02:22:42	Descent Burn
T + 03:05:00	T + 02:23:00	Landing Complete
T + 03:06:00	T + 03:00:00	Systems check, begin O2 pre-breathe
T + 03:07:00	T + 03:01:00	Donn EVA suits
T + 03:09:00	T + 03:03:00	De-pressurize cabin and exit
T + 00:01:30	T - 00:04:00	Enter LEVCM, Doff EVA Suits
T + 00:03:30	T - 00:02:00	Systems Check, Donn Partial Pressure Suits
T + 00:05:30	T + 00:00:00	LEV Ascent Burn
T + 00:05:41	T + 00:00:11	LEV Ascent Burn Complete
T + 00:08:30	T + 00:03:00	LEV rendezvous with LTV

T + 00:09:00	T + 00:03:30	Systems check, Snack
T + 00:10:30	T + 00:05:00	TEI Burn
T + 00:10:35	T + 00:05:05	TEI Burn Complete
T + 00:13:00	T + 00:07:30	Doff Suits, Stowage complete, MS1 prepare meal
T + 00:14:00	T + 00:08:30	Dinner
T + 00:15:00	T + 00:09:30	Prepare for Sleep Period
T + 00:16:00	T + 00:10:30	Begin Sleep Period
T + 01:00:00	T + 00:18:30	Wake Up, MS2 prepares breakfast
T + 01:01:00	T + 00:19:30	Breakfast
T + 01:02:00	T + 00:20:30	Mid-Course Correction Burn
T + 01:02:30	T + 00:21:00	Begin Scientific Activities
T + 01:05:30	T + 01:00:00	MS3 prepares lunch
T + 01:06:30	T + 01:01:00	Lunch
T + 01:07:30	T + 01:02:00	Continue Scientific Activities
T + 01:10:30	T + 01:05:00	MS4 prepares dinner
T + 01:11:30	T + 01:06:00	Dinner
T + 01:12:30	T + 01:07:00	Relaxation, PR
T + 01:15:00	T + 01:09:30	Prepare for Sleep Period
T + 01:16:00	T + 01:10:30	Sleep Period
T + 02:00:00	T - 01:18:30	Wake -up, MS1 prepares meals
T + 02:01:00	T - 01:19:30	Breakfast
T + 02:02:00	T - 01:20:30	Don Suits, Systems Checkout
T + 02:07:00	T - 02:01:30	Crew enters LEV, prepares for EOI Burn
T + 02:07:30	T + 02:02:00	EOI burn initiates
T + 02:07:41	T + 02:02:11	EOI burn completed
T + 02:10:30	T + 02:05:00	Rendezvous with SSF
T + 02:12:30	T + 02:07:00	Transfer to SSF in LEV



**Appendix B**  
Specification Sheet

**Description**

Carry the LEV and Cargo loaders to Lunar orbit and return them to LEO.

**Sub-System Mass Table**

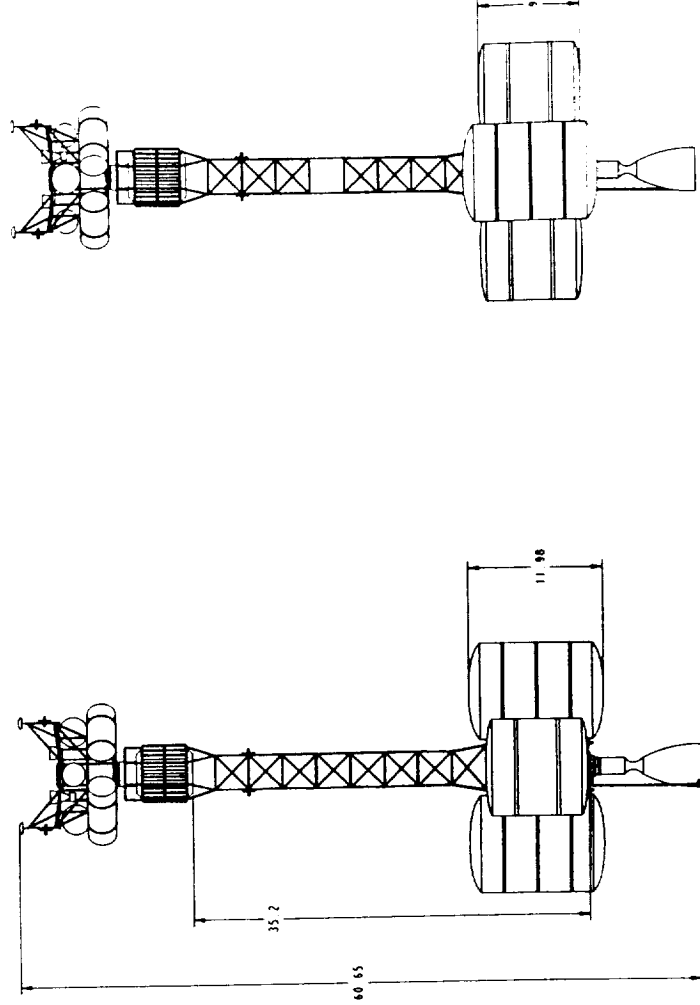
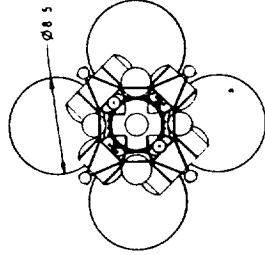
Component	Mass (lb)
Truss	5.5
Lunar Module	10,069
Primary Structure	3,312
Secondary Structure	1,651
Internal Components	712
Consumables	1,064
Miscellaneous	2,043
Power System	1,345
Primary Propulsion	13.0
MIR	8.5
Insulation Shield	4.5
RCS System	692
DTI Tank Mass	14,361
Miscellaneous	0
<b>Total</b>	<b>44,977</b>

**Fuel Mass Table**

Item	Mass (lb)
LEV	78.2
LOI	19.99
TEI	72.39
EOC	26.56
RCS Total Burn	2.07 (Storable)
<b>Total</b>	<b>197.71</b>

**CG and Moment Table**

Center of Gravity Location	Value (in)
X - Coordinate	0
Y - Coordinate	0
Z - Coordinate	9.91
<b>Moment</b>	<b>Value (lb-in)</b>
LEV	21,466
LOI	6,866



B-2

Lunar Excursion Vehicle  
Lunar Transportation System

SPECIFICATION SHEET  
University of Minnesota / NASA / USRA

Description

Transfer to & crew from lunar orbit to the lunar surface and back to lunar orbit.

Sub-System Mass Table

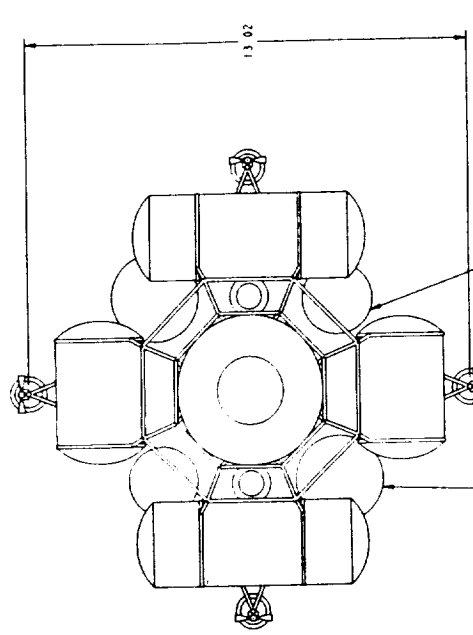
Component	Mass (MT)
Crew	3.75
Crew Module	9.95
Primary Structure	4.278
Secondary Structure	1.657
ECLSS	1.526
Consumables	6.98
Miscellaneous Items	1.781
Power System	1.746
Primary Propulsion	344
RL10A-4 (2)	1.977
Dry Tons	0.73
RCS System	0.73
Total Dry Mass	774

Fuel Mass Table

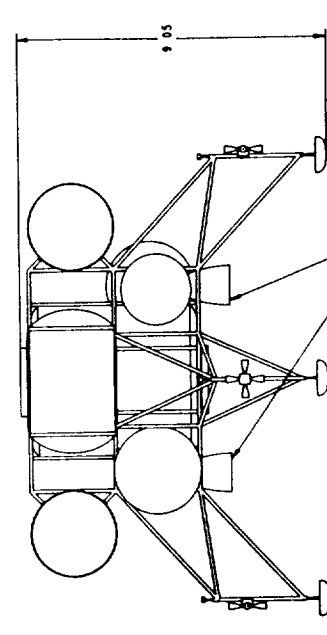
Item	Mass (MT)
Transfer from SSF	LM2 0.028 LOI 0.139
Descent	LM2 3.6 LOI 18.0
Ascent	LM2 7.12 LOI 10.6
Transfer to SSF	LM2 0.009 LOI 0.044
RCS Inert Mass	48 (Hydrazine)
Total	LM2 8.7% LOI 28.7%

CG and Moment Table

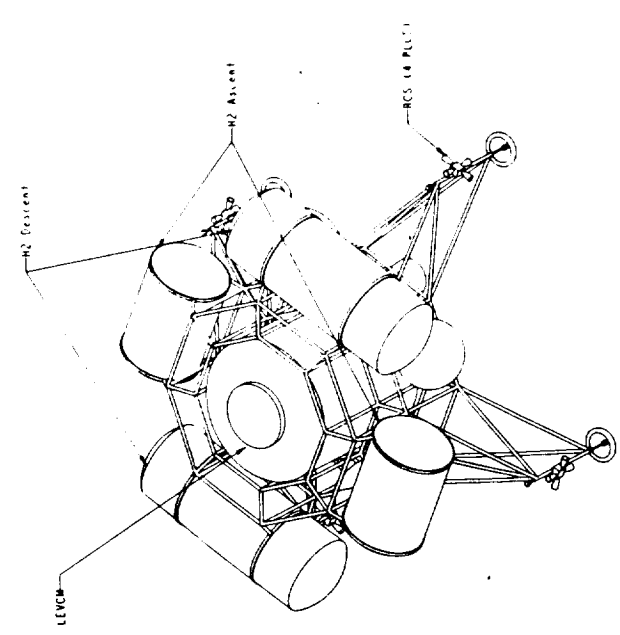
Center of Gravity	Coordinate (ft)
(x, y, z)	(0, 0, 5.73)
Moment	Value Page 3
Mass (MT)	5.244
CG (ft)	4.14x5



LOI Descent (2 PLCS)  
LOI Ascent (2 PLCS)



SCALE 0.015



SCALE 0.015

# **Appendix C**

## **Propulsion Spreadsheet**

MISSION TYPE	OPERATIONAL LIFE TIME (YRS)	OPERATIONAL LIFE TIME (MONTHS)	OPERATIONAL LIFE TIME (DAYS)	OPERATIONAL LIFE TIME (HOURS)	OPERATIONAL LIFE TIME (MINUTES)	OPERATIONAL LIFE TIME (SECONDS)	OPERATIONAL LIFE TIME (MILLISECONDS)	OPERATIONAL LIFE TIME (MICROSECONDS)	OPERATIONAL LIFE TIME (NANOSECONDS)	OPERATIONAL LIFE TIME (PICTURES)	OPERATIONAL LIFE TIME (BYTES)	OPERATIONAL LIFE TIME (KILOBYTES)	OPERATIONAL LIFE TIME (MEGABYTES)	OPERATIONAL LIFE TIME (GIGABYTES)	OPERATIONAL LIFE TIME (TERABYTES)	OPERATIONAL LIFE TIME (PETABYTES)	OPERATIONAL LIFE TIME (EXABYTES)	OPERATIONAL LIFE TIME (ZETTABYTES)	OPERATIONAL LIFE TIME (YOTTABYTES)
PROBLEMS TO SOLVE	33.7	33.7	33.7	33.7	33.7	33.7	33.7	33.7	33.7	33.7	33.7	33.7	33.7	33.7	33.7	33.7	33.7	33.7	33.7

PROPELLANT MASS FLOW RATE (G/SEC)	33.7	33.7	33.7	33.7	33.7	33.7	33.7	33.7	33.7	33.7	33.7	33.7	33.7	33.7	33.7	33.7	33.7	33.7	33.7
-----------------------------------	------	------	------	------	------	------	------	------	------	------	------	------	------	------	------	------	------	------	------

PROPELLANT MASS FLOW RATE (G/SEC)	33.7	33.7	33.7	33.7	33.7	33.7	33.7	33.7	33.7	33.7	33.7	33.7	33.7	33.7	33.7	33.7	33.7	33.7	33.7
-----------------------------------	------	------	------	------	------	------	------	------	------	------	------	------	------	------	------	------	------	------	------

PROPELLANT MASS FLOW RATE (G/SEC)	33.7	33.7	33.7	33.7	33.7	33.7	33.7	33.7	33.7	33.7	33.7	33.7	33.7	33.7	33.7	33.7	33.7	33.7	33.7
-----------------------------------	------	------	------	------	------	------	------	------	------	------	------	------	------	------	------	------	------	------	------

PROPELLANT MASS FLOW RATE (G/SEC)	33.7	33.7	33.7	33.7	33.7	33.7	33.7	33.7	33.7	33.7	33.7	33.7	33.7	33.7	33.7	33.7	33.7	33.7	33.7
-----------------------------------	------	------	------	------	------	------	------	------	------	------	------	------	------	------	------	------	------	------	------

PROPELLANT MASS FLOW RATE (G/SEC)	33.7	33.7	33.7	33.7	33.7	33.7	33.7	33.7	33.7	33.7	33.7	33.7	33.7	33.7	33.7	33.7	33.7	33.7	33.7
-----------------------------------	------	------	------	------	------	------	------	------	------	------	------	------	------	------	------	------	------	------	------

PROPELLANT MASS FLOW RATE (G/SEC)	33.7	33.7	33.7	33.7	33.7	33.7	33.7	33.7	33.7	33.7	33.7	33.7	33.7	33.7	33.7	33.7	33.7	33.7	33.7
-----------------------------------	------	------	------	------	------	------	------	------	------	------	------	------	------	------	------	------	------	------	------

PROPELLANT MASS FLOW RATE (G/SEC)	33.7	33.7	33.7	33.7	33.7	33.7	33.7	33.7	33.7	33.7	33.7	33.7	33.7	33.7	33.7	33.7	33.7	33.7	33.7
-----------------------------------	------	------	------	------	------	------	------	------	------	------	------	------	------	------	------	------	------	------	------

PROPELLANT MASS FLOW RATE (G/SEC)	33.7	33.7	33.7	33.7	33.7	33.7	33.7	33.7	33.7	33.7	33.7	33.7	33.7	33.7	33.7	33.7	33.7	33.7	33.7
-----------------------------------	------	------	------	------	------	------	------	------	------	------	------	------	------	------	------	------	------	------	------

PROPELLANT MASS FLOW RATE (G/SEC)	33.7	33.7	33.7	33.7	33.7	33.7	33.7	33.7	33.7	33.7	33.7	33.7	33.7	33.7	33.7	33.7	33.7	33.7	33.7
-----------------------------------	------	------	------	------	------	------	------	------	------	------	------	------	------	------	------	------	------	------	------

PROPELLANT MASS FLOW RATE (G/SEC)	33.7	33.7	33.7	33.7	33.7	33.7	33.7	33.7	33.7	33.7	33.7	33.7	33.7	33.7	33.7	33.7	33.7	33.7	33.7
-----------------------------------	------	------	------	------	------	------	------	------	------	------	------	------	------	------	------	------	------	------	------

PROPELLANT MASS FLOW RATE (G/SEC)	33.7	33.7	33.7	33.7	33.7	33.7	33.7	33.7	33.7	33.7	33.7	33.7	33.7	33.7	33.7	33.7	33.7	33.7	33.7
-----------------------------------	------	------	------	------	------	------	------	------	------	------	------	------	------	------	------	------	------	------	------

C-2

# Appendix D

## Thermal Analysis Program

```
program finelem
c
implicit real(a-h,n-y),complex(z),integer(i-m)
dimension t(60),energy(60)
complex findneighbor
dimension index(60)
real midd,out,in,junk1,junk2,junk3,junk4
common /ugh/ t(60),index(60),min,max
c
c initialize the element temperatures & indices -- guess a final
c temp of 265K
c
do 10 i=1,60
t(i)=265.
index(i)=i
10 continue
c
c calculate our inner and outer radiation surfaces
c also get the conduction length
c
in=3.1415926/30.0
out=in*.04
in=in*.05
midd=(in+out)/2.
cond=237
sig=5.67e-8
eps=0.9
c
c cp is really mass*Cp
c
cp=903*midd*.02*2700
open(unit=10,file='bs2',form='formatted',status='new')
c
c run main loop
c
do 20 i=0,15000
c
c calculate the conduction and solar flux into all 60 elem.
c
do 30 k=1,60
if ((index(k).ge.1).and.(index(k).le.30)) then
energy(k)=1400*0.36*out
else
energy(k)=0
endif
zget=findneighbor(k)
left=real(zget)
```

```

right=imag(zget)
energy(k)=energy(k)+.02*cond*(t(left)-t(k))/midd
energy(k)=energy(k)+.02*cond*(t(right)-t(k))/midd
energy(k)=energy(k)-out*sig*eps*t(k)**4
c
c calculate the interior radiation between all 60 elem.
c
do 40 l=1,60
  if ((k.eq.1).and.((l.eq.59).or.(l.eq.60))) goto 40
  if ((k.eq.2).and.(l.eq.60)) goto 40
  if ((k.eq.60).and.((l.eq.1).or.(l.eq.2))) goto 40
  if ((k.eq.59).and.(l.eq.1)) goto 40
  if ((l.gt.k+2).or.(l.lt.k-2)) then
energy(k)=energy(k)-.015*sig*eps*(t(k)**4-t(l)**4)*in
  endif
40 continue
30 continue
do 35 k=1,60
19 format (f,1a,f,1a)
t(k)=t(k)+energy(k)*.1/cp
if (t(k).lt.0.0) then
  t(k)=0.0
endif
c
c rotate at 1 rpm
c
if ((i/10).eq.(i/10.0)) then
  index(k)=index(k) - 1
  if (index(k).lt.1) then
    index(k)=60
  endif
endif
35 continue
c
c write out data every 10 sec
c
if ((i/100).eq.(i/100.0)) then
call minmax
write(unit=10,fmt=19) t(min),',',t(max),','
endif
20 continue
call minmax
print*,t(min),t(max),energy(min)
stop
end
c
complex function findneighbor (element)
c
c this function finds the left and right neighbors of the elem
c specified in element
c
integer element
complex zhold
c

```

```

if (element.eq.1) then
  zhold=cmplx(60,2)
else if (element.eq.60) then
  zhold=cmplx(59,1)
else
  zhold=cmplx(element-1,element+1)
endif
c
  findneighbor=zhold
  return
  end
c
c
c
  subroutine minmax
c
c  this subroutine finds the minimum and maximum temps in the c   beam
c
  common /ugh/ t(60),index(60),min,max
c
  min=1
  max=1
  tmax=t(1)
  tmin=t(1)
  do 100 i=1,60
    if (tmin.gt.t(i)) then
      tmin=t(i)
      min=i
    endif
    if (tmax.lt.t(i)) then
      tmax=t(i)
      max=i
    endif
100 continue
c
  return
  end

```



# Appendix E

## MLI Analysis and Code

The following is a detailed thermal analysis adopted from Sverdrup<sup>6.3</sup> used to quantify heat transfer between the tanks and their surroundings.

Assumptions made in this analysis are:

- (1) The tanks are covered with MLI for thermal control and an outer jacket to protect the tanks from dust and meteoroids (see figure 6.22).
- (2) No energy is stored in the outer jacket of the MLI. No space was assumed between the jacket and MLI and there is no conduction between the two surfaces. The thickness of the jacket was neglected. The jacket temperature was assumed to be 245 K. The absorptivity and emissivity of the outer jacket were assumed to be 0.36 and 0.9, respectively.
- (3) The cryogenes were assumed to be isothermal in the tank. Their temperatures are to be constant at saturation conditions and 20 psia. The tank wall thickness was neglected and the outer tank wall was assumed to be the temperature of the cryogen.
- (4) The MLI was assumed to consist of double aluminized Kapton shields separated by Dacron spacers. The shields were assumed to be .0076mm thick and stacked 24 shields/cm. Lexan pins and buttons, and velcro tabs were to be used and methods of attachment. The diameter of the pins was assumed to be .3175 cm. There were assumed to be seams in the MLI layer. These seams were assumed to be .3175 cm wide, and it was assumed that there were 1.772 meters of seam length per square meter of insulation. The density of the MLI was assumed to be 35.1 kg/m<sup>3</sup>. The emissivity of the MLI was assumed to be .04 and the total hemispherical emissivity was assumed to be .031. There was assumed to be one MLI blanket on each tank.
- (5) The structural heat leak was assumed to be 20 % of the MLI heat leak. The structural heat leak consists of heat leak due to support struts, plumbing, wires, etc.
- (6) No energy is stored in the insulation system.

A nodal representation of the thermal analysis is shown in figure 6.3.

Equations used in the analysis:

The heat leak into the tank is the sum of the heat leak through the MLI and the heat leak due to structural supports.

$$Q_{\text{boiloff}} = Q_{\text{mli}} + Q_{\text{structural}} \quad (W)$$

but

$$Q_{\text{structural}} = 0.2 Q_{\text{mli}} \quad (W)$$

therefore,

$$Q_{\text{boiloff}} = 1.2 Q_{\text{mli}} \quad (W)$$

The mass boiloff rate is:

$$Q_{\text{boiloff}} / \text{hfg} \quad (\text{kg/hr})$$

where hfg is the heat of vaporization for the cryogen.  
The heat leak through the MLI blankets consists of:

$$Q_{\text{mli}} = Q_{\text{conduction}} + Q_{\text{radiation}} + Q_{\text{seam}} + Q_{\text{pin}}$$

where,

- $Q_{\text{mli}}$  = heat rate through MLI (W)
- $Q_{\text{conduction}}$  = heat rate through MLI via spacer conduction (W)
- $Q_{\text{radiation}}$  = heat rate through MLI via radiation shields (W)
- $Q_{\text{seam}}$  = heat rate through MLI blanket seams (W)
- $Q_{\text{pin}}$  = heat rate through MLI blanket attachment pins (W)

The  $Q_{\text{conduction}}$  and  $Q_{\text{radiation}}$  terms represent the basic MLI performance. These are evaluated as:

$$Q_{\text{conduction}} = \frac{(8.95\text{E-}08) (\text{NLC}^2.56) (\text{T}_{\text{mli}}^2 - \text{T}_{\text{c}}^2)}{2(\text{N}-1)} \quad \text{A}$$

and,

$$Q_{\text{radiation}} = \frac{(5.39\text{E-}10) (\text{etot h}) (\text{T}_{\text{mli}}^{4.67} - \text{T}_{\text{c}}^{4.67})}{\text{N}-1} \quad \text{A}$$

where,

- $Q_{\text{conduction}}$  = heat rate through MLI via spacer conduction (W)
- $Q_{\text{radiation}}$  = heat rate through MLI via radiation shields (W)
- $\text{NLC}$  = number of layers of MLI/cm
- $\text{N}$  = total number of MLI layers
- $\text{etot h}$  = total hemispherical emittance of radiation shields
- $\text{T}_{\text{mli}}$  = temperature of outer MLI surface (K)
- $\text{T}_{\text{c}}$  = temperature of cryogen tank (K)
- $\text{A}$  = surface area of outer jacket

The heat leak through the MLI blankets due to seams can be evaluated using a one dimensional heat transfer approach:

$$Q_{\text{seam}} = \epsilon_1 \epsilon_2 F_{\text{seam}} L_{\text{seam}} W_{\text{seam}} (\text{T}_{\text{mli}}^4 - \text{T}_{\text{c}}^4)$$

where,

- $Q_{\text{seam}}$  = heat rate through MLI blanket seams (W)

e1 =	emissivity of outer side
e2 =	emissivity of inner side
Fseam =	one dimensional view factor
Lseam =	total length of seams along blanket layer (m)
Wseam =	width of seam (m)
o =	Stefan-Boltzman constant (W/m <sup>2</sup> K <sup>4</sup> )
Tmli =	temperature of outer MLI layer (K)
Tc =	temperature of cryogen tank (K)

The heat leak through on MLI blanket due to conduction through connecting pins is:

$$Q_{pins} = \frac{NPINS A_p K_{pin} (T_{mli} - T_c)}{DX}$$

where,

Qpins =	heat rate through MLI blanket attachment pins (W)
NPINS =	number of pins through insulation blankets
Ap =	cross sectional area of pin (m <sup>2</sup> )
DX =	total MLI thickness (m)
Kpin =	thermal conductivity of pin material (W/mK)
Tmli =	temperature of outer MLI layer (K)
Tc =	temperature of cryogen tank (K)

The previous equations cannot be evaluated unless the outer MLI surface temperature is known. It is assumed that all of the energy absorbed by the outer jacket is eventually transmitted through the MLI to the cryogen tank. Therefore, the energy received by the outer jacket is equal to the energy radiated from the outer jacket to the MLI outer layer and to the energy transmitted through the MLI to the cryogen tank.

$$Q_{in} = Q_{j-mli} = Q_{mli} \quad (W)$$

The energy transferred by radiation from the outer jacket to the outer surface MLI layer is:

$$Q_{j-mli} = o F_{j-mli} F_e A (T_j^4 - T_{mli}^4)$$

where,

Qj-mli =	energy transmitted from outer jacket to outer MLI layer (W)
o =	Stefan-Boltzman constant (W/m <sup>2</sup> K <sup>4</sup> )
Fj-mli =	configuration factor
A =	surface area of outer jacket (m <sup>2</sup> )
Tj =	temperature of outer jacket (K)
Tmli =	temperature of outer MLI layer (K)

and where  $F_e$ , the emissivity factor for concentric spheres or cylinders, is determined as:

$$F_e = (1/\epsilon_{mli} + (A_1/A_2)(1/\epsilon_j - 1))^{-1}$$

where,

- $A_1$  = area of outer jacket ( $m^2$ )
- $A_2$  = area of outer MLI layer ( $m^2$ )
- $\epsilon_{mli}$  = emissivity of outer MLI layer
- $\epsilon_j$  = emissivity of I.D. of outer jacket

Assuming no space between the outer jacket and the MLI outer layer ( $A_1=A_2=A$ ):

$$Q_{mli} = \frac{A_o (T_j^4 - T_{mli}^4)}{(1/\epsilon_{mli} + 1/\epsilon_j - 1)}$$

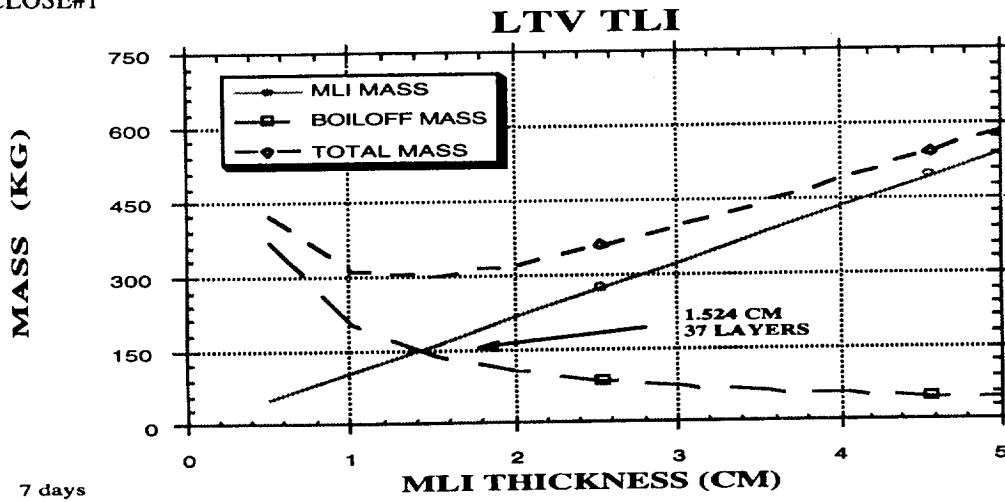
Modified code used to calculate MLI masses, MLI thicknesses, boiloff masses and total masses. This piece of code is for the LEV hydrogen ascent tank but it can be modified for all tanksets.

```
z$="LEV hydrogen ascent tank"
a=36.29
ar=1.25
lc=3.37
vol=16.56
tc=21.1
hfg=436823!
rho=71
rhomli=35.1
nlc=24
dx=0
asm=a
fjm=.5
fjs=.5
am=.93
aj=.36
ej=.9
eji=.9
em=.93
esm=.04
esmo=.04
qs=1394.3
stef=5.67E-08
lseam=1.772
wseam=.003175
apin=7.917E-06
nbl=1
```

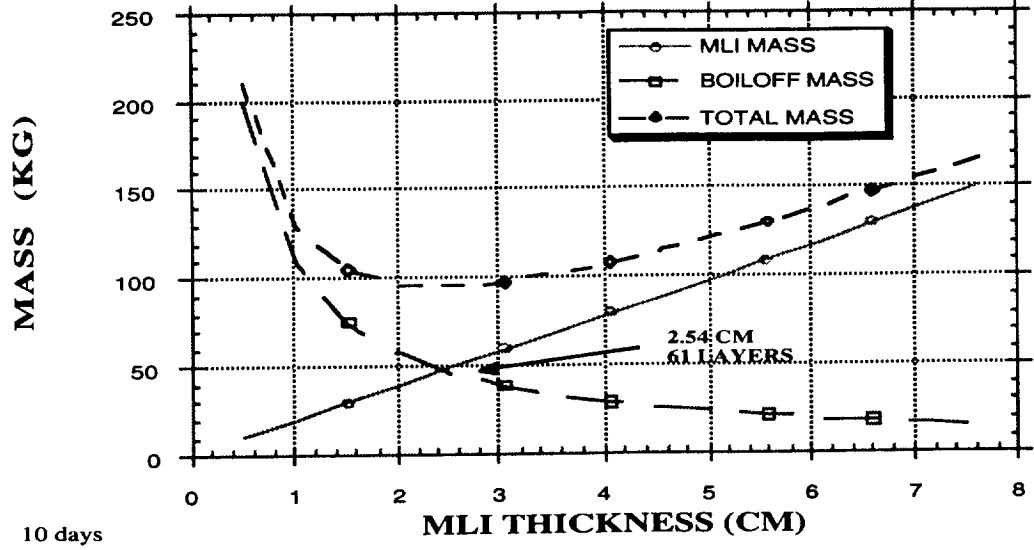
```

npin=11.302
tj=473
OPEN "levha.dat" FOR OUTPUT AS #1
FOR j=1 TO 40
dx=dx+.00508
wovt=dx/wseam
nl=(nlc*dx*100)+2*nbl
fseam=((1+(wovt/nbl)^2)^.5-wovt/nbl)/nbl
mi=rhomli*(((3.1415926#*(ar+dx)^2)*(lc+dx))-vol)
tmli=tj-1
FOR i=1 TO 20
tav=(tmli+tc)/2
kpin1=(.0323365+(.000335183#)*(tav)-(4.6414E-07)*(tav^2))
kpin=(kpin1+(.00000000323797#)*(tav^3))*1.7307
seam=ej*ej*fseam*stef*lseam*wseam*(tmli^4-tc^4)
pin=npin*kpin*apin*(tmli-tc)/dx
basic1=(8.95E-08*nlc^2.56*(tmli^2-tc^2))/(2*(nl-1))
basic2=(5.39E-10*.031*(tmli^4.67-tc^4.67))/(nl-1)
qmli=asm*(seam+pin+basic1+basic2)
tmli=(-qmli*(1/esmo+1/eji-1)/(stef*a)+tj^4)^.25
NEXT i
qt=qmli*1.2
bo=(qt/hfg)*3600
botot=bo*576
tmass=mi+botot
thick=dx*100
WRITE#1,thick,mi,botot,tmass
PRINT thick,mi,botot,tmass
NEXT j
CLOSE#1

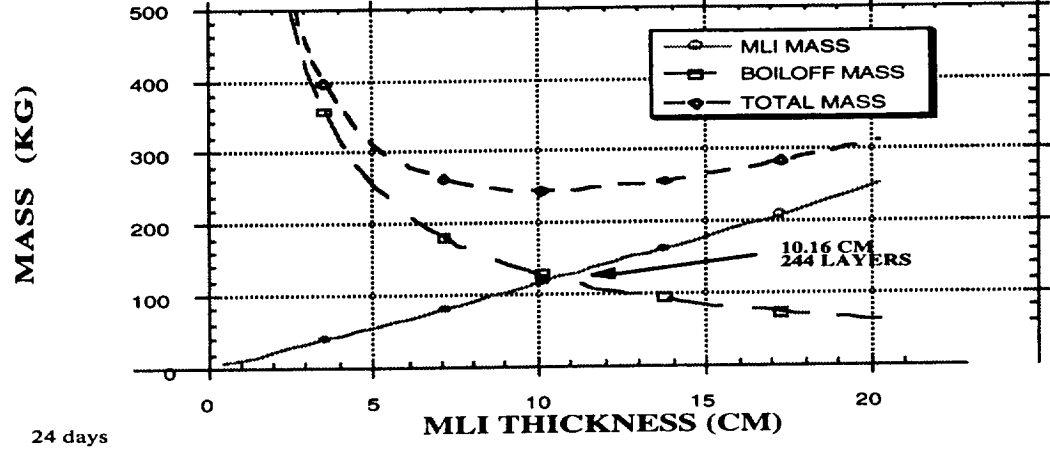
```



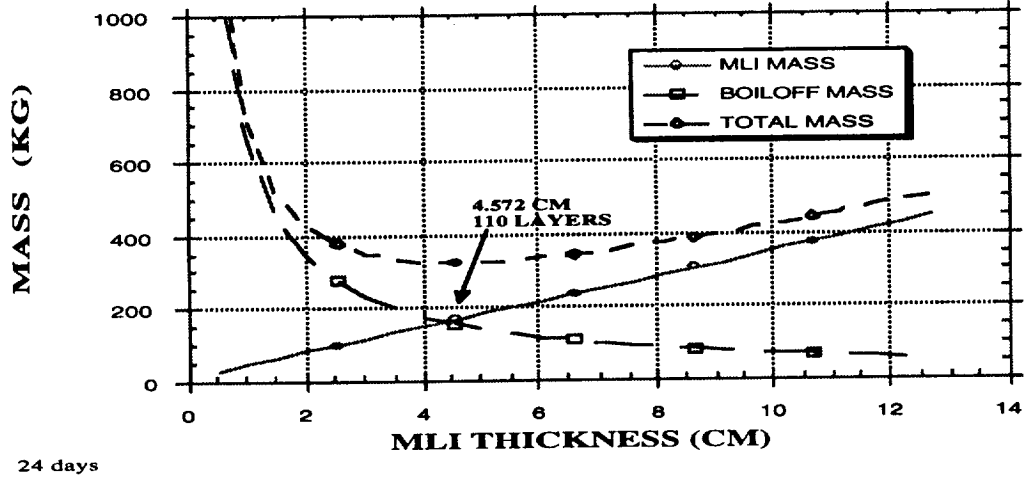
### LEV HYDROGEN DESCENT TANK



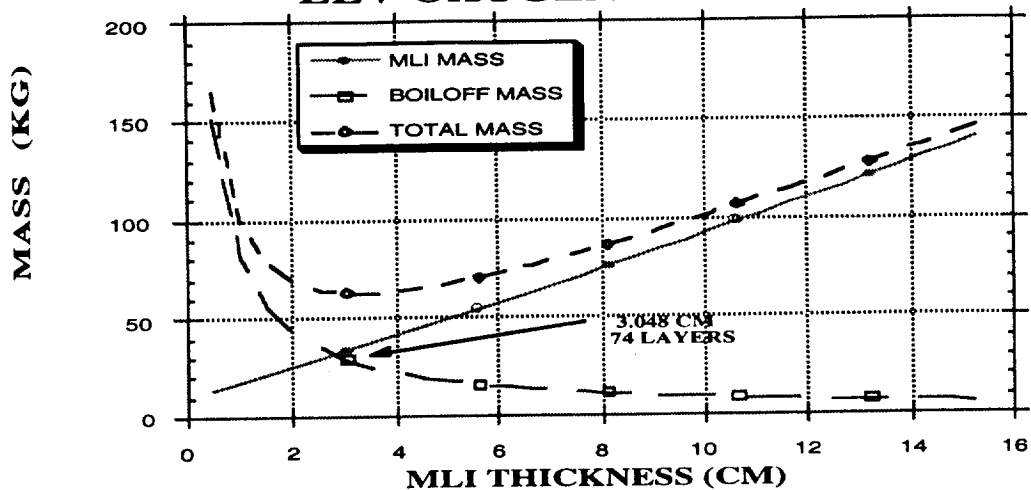
### LEV HYDROGEN ASCENT



### LTV TEI

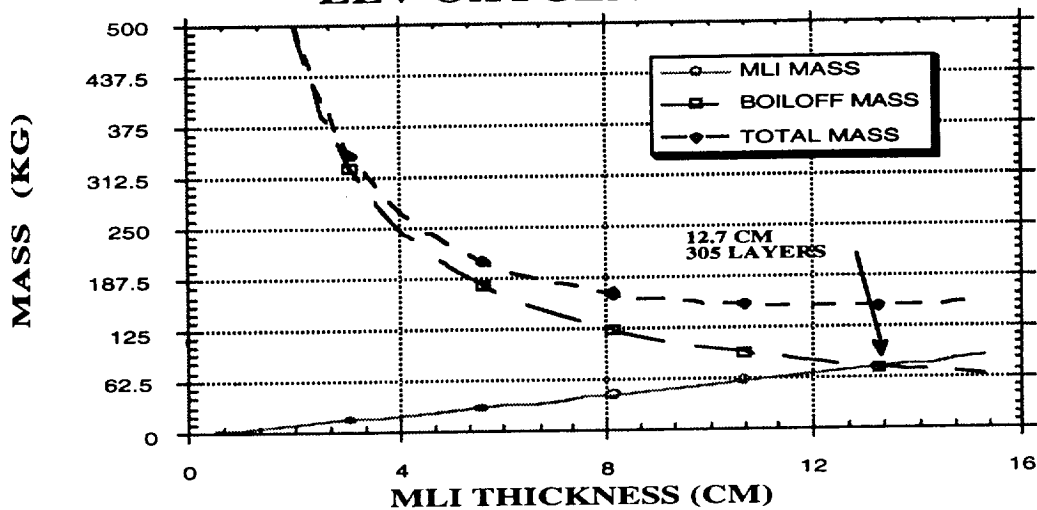


### LEV OXYGEN DESCENT



10 days

### LEV OXYGEN ASCENT



24 days

# Appendix F

## LTVCM Structure

Structural Component	Mass (kg)	Total Mass (kg)
Cylinder Skin (5m)	178	
Aft Bulkhead	581	581
Forward Bulkhead	577	577
Intermediate Rings (2)	107.5	215
Endcone Mounting and Standoff Structure	1016	1016
Hatch (2)	233	233
Docking Ring	200	200
<b>Total</b>		<b>3712</b>

### Secondary Structure

Subsystem	Mass (kg)
Rack structure - double	654
80" single bay rack	218
75" crossover rack	408
Rack attachments	297
Removable center panel	80
<b>Subtotal</b>	<b>1657</b>

### ECLSS LTVCM

Subsystem	Mass (kg)
Temperature and Humidity Control (THC)	520
Atmosphere Control and Supply (ACS)	280
Air Revitalization (AR)	400
Fire Detection and Suppression (FDS)	136
Water Storage Tanks (7)	33
Water Storage Tank Support	108
High Pressure Tanks (O2)	85
High Pressure Tanks (N2)	190
<b>Total</b>	<b>1752</b>

### Internal Components LTVCM

Subsystem	Mass (kg)
Commode/Urinal	122
Galley	50
Stowage Lockers	100
Science Station	500
<b>Total</b>	<b>772</b>



**Miscellaneous Items LTVCM**

Subsystem	Mass (kg)
Clothing	14
Personal Hygiene	3
Medical Supplies	2
Tools	3
Miscellaneous	10
<b>Total</b>	<b>32</b>

**Consumables LTVCM**

Subsystem	Mass (kg)
Food	34
Oxygen	200
Nitrogen	650
Water (720 kg for crew consumption, 280 kg for science station)	1000
<b>Total</b>	<b>1884</b>

**LTVCM Subsystem Total**

Subsystem	Mass (kg)
Primary Structure	3712
Secondary Structure	1657
ECLSS	1752
Internal Components	772
Consumables	1884
Miscellaneous Items	32
<b>Total</b>	<b>9809</b>

F-2

C-2

# Appendix G

## LTS POWER REQUIREMENTS

System	Power Requirement	
	Connected Load (W)	Average Load (W)
THC	1065	915
ACS	26	26
ARS	1300	1194
FDS	838	40
GCA	240	240
Vacuum	238	12
Water Dispenser	707	393
<b>Total</b>	<b>4414</b>	<b>2820</b>

## LTVCM POWER REQUIREMENTS

System	Power Requirement	
	Connected Load (W)	Average Load (W)
THC	1065	915
ACS	26	26
ARS	1300	1194
FDS	838	40
GCA	240	240
Galley	1629	444
Water Storage	70	14
Science Station	500	400
Waste Management	205	27
Hygiene	500	110
<b>Total</b>	<b>6373</b>	<b>3410</b>

# Appendix H

## LEVCM Structure

Structural Component	Mass (kg)	Total Mass (kg)
Cylinder Skin (5m)	178	890
Aft Bulkhead	581	581
Forward Bulkhead	577	577
Intermediate Rings (2)	107.5	215
Endcone Mounting and Standoff Structure	1016	1016
Hatch (3)	233	699
Flight Deck Floor	200	200
Docking Ring	100	100
<b>Subtotal</b>		<b>4278</b>

### Secondary Structure

Subsystem	Mass (kg)
Rack structure - double	654
80" single bay rack	218
75" crossover rack	408
Rack attachments	297
Removable center panel	80
<b>Subtotal</b>	<b>1657</b>

### ECLSS LEVCM

Subsystem	Mass (kg)
Temperature and Humidity Control (THC)	520
Atmosphere Control and Supply (ACS)	280
Air Revitalization (AR)	400
Fire Detection and Suppression (FDS)	136
High Pressure Tanks	190
<b>Subtotal</b>	<b>1526</b>

### Miscellaneous Items LEVCM

Subsystem	Mass (kg)
Crew (82 kg/person)	492
Pressure Suits (14 kg/suit)	84
EVA suits (70 kg/suit)	420
Stowage Lockers	100
Seats (16.5 kg/seat)	100
Medical Supplies	2
Tools	3
<b>Subtotal</b>	<b>1201</b>

**Consumables LEVCM**

<b>Subsystem</b>	<b>Mass (kg)</b>
Food	8
Oxygen	130
Nitrogen	500
Water Storage Tank and Plumbing	60
<b>Subtotal</b>	<b>698</b>

**LEVCM Subsystem Total**

<b>Subsystem</b>	<b>Mass (kg)</b>
Structure	4278
ECLSS	1526
Secondary Structure	1657
Consumables	698
Miscellaneous Items	1201
<b>Total</b>	<b>9360</b>

# Appendix I

## LEV Avionics

The left-hand column shows all of the avionics for the LEV. The next three columns show the quantity, weight, and power of the items. The next three columns show which piece of equipment that needs power for each of the mission phases as defined by power required.

LEV Avionics Equipment				LEV Avionics Power Demanded		
Item	Quantity	Item Unit Power (W)	Item Total Weight (kg)	LTV and LEV (docked)	LEV (undocked)	LEV (unoccupied)
Mounted Video Cameras	4	7.5	28	30	30	30
Pan/Tilt Units for Cameras	4	15	21.6	60	60	60
Internal Camera	1	7.5	7	7.5	7.5	7.5
Digital TV Processor	2	30	13.6	60	60	60
Video Controller	1	60	6.8	0	60	0
EVA VHF Antenna	1	30	0.9	0	30	30
S-Band Omnidirectional Antenna	2	15	2.2	0	30	30
Ku-Band Omnidirectional Antenna	4	15	4.4	0	60	60
S-Band Transceiver/Transmitter	1	0.8	9.1	0	0.8	0.8
Ku-Band Transceiver/Transmitter	1	0.8	9.1	0	0.8	0.8
Radio Power Amplifier	2	72	17.2	0	144	144
Radio Frequency Assembly	2	50	11	0	100	100
Keyboard/Display	2	40	13.2	0	80	80
Caution/Warning Electronic Assembly	1	13	8.3	13	13	13
Internal Lights	10	15	5	150	150	150
Star Trackers	6	10	26	0	60	0
Sun Sensors	8	2.5	14	0	20	0
Hexad Navigation Unit	1	75	16	0	75	0
Mounted Video Cameras	2	7.5	14	0	15	0
Landing Radar	1	123	38	0	123	0
Landing Lights	2	130	22	0	260	0
Navigation Sensor: Landing	1	100	13.2	0	100	0
Control Electronics	1	150	70	0	150	0
Data Storage Unit	2	25	9	0	50	0
Data Management Processor	2	75	20	0	150	0
Flight Processor	2	20	13.6	0	40	0
Command and Telemetry Processor	2	30	10	0	60	60
<b>LEV Totals (power in integer values)</b>			423.2	320	1929	826

Indicates Estimate

# Appendix J

## LTV Avionics

The left-hand column shows all of the avionics for the LTV. The next three columns show the quantity, weight, and power of the items. The next two columns show which piece of equipment that needs power for each of the mission phases as defined by power required.

LTV Avionics Equipment				LTV Avionics Power Demanded	
Item	Quantity	Item Unit Power (W)	Item Total Weight (kg)	LTV and LEV (docked)	LTV (with LEV undocked)
Internal Camera	1	7.5	7	7.5	0
Digital TV Processor	2	30	13.6	60	0
Video Recorder	1	50	10	50	0
S-Band Steerable Antenna	1	50	12.7	50	50
Ku-Band Steerable Antenna	1	50	12.7	50	50
S-Band Omnidirectional Antenna	2	15	2.2	30	0
Ku-Band Omnidirectional Antenna	4	15	4.4	60	0
S-Band Transceiver/Transmitter	1	0.8	9.1	0.8	0.8
Ku-Band Transceiver/Transmitter	1	0.8	9.1	0.8	0.8
Radio Power Amplifier	2	72	17.2	144	144
Radio Frequency Assembly	2	50	11	100	100
Keyboard/Display	2	40	17.2	80	0
Caution/Warning Electronic Assembly	1	13	8.3	13	13
Internal Lights	10	15	10	150	0
Video Controller	1	60	6.8	60	0
Hexad Navigation Unit	1	75	16	75	75
Star Trackers	3	10	13	30	30
Sun Sensors	4	2.5	7	10	10
Navigation Sensor: Rendezvous	1	200	20.5	0	200
Rendezvous and Docking Radar	1	123	38	0	123
Docking Lights	2	130	22	0	260
Video Cameras	2	7.5	14	0	15
Control Electronics	1	150	70	150	0
Data Storage Unit	2	25	9	50	50
Data Management Processor	3	113	30	337.5	337.5
Flight Processor	2	20	13.6	40	40
Command and Telemetry Processor	2	30	10	60	60
<b>LTV Totals</b>			414	1608	1559

Indicates Estimate

# References

- 2.1 *Space Exploration Initiative: A Modified Scenario*, Spacecraft Design Team, University of Minnesota, 1992.
- 2.2 Cook, Stephen; Hueter, Uwe; *Launch Vehicles For The Space Exploration Initiative*, AIAA 92-1546, NASA-Marshall Space Flight Center, Huntsville, AL.
- 2.3 "STME: Streamlining the Engine of Change." *Aerospace America* July 1992: 22.
- 2.4 "ASRM: Turning in a Solid Performance." *Aerospace America* July 1992: 26.
- 2.5 Isakowitz, Stephen J., *International Reference Guide to Space Launch Systems*, AIAA 1991.
- 2.6 *First Lunar Outpost Heavy Lift Launch Vehicle Design and Assessment*, Preliminary Status Report, May 1992.
- 2.7 *ibid.*
- 2.8 Hall, Al ed. *Petersen's Book of Man in Space. Volume V. Beyond the Threshold*. Los Angeles: Petersen, 1974.
- 2.9 Buden, David, *Nuclear Rocket Safety*, ACTA Astronautica, Volume 18, 1988, pp. 217-224.
- .1. NASA Office of Technical Information: *Lunar Flight Handbook*, Volume 2: Lunar Mission Phases. NASA N63-21105, 1963.
- 4.2. Bate, Roger R., Mueller, Donald D., and White, Jerry E., *Fundamentals of Astrodynamics*, Dover Publications, Inc., New York, 1971.
- 4.3 Griffin and French, *Space Vehicle Design*, American Institute of Aeronautics and Astronautics, Inc., Washington, DC, 1991.
- 4.4. Gennaro Avvento, *Automated Rendezvous Techniques*, University of Houston, May 1986.
- 5.1 David L. Black and Stanely Gunn, "A Technical Summary of Engine and Reactor Subsystem Design Performance During the NERVA Program", AIAA 91-3450.
- 5.2 W.H. Robbins and H.B. Finger, "An Historical of the NERVA Nuclear Rocket Engine Technology Program", AIAA 91-3451.
- 5.3 S.K. Borowski, "The Rational/Benefits of Nuclear Thermal Rocket Propulsion for NASA's Lunar Transportation System", 27th Joint Propulsion Conference, Sacramento, California, June 24-26, 1991.
- 5.4 D. Peaccio, C. Scheil, and J. Collins, "Near Term Lunar Nuclear Thermal Rocket Engine Options", 27th Joint Propulsion Conference, Sacramento, California, June 24-26, 1991.
- 5.5 James T. Walton, "An Overview of Tested and Analyzed NTP Concepts", AIAA 91-3503.
- 5.6 M. Stancati and J. Collins, "Mission Design Considerations for Nuclear Risk Mitigation", Space Applications International Corporation, Technical Report.
- 5.7 *Lunar Transportation Systems*, NASA Technical Document, Volume 2, Marshall Space Flight Center, Huntsville, Alabama, 1990.

## References (cont.)

- 5.8 *FLO Lander and Return Stage Propulsion System Trade Study*, NASA Propulsion Workshop II, Johnson Space Flight Center, Houston, 1992.
- 5.9 *Design of a Lunar Excursion Vehicle*, NASA Technical Paper 1-1828-1-35D, Marshall Space Flight Center, Huntsville, AL, 1991.
- 5.10 *Lunar Transportation Systems*, NASA Technical Document, Volume #2, Marshall Space Flight Center, Huntsville, AL, 1990.
- 5.11 Griffin and French, *Space Vehicle Design*, American Institute of Aeronautics and Astronautics, Inc., Washington, DC, 1991.
- 5.12 *Lunar Lander Conceptual Design*, EEI Report # 88-181, NASA LBJ Space Center, 1988.
- 5.13 *Space Shuttle Spacecraft Systems*, NASA Press Release, Rockwell International, 1984.
- 5.14 Rockwell International Technical Document #172 P02
- 5.15 *Lunar Module Reaction Control System*, NASA Technical Paper TN D-6740, Manned Spacecraft Center, Houston, TX, 1972
- 5.16 *First Lunar Outpost (FLO) Study*, NASA Space Transit Subsegment Subteam, 1992
- 6.1 *Metals Handbook - Volume I Tenth Edition, Properties and Selection: Irons, Steels, and High-Performance Alloys*. American Society for Metals, Metals Park, Ohio: 1990
- 6.2 Griffin and French, *Space Vehicle Design*, American Institute of Aeronautics and Astronautics, Inc., Washington, DC, 1991.
- 6.3 "*Cryogenic Boiloff in Low Earth Orbit - A Parametric Study Utilizing Multilayer Insulation*", Sverdrup Technology, Task Number 313-002, February 12, 1990.
- 6.4 "*In-House Study - Design of a Lunar Excursion Vehicle* ", Marshall Space Flight Center Program Development, December 1991.
- 7.1 *Designing for the Human Presence in Space*
- 7.2 *Manned Systems Integration Standards*, NASA 1989
- 7.3 *Space Shuttle Transportation System*, Rockwell International, 1984
- 7.4 *FLO Trade Study*, MSFC 1992
- 7.5 *Space Shuttle Systems Handbook* NASA JSC 1991
- 7.6 Schitzler, B.G. and Borowski, S.K, *Radiation Dose Estimate for Typical NTR Lunar and Mars Mission Engine Operations*, 1991.
- 7.7 Griffin and French, *Space Vehicle Design*, American Institute of Aeronautics and Astronautics, Inc., Washington, DC, 1991.



